THE UNIVERSITY OF CHICAGO

ANDROGEN RECEPTOR MEDIATED GENDER BIAS IN AUTOIMMUNITY

A DISSERTATION SUBMITTED TO
THE FACULTY OF THE DIVISION OF THE BIOLOGICAL SCIENCES
AND THE PRITZKER SCHOOL OF MEDICINE
IN CANDIDACY FOR THE DEGREE OF
DOCTOR OF PHILOSOPHY

COMMITTEE ON CANCER BIOLOGY

BY
JEAN LEE

CHICAGO, ILLINOIS
DECEMBER 2022

Amor Fati

TABLE OF CONTENTS

LIST OF FIGURES

LIST OF TABLES

ACKNOWLEDGMENTS

First off, I thank my dearest advisor, Alexander V. Chervonsky. Sasha has shown me unwavering support and patience throughout the years I have worked with him, and I am forever grateful for the space and time he has allowed me to discover joy in entertaining independent ideas. He has shown me the beauty of practicing science for reasons no other than to foster curiosity and explore the unknowns. It was a great privilege to learn from the incredible insight and brilliance in his approach to science. Beyond science, Sasha, you have been a father and a dear friend I relied on for really, anything life threw at me. It has been a great solace to always know that I can always stop by your office door at any time, and that you will listen to me for whatever I have to say whether it is science or non-science related. I will miss stomping down to your office door to alert you that I am coming 'unannounced'. Thank you for creating the best home in Chicago for me, where I can freely enjoy science, but also to feel loved, respected, and cared for, for who I am.

I would like to thank my dear special mentor, Tatyana Golovkina. Tanya has taken me under her wings from day 1 and has been both my most critical mentor and best cheerleader over the years. I am forever grateful to her for sharing the rigorous scientific training and dedication to science with me, without which I would not have advanced to the scientist I am today. I will always remember the conversation we had over lunch one day about the idea of designing my very first T cell transfer experiment, and how that one discussion kicked off my drive to think independently. Thank you for being you, my mentor, friend, and family.

Thank you to both Sasha and Tanya, for being by my side, through my personal growth over the years. Without you, I would not be who I am today.

I would like to thank my committee members, Russell Szmulewitz, Geoffrey Greene, and Justin Kline, for steady support and helpful discussions. It was always a pleasure and a privilege to discuss data and ideas with you.

I thank my collaborator, Aly Khan, for kicking off the AR project with Lonya. I am

thankful for his insight and extreme patience with my naïve questions over the years.

I thank past and present members of our labs, all of whom brought immense joy to my daily life in lab: Leonid Yurkovetskiy, Joseph Pickard, Matt Funsten, Renee de Pooter, Andrey Kuznetsov, Samara Singh, Katie Senter, Yunisse Gonzalez, Zoe Strong, Grace Ryan, Katie Fox, Laura Sams, Brandon Hawkins, Emily Cullum, Jessica Spring, Helen Beilinson.

Lonya and Joe, thank you for showing me how to have real fun with science. I am extremely lucky to have had you as grad students who exposed me to research. Matt, thank you for being my wonderful partner soldier over the years. I will miss your silly jokes from across the bay. Renee and Andrey, thank you for feeding me and taking care of me like a family. Emily, Jessica, and Helen, thank you for making my tough days always much easier and bearable. To all the undergrads and technicians: thank you for making me laugh, revealing the joy of sharing and teaching science, and most of all, being my sisters and brother.

I thank my dear old friends outside of science, Julia Park and Jisoo Lee, for being present for me no matter what or where we are. Julia, I do not know where I would be without your love and support in my life.

I would like to thank my friends who helped me push through the difficult period of my life towards the end of my Ph.D career, including Grace Ryan, Emily Cullum, Elaine Kouame, Allen Zhu, Daniel Dongjoo Lee, Julia Park, Jisoo Lee, Samara Singh, Yunisse Gonzalez, Laura Sams, Brandon Hawkins, Katie Fox, Jessica Spring, Helen Beilinson, Sasha Chervonsky, and Tanya Golovkina.

Grace, thank you for being the little sister I never had, for being "happier beings" with me, for loving me for who I am. Emily, thank you for being there for me and looking out for me no matter what, even when I don't ask. I will always remember the love you have given me when I found myself in the dark. Elaine, thank you for being my strong, independent female friend and an awesome scientist. I will miss laughing and spending time with you

dearly. Helen, thank you for finding silver linings and lending me a shoulder to cry on. Dan, thanks for being a silly and endearing brother to me. And Allen, thank you, for the friendship, understanding, and love you have shown me. My heart will always remember that you put peanut butter on the bread I would eat.

I would like to thank Ruben Young Seok Kim, for being my friend and family over the years. Know that I always wish the best for you, and will only have love and support for you.

Thank you to my lovely two pets, Monji and Baki. I miss you every day, very much.

Lastly, I thank my family, who taught me how to be resilient. I thank them for loving and supporting me, whatever shape or form I am in. For making me who I am today, teaching me to never give up, and helping me believe I can live a meaningful life. I would like to thank my sister, Hannah, for being my lighthouse for the entire life I have known.

ABSTRACT

A sex bias exists in major autoimmune diseases with females suffering from increased susceptibility compared to males. The male sex hormones—androgens—have been implicated in contributing to protection from autoimmunity, but cellular and molecular mechanisms underpinning androgen-mediated suppression of autoimmunity remained unclear. Here, we define the canonical androgen signaling pathway through the androgen receptor (AR) in T cell-intrinsic fashion to be sufficient in dampening $\alpha\beta$T cell autoreactivity in the NOD/ShiLtJ (NOD) mouse model of spontaneous type I diabetes (T1D). Mechanistically, T cell-intrinsic AR signaling modulated capacity of $CD8^+$ T cells to proliferate and secrete IFNγ in an antigen-specific manner. Moreover, we reveal that androgens influence the shaping of the thymic TCR repertoire and function of autoimmune regulator (AIRE) in a T cell-extrinsic fashion. An analysis of AR targets in T cells identified *Ptpn22*, a gene encoding a lymphoid-specific phosphatase that negatively regulates T cell activation, as a candidate player for AR-mediated regulation of male protection from autoimmunity. PTPN22 deletion resulted in the loss of gender bias in the B6.NZM mouse model of systemic lupus erythematosus (SLE). In addition, mutagenesis of the newly identified AR binding site in the regulatory region of *Ptpn22* by CRISPR/Cas9 in NOD mice yielded generation of more aggressive autoimmune T cells. However, T cell-intrinsic AR signaling or AR-mediated modulation of *Ptpn22* alone was not sufficient to establish male protection from spontaneous T1D in NOD mice. In humans, the penetrance of autoimmunity-associated mutation in PTPN22 (R620W) was found to inversely correlate with the degree of a disease sexual dimorphism, and no sex-dependent difference in the frequency of the mutant allele was detected in patients with autoimmunity. Collectively, our data supports a possibility that PTPN22 most common 'normal' allele does contribute to disease development in a hormone dependent manner, making this protein, as well as potentially multiple other proteins that are controlled by androgens, a valid target for therapeutic interventions. Furthermore, our findings warrant investigation of additional

networks and cell types that contribute to protection from autoimmunity in sex-dependent manner.

CHAPTER 1

INTRODUCTION

1.1 Gender bias in immune responses

A sex bias in immunity is a conserved trend that spans across vertebrates and a set of invertebrates [1, 2]. Females generally exhibit stronger immune responses than males, and therefore, fare better against cancers and infectious diseases [3–5]. With cancers of nonreproductive organs, males are disproportionately more susceptible to acquiring cancer in urinary bladder, liver, oral cavity, kidney, and lung compared to females [3]. Similarly, males display increased sensitivity to various types of bacterial, parasitic, fungal, and viral infections over females [4]. The flip side of this trend is present in autoimmunity: females are generally more prone to developing autoimmune disorders than males are [5]. Major autoimmune diseases such as systemic lupus erythematosus (SLE), multiple sclerosis (MS), rheumatoid arthritis, and Graves' disease display a striking female bias, with a female-to-male incidence rate ratio ranging up to 9:1 in SLE [5]. Even in Type 1 diabetes (T1D), where overall incidence rate seems to be equivalent between sexes, a subset associated with polyglandular autoimmune syndrome II-IV displays a strong female bias [6].

The trend of gender bias in autoimmunity extends to mouse models of autoimmune diseases. In NOD/ShiLtJ (NOD) mouse model of spontaneous T1D, sex bias is evident in animals raised in the specific pathogen-free (SPF) conditions with an average of 75% incidence of T1D in females, in contrast to an average of 25% incidence in males, by 30 weeks of age [7]. Several mouse models of SLE also exhibit autoimmunity in a sexually disparate manner with increasingly severe pathology manifested in females compared to males [8, 9]. In addition, in the SJL model of experimental autoimmune encephalitis (EAE) for MS, EAE-inducing proteolipid antigen elicits chronic autoimmunity in females but restricted, monophasic form of autoimmunity in males [10, 11].

1.2 Candidate regulators of gender bias in autoimmunity

Several players may contribute to the sexually dimorphic display of autoimmunity. The X chromosome represents an interesting genetic candidate because of an incomplete nature of X chromosome inactivation (XCI). XCI is an epigenetic silencing mechanism that randomly silences one of the two X chromosomes present in all female cells in order to normalize the double dosage of X chromosomes present in females compared to males. The process involves non-coding RNA transcribed from *X-inactive specific transcript* (*Xist*) that covers and silences X chromosome in *cis*. The X chromosome encodes for several important immune regulators, including FOXP3, TLR7, IL2RG, among others, and any gene that escapes said epigenetic silencing can be expressed in an increased dosage in females. Therefore, depending on the targets of partial X chromosome inactivation, X-linked genes may play a role in driving the sex biased display of autoimmunity. However, to date, there has not been a direct evidence for a one-to-one linkage between an X-linked gene and gender bias in autoimmune conditions.

The male sex hormones—androgens—represent an interesting category of candidates that could influence gender bias in autoimmunity. Androgens define a group of steroid hormones that are critical for proper fetal and male pubertal developmental events [12]. In male humans, androgens are synthesized by testes and adrenal glands. Male mice, on the other hand, lack the enzyme 17 α-hydroxylase in the adrenals, which leaves testes to be the primary organ for androgen production. Testosterone and its active metabolite dihydrotestosterone (DHT) are the principal forms of androgens in systemic circulation [13].

Epidemiological studies that stratified autoimmunity incidence prior to and post puberty reported greater risk of autoimmunity following the onset of puberty, which coincides with increased production of sex hormones including testosterone [14, 15]. The importance of androgens in mediation of male protection from autoimmunity has been highlighted in several mouse studies utilizing models of gender biased autoimmune conditions. For example,

removal of androgens via surgical castration in NOD males was sufficient to reverse male protection from T1D [16]. This finding was complemented by an exogenous supplementation of DHT, which was sufficient to restore protection in castrated males. These findings were recapitulated with the NZB/NZW F_1 mouse meodel of SLE and the experimental autoimmune encephalitis (EAE) model of MS, where castration removed male protection from autoimmunity and androgen treatment restored male protection [17, 18]. In light of these findings, the role of female sex hormone, estrogens, in exacerbating autoimmunity has been examined in NOD and NZB/NZW F_1 mouse models of T1D and SLE, respectively. When provided with a physiological dose of estrogens, NOD females did not show consistent difference in the rate of T1D [19]. In the NZB/NZW F_1 model of SLE, treatment with supraphysiological levels of estrogen resulted in an increased morbidity due to symptoms irrelevant to characteristic lupus parameters but related to toxicity from estrogens [19]. These data suggest that the role of estrogens in modulation of gender bias is not necessarily linear and may be influenced by additional factors whose identities and roles need to be characterized.

Lastly, work from our own lab and others revealed the involvement of the microbiota in mediating gender bias in autoimmunity. A rederivation of NOD mice into germ-free (GF) settings rendered both females and males highly susceptible to T1D development over the course of 30-weeks [20], underscoring the importance of microbes in establishing male protection from T1D. Collectively, our data delineated that two required signals—signals from androgens and the microbiota—crosstalk to offer the protection from T1D in NOD males. In this network, androgens harness an environment appropriate for certain microbes to propagate, whereas the microbes can regulate systemic levels of androgens in circulation.

1.3 Protective effects of androgens against T1D in microbiota-independent fashion

Through the lens of a recent analysis of the cumulative T1D incidence within our GF colony of NOD mice, we learned that under appropriate genetic contexts, androgen signal alone has the capacity to establish male protection from T1D in NOD mice in the absence of microbes. Previously, gender bias in T1D incidence was absent in GF colonies of NOD mice, primarily due to a loss of male protection in a sterile condition [20]. However, with potential genetic alterations that may have resulted from a genetic drift within our GF NOD colony over time, we observed some partial protection from T1D in NOD males even in the absence of the other required signal, the microbial signal **(Figure 3.1)**. This finding warrants further investigation of the mechanisms by which androgen signaling elicits protection from T1D in NOD males.

To date, multiple research groups examined the effects of androgens on cells of the immune system *in vitro* to demonstrate that androgens can directly or indirectly affect various cell types including monocytes, macrophages, ILC2 progenitors, neutrophils, mast cells, and T cells [21]. However, despite these efforts, understanding of the precise cellular and molecular mechanisms underpinning androgen interaction with immune cells *in vivo* that drive gender bias in autoimmunity is still incomplete.

CHAPTER 2

MATERIALS AND METHODS

2.1 Animals

NOD/ShiLtJ (NOD), NOD.Cg-*Prkdc*^{scid}/J (NOD.SCID), NOD.Cg-Tg(TcraTcrbNY8.3)1 Pesa/DvsJ (NOD.8.3), NOD.Cg-Tg(TcraBDC2.5,TcrbBDC2.5)1Doi/DoiJ (NOD.BDC2.5), C57BL/6J (B6J), B6;NZM-Sle1$^{NZM2410/AegSle2NZM2410/Aeg}$ Sle3$^{NZM2410/Aeg/LmoJ}$ (B6.NZ M), and B6.Cg-*Ptpn22*^{tm2Achn}/J (B6.PTPN22$^{-/-}$) mice were purchased from The Jackson Laboratory. NOD.Cg-*Tcra*^{tm1Mjo}Tg(TcrbG9C8)2Fsw/J (NOD.G9C8) [22] and NOD.PTPN2 2^{AREmut} mice produced by us were maintained at the University of Chicago. NOD.PTPN22 ^{AREmut} mice were crossed to NOD.G9C8 mice to generate NOD.PTPN22^{AREhet}G9C8$^{+/-}$ mice, and the resulting NOD.PTPN22^{AREhet}G9C8$^{+/-}$ mice were intercrossed to obtain NOD.PTPN22^{AREwt}G9C8$^{+/-}$ and NOD.PTPN22^{AREmut}G9C8$^{+/-}$ mice, which were used for experiments. B6.NZM mice were crossed to B6.PTPN22$^{-/-}$ mice, and the resulting B6.NZM.PTPN22$^{+/-}$ mice were intercrossed to obtain B6.NZM.PTPN22$^{+/+}$ and B6.NZM. PTPN22$^{-/-}$ mice. PCRs specific for the NZM SLE (*Sle*) 1/2/3 loci mapped to chromosomes 1, 4, and 7 were done with primers at proximal, intermediate, and distal locations of each of the loci using the primers listed in Table 2.1. The studies described in this study have been reviewed and approved by the Animal Care and Use Committee at the University of Chicago.

2.2 CRISPR/Cas9-mediated generation of mice

CRISPR guide RNAs (crRNA and tracrRNA annealed) were designed using Custom Alt-R CRISPR-Cas9 guide RNA design tool (Integrated DNA Technologies, Inc., Coralville, IA). Alt-R S.p. Cas9 Nuclease 3NLS protein (IDT) was prepared in mouse embryo-grade H2O (Sigma-Aldrich) on the day of injection. AR flox plasmid HDR template with the homology

arms and floxed exon 2 sequence was custom generated using EcoRV insertion sites in pUC57 by GenScript. ssODN HDR donor for the generation of Ptpn22$^{\text{AREmut}}$ mice was custom generated by IDT. The injection mixes were prepared as follows. Lyophilized crRNA and tracrRNA were resuspended in TE buffer (1mM Tris-HCl, pH7.5, 0.1mM EDTA). 5 μg of crRNA (5 μl of 1 μg/μl) and 10 μg of tracrRNA (10 μl of 1 μg/μl) were combined in a PCR tube and were annealed in a thermocycler (95°C for 5 min followed by ramp down to 25°C at 5°C/min). The annealed crRNA and tracrRNA (guide RNA) were diluted in H_2O and mixed with Cas9 protein, followed by 10-15 minute incubation at room temperature to obtain the RNP mix. The final concentration of components in RNP mix was 30ng/μl of each guide RNA and 50ng/μl Cas9 for AR flox, and 80ng/μl of guide RNA and 100ng/μl Cas9 for Ptpn22$^{\text{AREmut}}$. The plasmid or ssDNA donors were mixed with the RNP mixes at the final concentration of 12.5ng/μl for the plasmid and 60ng/μl for the ssDNA. The final injection mixes were spun at 20,000xg for 10 min at room temperature. Microinjections were performed by the Transgenics/ES Cell Technology Mouse Core Facility at the University of Chicago.

2.3 Surgical castration

Gonads were excised using Change-A-Tip handheld cauterizer (Bovie Medical Corporation, Clearwater, FL) from 4-week-old males anesthetized with isoflurane. Wounds were closed with Vetbond (3M, Saint Paul, MN). Sham-operated mice had an incision made followed by wound closer with Vetbond (3M).

2.4 Diabetes tracking

Diabetes development was monitored by weekly testing of urine glucose with Diastix Reagent Strips (Bayer, Elkhart, IN). All mice monitored for T1D were littermates.

2.5 Intraperitoneal glucose tolerance test (IPGTT)

Mice were fasted overnight for 12 h and baseline blood glucose level was measured using a glucometer (timepoint 0). Mice were then intraperitoneally injected with 20% glucose solution in PBS (2g/kg body weight) and blood glucose levels were measured at 15, 30, 60, 90, and 120 minutes following injection. Blood glucose level is normalized by taking the difference in glucose level between each time point and timepoint 0.

2.6 Microbiota colonization

SPF B6.NZM donor females from U of C and U of F were euthanized at each respective institution and the cecal contents was immediately frozen at $-80\,^{\circ}\mathrm{C}$. On the day of colonization, cecal contents were immediately homogenized in sterile PBS and 400μl was gavaged into each GF recipient. The recipients were housed at isolators and bred to produce G_1 colonies, which were analyzed for SLE parameters at indicated ages.

2.7 T cell transfer

Single cell suspensions of lymph nodes and RBC-lysed splenocytes from 8-week-old donor mice were pooled and subjected to B cell panning, which involved incubation in 10-cm petri dish (Thermo Fisher Scientific, Hampton, NH) pre-coated with 10μg/ml rabbit anti-mouse IgG antibody for 1h at RT. Non-adherent fraction was collected and analyzed by FACS to confirm enrichment with T cells. For $CD4^+/CD8^+$ mix transfers, B cell panned fraction was further purified by CD4 (L3T4) MicroBeads (Miltenyi Biotec, Bergisch Gladbach, North Rhine-Westphalia, Germany) or CD8a (Ly-2) MicroBeads (Miltenyi Biotec) by negative selection. A total of $20\text{x}10^6$ T cells were *i.v.* transferred into each host. Diabetes was monitored weekly up to 130 days.

2.8 T cell proliferation *in vitro*

2x10^6cells/ml RBC-lysed, irradiated splenocytes were seeded with 5% FBS-supplemented Click's media in 96-well round bottom tissue culture treated plates. Splenocytes were treated with 1ng/ml LPS for 24 h at 5% CO_2 at 37 °C. Splenocytes were washed twice with 5% FBS-supplemented Click's media and 10^5 CTV stained T cells were seeded. 2μg/ml cognate peptides were added to each well. 72 h later, cells were collected and analyzed by FACS for T cell proliferation.

2.9 IFNγ ELISA

Cells were prepared as described in T cell proliferation *in vitro*. At the end of the stimulation with cognate peptide for 72 h, supernatant was collected and used for IFNγ ELISA using mouse IFNγ ELISA set (BD Biosciences) following manufacturer's protocol.

2.10 T cell proliferation *in vivo*

Single cell suspensions of lymph nodes and RBC-lysed splenocytes from 8-week-old donor mice were pooled and subjected to B cell panning. The resulting T cell fraction was stained with CellTrace Violet (Invitrogen, Carlsbad, CA) using manufacturer's protocols. 2-3x10^6 T cells were *i.v.* transferred into NOD hosts. After 72 h, PLN and inguinal lymph node (ILN) were isolated from each host and analyzed by FACS for T cell proliferation.

2.11 Lymphoid cell isolation, FACS analysis, and sorting

Single cell suspensions prepared from RBC-depleted splenocytes or pancreatic lymph nodes were stained with the following antibodies following the manufacturer's protocol to characterize profiles of T cells and B cells: Fc-Block (BD Biosciences, Franklin Lakes, NJ),

anti-CD4 (eBioscience, San Diego, CA), anti-CD8a (Invitrogen), anti-CD62L (BioLegend, San Diego, CA), anti-CD44 (BioLegend), anti-CD69 (Invitrogen), anti-CD93 (BioLegend), anti-B220 (BioLegend), anti-IgM (Invitrogen), anti-CD23 (BioLegend), anti-CD21/CD35 (BioLegend), and anti-CD1d (Invitrogen). Dead cells were gated out by staining with propidium iodide (Sigma-Aldrich, Burlington, MA). To confirm enrichment of T cells from B cell panning, non-adherent fraction was stained with Fc-Block (BD Biosciences), anti-CD4 (eBioscience), anti-CD8a (Invitrogen), anti-CD19 (BioLegend), anti-B220 (BioLegend) antibodies following the manufacturer's protocol. Dead cells were gated out by staining with propidium iodide (Sigma-Aldrich). To measure T cell proliferation, single cell suspensions of PLN and ILN were stained with Fc-Block (BD Biosciences), anti-CD4 (eBioscience), and anti-CD8 (Invitrogen). Dead cells were gated out by staining with propidium iodide (Sigma-Aldrich). $PI^-CTV^+CD8^+$ T cells were gated to calculate the proliferation index. All data were acquired using LSRFortessa (Becton, Dickinson & Company, Franklin Lakes, NJ) and analysis was performed using FlowJo software (Becton, Dickinson & Company). For sorting thymocyte subpopulations, single cell suspension of the thymus was stained with the following antibodies using manufacturer's protocols: Fc-Block (BD Biosciences), Ter119-Biotin (BioLegend), CD19-Biotin (BioLegend), CD11c-Biotin (Invitrogen), CD11b-Biotin (BioLegend), anti-CD4 (eBioscience), anti-CD8a (Invitrogen), and Streptavidin-APCCy7 (BioLegend). Dead cells were discriminated with propidium iodide (PI) staining. On FACSAria Fusion 5-18 (Becton, Dickinson & Company), $PI^-Ter119^-CD19^-CD11c^-CD11b^-$ cells were sorted into following populations: DN ($CD4^-CD8^-$), DP ($CD4^+CD8^+$), CD4SP ($CD4^+CD8^-$), and CD8SP ($CD4^-CD8^+$).

2.12 Histology

Kidney pathology was scored using 5-μm, PAS-stained sections with 40-μm intervals and scored as follows by a renal pathologist, Anthony Chang: 0, no visible change; 1, focal mesan-

gial proliferative changes; 2, diffuse mesangial proliferative disease; 3, diffuse proliferative glomerulonephritis (GN) with focal crescents; and 4, diffuse GN with crescents in >50% of glomeruli.

2.13 Anti-nuclear Ab staining

HEp-2 slides (Bio-Rad Laboratories, Hercules, CA) were incubated with serum samples diluted at 1:100 in FACS buffer (1% FBS, 0.02% NaN_3 in 1XPBS), and counterstained with tetramethylrhodamine-labeled donkey anti-mouse IgG (Jackson ImmunoResearch, West Grove, PA) diluted at 1:100 in FACS buffer. After washes in FACS buffer, slides were wetted with 50% glycerol and covered with glass coverslips (IMEB, San Marcos, CA). The imaging and scoring were performed on the Leica DMLB fluorescent microscope.

2.14 Cryosectioning and immunohistochemistry

Kidney samples embedded in OCT (Sakura Finetek USA, Torrance, CA) were cut with a cryostat into 8-μm-thick sections, which were transferred to microscope slides. Slides were fixed in $-20\,^{\circ}$C acetone, dried, and stained with tetramethylrhodamine-coupled anti-mouse IgG (Jackson ImmunoResearch) or anti-mouse FITC-labeled C3a Ab (MP Biomedicals, Irvine, CA) in FACS buffer. After washes in FACS buffer, slides were wetted with 50% glycerol and covered with coverglass (IMEB). The slides were stored at $4\,^{\circ}$C until imaging using a DMLB microscope (Leica Microsystems, Wetzlar, Germany) equipped with a SPOT camera (Diagnostic Instruments, Sterling Heights, MI).

2.15 RNA extraction, reverse transcription, and RT-PCR

Total RNA was extracted for RT-PCR analysis from thymocytes and Jurkat cells with Purelink RNA mini kit (Thermo Fisher Scientific) following manufacturer's instructions.

RNA was retrotranscribed using Superscript IV reverse transcriptase (Invitrogen) according to the manufacturer's instructions. cDNA was amplified with specific primers for the mouse genes *Ar*, *Ptpn22*, *Axin2*, *Ctnnb1*, *Nur77*, and *Actin* using TaqMan Probes (Thermo Fisher Scientific) or iTaq Universal SYBR Green Supermix (Bio-Rad Laboratories) on QuantStudio 3 Real-Time PCR System (Applied Biosystems, Waltham, MA).

2.16 Transient transfection

HEK293T cells were seeded into 24-well plates (Corning, Corning, NY) at a density of $3x10^4$ cells/well, cultured for 24 h to 70% confluence, and co-transfected with pGL4.23 mouse Ptpn22 promoter-luciferase reporter plasmid or pGL4.23 human Ptpn22 promoter-luciferase reporter plasmid, pIRES2-zsGreen-1-AR, and pRL-CMV. pRL-CMV was used as an internal control for transfection efficiency. Transfection was performed with Lipofectamine LTX (Thermo Fisher Scientific) according to the manufacturer's instructions. Complexes were incubated for 20 min at RT prior to transfection. Cells were incubated at 37°C for 24 h before treatment with 10nM of R1881. At 48 h post transfection, cells were collected for luciferase assay.

2.17 Molecular cloning

Mouse *Ptpn22* promoter and AR sequences were amplified from the tail DNA of NOD/ShiLtJ prepared using DirectPCR Lysis Reagent (Viagen Biotech, Los Angeles, CA). Human *Ptpn22* 56bp promoter sequence was generated by annealing sense and antisense oligonucleotides (Sigma-Aldrich) to be used as an insert in the ligation reaction. *Ptpn22* promoter sequences with KpnI and XhoI sites were generated using forward and reverse primers with KpnI and XhoI sites. Alternatively, sense and antisense oligonucleotides of *Ptpn22* promoter sequences with KpnI and XhoI sites were annealed to form double-stranded oligonucleotides. *Ptpn22*

sequences and pGL4.23 were digested with KpnI and XhoI (New England Biolands, Ipswich, MA) according to the manufacturer's protocol. Digested products were gel purified with NucleoSpin Gel and PCR Clean-up kit (Macherey-Nagel, Düren, Germany) according to the manufacturer's protocol. Insert and vector were ligated with T4 DNA ligase (Invitrogen) and introduced into E. coli DH5α (Invitrogen) by electroporation. Colonies on LB+ampicillin (Amresco, Dallas, TX) plate was screened by QIAprep Spin Miniprep Kit (Qiagen, Hilden, Germany). E. coli carrying the pGL4.23 reporter with insert were grown overnight at 37°C in Luria-Bertani broth (LB) supplemented with ampicillin. Plasmids were isolated with NucleoBond Xtra Midiprep kit (Macherey-Nagel) and sequenced with primers flanking the insert. The 56bp ARE region of *Ptpn22* promoter is as follows: mouse 5'-TCTAGGGCTTGTGATGAAGTCAGTAAACCACAGCCTCCAGCACGCTGTGCTCCTGC-3', and human 5'-TCTAGGGCTTGTGATGAAGTCAGTAAACCACAGCCTTCAGCATGCTCTGCTCAGGC-3'. pIRES2-ZsGreen1 containing mouse AR sequence was generated as above, using XhoI and PstI restriction enzymes (New England Biolabs) and kanamycin (Sigma-Aldrich) for antibiotic selection.

2.18 Dual-luciferase assay

Luciferase expression was measured using Dual-Luciferase Reporter Assay System (Promega, Madison, WI) according to the manufacturer's protocol. Briefly, cells were washed in 1xPBS and harvested in 65µl of 1x reporter lysis buffer, lysed for 15 minutes at RT on a shaker. 20µl of lysates were used for the measurements of firefly and *Renilla* luciferase activities on a SpectraMax M3 luminometer (Molecular Devices, San Jose, CA). The firefly luciferase activities were normalized to *Renilla* luciferase activities.

2.19 AR stimulation in Jurkat cells

Androgen receptor was cloned from pLENTI6.3/AR-GC-E2325 (Addgene, Watertown, MA) by PCR into lentiviral expression plasmid pscALPS-Puro (Addgene). For lentivirus production, HEK293 cells were seeded at 80% confluency in 6 well plates and transfected with 2.5μg of total plasmid DNA with either pscALPS-Puro (empty plasmid control) or pscALPS-puro expressing AR, psPAX2 gagpol expression plasmid, and the pMD2.G VSV-G expression plasmid at a DNA ratio 4:3:1 using TransIT-LT1 lipid reagent (Mirus Bio LLC, Madison, WI) according to manufacturer protocol. Media was changed to FBS supplemented RPMI FBS 16 h following transfection, and viral supernatant was harvested 2 days later to be filtered through a 0.45μm filter. To generate AR expressing and control cells, 10^6 Jurkat cells were plated in 1mL of FBS supplemented RPMI to which 500μL of viral supernatant was added, followed by selection with 1μg/mL puromycin 2 days later. Jurkat cells transduced with AR-encoding construct or empty plasmid were grown to 60% confluence in Click's medium supplemented with 5% FBS (GeminiBio, West Sacramento, CA). Cells were washed twice with serum-free Click's medium and seeded in 6-well plates (Corning) using Click's medium supplemented with 5% charcoal-stripped FBS (Thermo Fisher Scientific) at 1.75x10^5 cells/well. After incubation for 48 h in 37 °C CO_2 incubator, cells were stimulated with R1881 (Sigma-Aldrich) (5nM) or carrier (0.1% EtOH) for 16 h in 37 °C CO_2 incubator. At the end of the incubation period, cells were harvested and lysed for RNA extraction following manufacturer's protocol.

2.20 Preparation of thymocytes for qPCR and TCR repertoire analysis

Thymi were collected in 5%FBS+1XPBS. For RNA isolation from bulk thymocytes, thymus was homogenized and lysed with Purelink RNA mini kit (Thermo Fisher Scien-

tific) according to the manufacturer's protocol. For RNA isolation from DN ($CD4^-CD8^-$), DP ($CD4^+CD8^+$), CD8SP ($CD8^+CD4^-$), CD4SP ($CD4^+CD8^-$) thymocytes, single cell suspension of thymocytes at $20x10^6$ cells/mL was prepared in 5%FBS+1XPBS. Thymocytes were stained with Fc-Block (BD Biosciences), CD19-biotin (BioLegend), CD11c-biotin (BioLegend), CD11b-biotin (BioLegend), TER119-biotin (BioLegend), SA-PerCPCy5.5 (Invitrogen), CD4-APC (BioLegend), CD8a-PacBlue (Invitrogen), and Propidium Iodide (PI) (Sigma-Aldrich), following manufacturer's protocol. $FoxP3^+$ cells were detected with GFP. Stained thymocytes were sorted using BD FACSAria™ Fusion Cell Sorter.

2.21 TCR sequencing

To characterize the thymic TCR repertoires of castrated and sham-operated male mice, NOD.$Foxp3^{GFP}$ mice were bred to NOD.TCR$\alpha^{-/-}$ mice to obtain NOD.$Foxp3^{GFP}$TCR$\alpha^{+/-}$ males. Males were either castrated or sham-operated as described above at 4 weeks of age. At 8 weeks of age, thymi were collected and single cell suspensions were stained as described above. The same crosses and analyses were performed using mice on C57BL/6J background. For the generation of TCRα chain library, RNA was isolated from sorted thymocytes using RNeasy Micro kit (Qiagen). 1^{st} strand cDNA was synthesized using a primer against the constant region of mouse TCRα chain mRNA. Template switch was carried out with SMARTScribe Reverse Transcriptase (Clontech) and template switch adapter. 1^{st} strand cDNA was PCR amplified using Q5 polymerase (New England Biolabs), nested primer for the constant region of TCRα cDNA, and step-out primers complementary to the switch adapter. 2^{nd} PCR amplification was performed with a nested primer against the constant region of TCRα cDNA and a nested primer complementary to the switch adapter. NEBNext Ultra DNA Library Prep Kit for Illumina sequencing with standard protocol according to the manufacturer's recommendations was used for Illumina adaptor ligation. Target library was purified using agarose gel purification and amplified with PCR. The library was analyzed

using paired end Illumina NextSeq sequencing.

2.22 Chromatin Immunoprecipitation

Thymi were harvested from pre-pubescent male NOD mice (4-5-week-olds). DN and CD8SP thymocytes were enriched through negative selection of $CD4^+$ cells. Chromatin was cross-linked and immunoprecipitated (ChIP-ed) with antibodies to AR in the presence of 100nM DHT in DMSO (treated) or DMSO (untreated). To boost signal from noise and increase the specificity of our results, we performed ChIP using two different antibodies that recognized different epitopes of the AR protein. Ab1 identified an epitope corresponding to amino acids in 91-370 of AR (sc-13062, Santa Cruz Biotechnology, Inc., Dallas, TX), whereas Ab2 identified an epitope mapping to the N-terminus of AR (sc-816, Santa Cruz Biotechnology, Inc.). ChIP sequencing was performed by the Genomics facility at the University of Chicago.

2.23 ChIP-seq analysis

DHT-dependent AR binding sites were identified using untreated AR-ChIP samples and chromatin input as background, and ChIP-seq binding sites from both antibodies were integrated using the IDR algorithm [citation]. Non-specific binding sites were filtered out by identifying DHT-dependent AR binding sites in the context of known genomic regions that often produce artifact signals in functional genomics assays (e.g. ChIP-seq, MNase-seq, DNase-seq, FAIRE-seq) [encode citation]. AR binding sites were highly enriched in the promoter region of genes as defined by the 5'UTR and 5K upstream of the TSS ($p<10^{-77}$ and $p<10^{-300}$, respectively; binomial test).

2.24 ImmGen analysis

To determine the relative Ar expression level in cells of the hematopoietic lineage, nearly 200 different myeloid and lymphoid immune cell types curated by the ImmGen consortium were analyzed.

2.25 PTPN22 R620W (SNP C1858T) association analysis

The published epidemiological data reporting percentage of female incidence in autoimmune diseases and the published odds-ratios of autoimmune diseases significantly associated with the common C1858T (rs2477601) R620W nonsynonymous single nucleotide polymorphism of PTPN22 in various GWAS studies were integrated.

2.26 Genotyping human subjects, performed by the Kahaly lab

Genotyping procedures for the subjects used in the association study were described previously [23]. In brief, DNA from peripheral venous blood was extracted using QIAamp Blood Mini Kit (Qiagen). Exon 14, which has the SNP C1858T (rs2476601), was amplified by PCR. PCR products were treated with ExoSAP-IT (USB Europe, Staufen, Germany) and sequenced with an ABI PRISM 3100 Genetic Analyzer (Applied Biosystems, Darmstadt, Germany) following the manufacturer's protocol. Data was analyzed using GeneMapper software version 3.2 (Applied Biosystems).

2.27 Metascape gene set enrichment analysis

A list of significant ($p<0.05$) AR target genes from ChIP-seq analysis was subjected to Gene Ontology analysis using Metascape [24]. Genes were analyzed for enrichment for Functional Set and Pathway.

2.28 Statistical analysis

All statistical analyses were performed with Prism 9 (GraphPad) unless mentioned otherwise. Results are expressed as means ± SEM. The statistical difference between two groups was determined by unpaired t test. T1D incidence data was analyzed by Kaplan-Meier. A p-value < 0.05 was considered statistically significant. *$p<0.05$, **$p<0.01$, ***$p<0.001$, ****$p<0.0001$. For PTPN22 R620W association study (AITD, T1D, APS3v), all statistical analyses were performed with SPSS software package, release 15.0 (SPSS Inc., Chicago, IL). Genotypes of each cohort were tested for deviation from Hardy-Weinberg equilibrium with chi-square tests.

Table 2.1: Genotyping Primers

Primer Name	Sequence	Use
Proximal Sle1 forward	5'-GTGTCTGCCTTTGCACCTTT-3'	Sle1 Genotyping
Proximal Sle1 reverse	5'-CTGCTGTCTTTCCATCCACA-3'	Sle1 Genotyping
Intermediate Sle1 forward	5'-TCCACAGAACTGTCCCTCAA-3'	Sle1 Genotyping
Intermediate Sle1 reverse	5'-ATACACTCACACCACCCCGT-3'	Sle1 Genotyping
Distal Sle1 forward	5'-CTGACCTCCACACGACCC-3'	Sle1 Genotyping
Distal Sle1 reverse	5'-GCTTGGGAAACTGGATGAAA-3'	Sle1 Genotyping
Proximal Sle2 forward	5'-TGGCCAACCTCTGTGCTTCC-3'	Sle2 Genotyping
Proximal Sle2 reverse	5'-ACAGTTGTCCTCTGACATCC-3'	Sle2 Genotyping
Intermediate Sle2 forward	5'-GGCTTTGCAATGCTATGCAT-3'	Sle2 Genotyping
Intermediate Sle2 reverse	5'-TGGCAGGAGGTATGACAGAA-3'	Sle2 Genotyping
Distal Sle2 forward	5'-GCTTGCTTTAGGAGTGTGCC-3'	Sle2 Genotyping
Distal Sle2 reverse	5'-TATTTGCTCTCCATTTCCCC-3'	Sle2 Genotyping
Proximal Sle3 forward	5'-CCAGACCATCTGATCCAGATC-3'	Sle3 Genotyping
Proximal Sle3 reverse	5'-GGAGGTTGCAGTGAATTCAAG-3'	Sle3 Genotyping
Intermediate Sle3 forward	5'-CCCACCAGAGATCACCAAGT-3'	Sle3 Genotyping
Intermediate Sle3 reverse	5'-CACAATGAAGGCTGAAAGCA-3'	Sle3 Genotyping
Distal Sle3 forward	5'-CACTTGGGGAACGTCAAGAC-3'	Sle3 Genotyping
Distal Sle3 reverse	5'-TGTAGACCATAGCCCATAAGCC-3'	Sle3 Genotyping

Table 2.2: crRNA

crRNA	Sequence	Mouse line
AR crRNA1	5'-TATTTGATAAGGCTGATCAT-3'	NOD.AR$^{f/y}$ and NOD.ARKO
AR crRNA2	5'-CATCATTGCTTGTACAACCA-3'	NOD.AR$^{f/y}$ and NOD.ARKO
PTPN22 crRNA1	5'-GCAGGCTAACCTAGTGCTGG-3'	NOD.Ptpn22^{AREmut}

Table 2.3: HDR template

AR$^{f/y}$ (inserted in pUC19)

5'-TTTTTCTTCCTCCTTTGGTAGAGAAACACAGATAAATCATGGATGTTGTAGTTCCATGGCTACGAGTGTGG
ACAATTGTCATCTTTAAGGCAGATTAACATAACATAAGAGGTCACTTATAATTTATTAATTTTTTACATAGAAC
ATGGAACATAGACAAAATTTGATATTTGGTTAGCAAGAAGCATATTCTAGTTGGAAAAATGAAGTCATTATTA
AAAGAGATGGAGAACTAATATACAGTGAGGAGTTTAGAATTGTTTTTCTATCTCATTACTTTCATATTTACCC
GAAAAGTGTAGACACAGATCTTGGAGCTAAGCACTTAGACTAGCATGATCCTCATCCAGGAAACCTAGAAGT
CTTGTAAAGGTTTTGACAGCATCCCTCAAACTATTCAACAGTGCTGTGTATCGTTTCTCAGGAAAAGTGCAT
GGTACAAGGATTCTATTACATTTTTTTTATTAGGTATTTTCCTCCTTTACATTTTCAATGCTATCCCAAAGGT
CCCCCATACCCACCCCCCCAATCCCCTACCCACCCACTCCCCCTTTTTGGCCCTGGCGTTCCCCTGTACTGG
GGCATATAAAGTTTGCAAGTCCAATGGGCCTCTCTCTTTGCCATGATGGCCGACTAGGCCATCTTTTGATAC
ATATGCAGCTAAAGACAAGAGCTCCCGGGTACTGGTTAGTTCATATTGTTGTTCCACCTATAGGGTTGCAGT
TCCCTTTAGCTCCTTGGGTAATTTCTCTAGCTCCTCCATTAGGGGCCGTGTGACCCATCCAATAGCTGACTG
TGATCATCCACTTCTGTGTTTGCTAGGCCCCGACATAGTCTCACAAGAGAGAGCTATAACTGGGTCCTTTCA
GCGAAATCTTGCTAGTGTATGCAATGGTGTCAGCATTTGGAAGCTGATTATGGGATGGATCCCTGCATATGG
CATCTATTACATTTTTGTTACAGAACAGGGAAAGGGACACTGAGAGACTCAAGAAGAAAGAAAAGGAATTAA
TACAAAAGAACAGTGAAAGCTGGTATGATAATACTAATTTATCCTTTACTTGTATATTAATATCAAGAGTAACT
CATACATCTGATTTATGTTGTCAGAGCAATAACTCAGTACTACTGGTAGCAATATTGCTGTTTTACAGGTAAG
ACTCTAGGCTCCAAGAGCTAAAATATATAAAATTCTTCTGGTATTTGATAAGGCTGATCATAGCCCTCTCTCT
GGAAGAAGTAAGATAGAGTTATGTTCATGCCATTTAATGACTGTATATGTCGTCATTAATGCATCACATTAAG
TTGATACCTTAAATAACTTCGTATAGCATACATTATACGAAGTTATCCTCTGCTTAACTTCCTTCTCTTACAAA
TGCAGAGCTCATGAGATTGGCTATTCCCTCAGAACCTGTTTAATTCCTTGGCAGGATTCAAAGTGTCCATAG
GAAACCTTACAAACACTCTGTCCAGAGAAGGTCTCAAAAGAGTTCAGCTTTACACTGATTCACTCGAGCAAT
CCATAGAATAGTCACTTGGATGTATGTACAGTTTCTCAGAAGACCGTAGAATTCTGATCGATGTCTGCCATCC
ACTGACATATGTTGCTTTGTTCTCTCTCTGTCTCTGTGTGTGTCTTTTCAGTTTGGACAGTACCAGGGACCA
TGTTTTACCCATCGACTATTACTTTCCACCCCAGAAGACCTGCCTGATCTGTGGAGATGAAGCTTCTGGCTG
TCACTACGGAGCTCTCACTTGTGGCAGCTGCAAGGTCTTCTTCAAAAGAGCCGCTGAAGGTAAAAAGTCTT
ACCTACTTCCTGATATTTTCCCCTTCTCTTTTGCCTAGCAGAGAATGACAGTGACCTTCCAGGGCATTCTGA
ATAACTTCGTATAGCATACATTATACGAAGTTATTAATCCCAGAGACTGAGTCATTAGCAAGGGCCCTCTCAC
AGTACATGTAAGATCAAAGAAGCCCATGGTTATATTTGCTGAGCTGTCTTGGCTGGCCTGGTTGTACAAGCA
ATGATGGTGATGTAGGTGGTCCCAGCTGGTGCTTGGTGGCTCCCAGGACTGGAAGCAAAATTAATGATTTG
AAAAATTAAATTTCCTTCCTGCTTGTTTTCAACTCTGCTTCCTAGTGAGGAAAAGAAAACTTGTCCTTATTA
GAGAGGTTAGAAGTGGAGAAACCCCAACTGAGTATACAGGCTGTTTTCTGTAGAGAATATGAGACTGTTCC
TTAGCAAAAGCTTCCTGGCTTTAACCCCAGAAAAGGAAGTGTTCTCACTGTTCAGCAGACCATCAGTGTCT
GCACCTGCTCCCTCCTGCTTGCTGCCTCTTTGGGACCTCTCTTTGCAATAAGGACTCCAAGGCAGGAAAAA
ACTCAGAGAGAAGCATCAGAGGACTGCTTTCAGGGCATGACAGTTGGTTCAGAATCCCAACGTAACTTGCA
TTTTGTATCCAGCTAAGTGGGATGGAGCCTTTACTTGTTATCTGCACTAATTATGATGTTTCTAACCTACAT
CATCTAGCAGAAACACCCACTCCAGGCCTTTACTGTAGTCTTAGTGATCCCTCCCTTCTTAATCACAGGGTG
GGGGTGGGAGCTTAAACCTTTATTCATACACTCTACTACCATCCCTCAGTCTGGTACTCCTTTCTCAAAGAG
TCACTGGAAAGCTGCCCCTACATGGTCTACTGTGGCTGCAGACTCAGTTTTAAAGATTCCTTTGCAACTCT
GCCCTGGTCTCTGGCTTCCCACCAAGGGGGAGCTTCCGGCCAGGGAGGTTTTCCTTCTTTCTAACAGGTC
AGGAAGAGCTTAAATCAGAACCAAAACAGACAGCCCTTTATCATACAAAAGAAGCATCAGCATCAGAAAAG
AAATTCATTTCCTGAGAAATATGCTCAGCACAACAGAAGCACAAGGGAATACCTGGCAACAAGAGCTGTCC
TCACTGACAGCCAATCTAACAATGATTTTAATGTCAGCATTTTAGTAGGTGGGAGAAATACATTCAAAACAC
AAAGCTACCCTTTTCTTTTCTTCCAGTTCCCCAAGGCATGAGGAGGCAAACAGGCACTTTGTAATAGTGAA
AATGAGCTACATGTTTCACCTCTACTCCCCAATGGCCCCTTTGCTGCTGTCCATAGTAGACTAGCATGAGAT
CCAAGGCCCTAAGGCATAATAAGCTTGGACCTTTAGAAAAGTCTTAAAGCGATGCCTTCCTTTCT-3'

PTPN22^{AREmut}

5'-TGGCCAAGGCAGCACCAAGAAGCCACTGCTGCTGCAGGCTAACCTAGTGCTGGAGGCTGTGGTTTACTGA
CTTCATCACAAGCCCTAGAGGAAATTAGTACAAAACTAGCTTCTGTGGTCACACAACAAAGCCATCATCT-3'

Table 2.4: TCR sequencing oligonucleotides

Primer	Application	Sequence
1st strand cDNA synthesis		
SmartNNNa	5' – template switch adapter	(AAGCAGUGGTAUCAACGCAGAGUNNNNUNNNNUNNNNUCTT(rG)$_4$)
Mus α synt3	Primer for cDNA synthesis, mouse TCR α chain mRNA, C-region	AGTCAAAGTCGGTGAAC
BCmus syn2	Primer for cDNA synthesis, mouse TCR β chain mRNA, C-region	ATCTCTGCTTTTGATG
1st PCR amplification		
Step-out primer mix: Smart 20 Step1	Step-out mix, anneals on the switch adapter	CACTCTATCCGACAAGCAGTGGTATCAACGCAG-3'/ CACTCTATCCGACAAGCAGT-3'
Mus α rev2	Nested primer, TCR α cDNA, C-region	GCTGTCCTGAGACCGAGGAT
Mus BC4	Nested primer, TCR β cDNA, C-region	ATGGCTCAAACAAGGAGACC
2nd PCR amplification		
M1s i	Slightly nested primer, anneals on the switch adapter	(N)$_{2-4}$(XXXXX)CAGTGGTATCAACGCAGAG
Mus acj i	Nested primer, TCR α cDNA, C-region	(N)$_{2-4}$(XXXXX)CAGGTTCTGGGTTCTGGATGT
Mus bcj i	Nested primer, TCR β cDNA, C-region	(N)$_{2-4}$(XXXXX)AGTCACATTTCTCAGATCCT

CHAPTER 3

RESULTS

3.1 Androgen receptor signaling in T cells modulates T cell autoreactivity.

3.1.1 Surgical castration is sufficient to reverse protection from T1D in NOD males

To establish that androgens confer protection from T1D in our colony of NOD males, we subjected prepubescent NOD males to either sham-operation or surgical castration. As expected, sham-operated males displayed low T1D incidence over the course of 30 weeks. In contrast, surgical castration resulted in a loss of protection in which castrated males exhibited high T1D. Therefore, surgical castration was sufficient to reverse protection from T1D in NOD males **(Figure 3.2)**.

3.1.2 Canonical androgen signaling through the androgen receptor is involved in establishing protection from T1D in NOD males

We next sought to understand the downstream signaling pathway of androgens responsible for conferring protection from T1D in NOD males. Androgens are understood to signal through the canonical or noncanonical pathway [25]. The canonical androgen signaling is mediated through the intracellular, cognate nuclear hormone receptor, androgen receptor (AR), which is encoded by the X chromosome [25]. The expression pattern of AR is broadly distributed [26], where AR carries out nuclear signaling by functioning as a transcription factor in a ligand dependent manner. Androgens including testosterone normally circulate systemically, being bound by carrier proteins such as sex hormone binding globulins [27].

Upon entering the cytoplasm of the target cell through passive diffusion, the enzyme 5α-reductase converts testosterone to an active metabolite called dihydrotestosterone (DHT) [27]. The presence of DHT in the intracellular compartment prompts AR, which normally remains sequestered in the cytoplasm by the chaperone proteins such as heat shock proteins, to be released and associate with DHT [27]. DHT-bound AR translocates into the nucleus as a homodimer and recognizes a specific sequence termed *androgen response element* (*ARE*) motif that is usually composed of short sequences at the 5' regulatory region of target genes [28, 29]. This sequence-specific binding of AR to the genome initiates recruitment of other transcriptional coregulators that, in sum, yields transcriptional control of target gene expression. On the other hand, the noncanonical signaling of androgens is understood to result in more rapid outcomes (seconds to minutes) that are mediated by non-genomic pathways [30]. Noncanonical receptors for androgens include membrane receptors such as GPCRs and have been shown to modulate intracellular second messenger signaling intermediates or Ca^{2+} levels [30].

To identify the primary downstream signaling pathway androgens utilize to confer protection from T1D in NOD males, we tested whether the canonical signaling through AR is involved in male protection from T1D in NOD mice. For this, we generated a NOD.ARKO line using CRISPR/Cas9 **(Figure 3.3)** for observation of spontaneous T1D development over the course of 30 weeks. As expected, control animals sufficient in AR presented clear gender bias with a higher T1D susceptibility in females over males **(Figure 3.4)**. However, NOD.ARKO males demonstrated an overall T1D incidence similar to that of control females, a phenotype that recapitulates the T1D incidence of castrated NOD males **(Figure 3.4)**. This data indicates that the canonical androgen signaling through AR, instead of the noncanonical pathway, is the primary pathway involved in establishing androgen-mediated protection from T1D in NOD males.

3.1.3 T cells, among the hematopoietic cells, have the highest level of Ar at the level of transcript

Because the expression of AR is broadly distributed [26], we first sought to identify the candidate immune cell type AR signaling primarily acts on. We used the gene expression data available from the ImmGen database [31] to compare the relative expression level of AR encoding gene, *Ar*, within the immune cell populations of the hematopoietic lineage. This computational analysis identified T cells as the major population with the highest relative expression of *Ar* **(Figure 3.5)**. Among the thymic T cell subpopulations, immature double-negative (DN, $CD4^{-}CD8^{-}$) and immature $CD8^{+}$ single-positive (CD8SP, $CD4^{-}CD8^{+}$) cells **(Figure 3.6.A)** displayed the highest level of *Ar* expression. Results of the computational analysis were validated by the quantitative measurement of *Ar* in DN and CD8SP thymocytes isolated from postpubescent male C57BL/6J (B6J) mice **(Figure 3.6.B)**. This pattern of *Ar* expression in DN and CD8SP was not a peculiarity of the genetic background of B6J mice, as a similar observation was made with DN and CD8SP from T1D-prone NOD mice **(Figure 3.6.C)**. Thus, the effect of androgens-AR signaling on T cells became the focus of our subsequent analyses.

3.1.4 Androgens influence T cell autoreactivity

While several groups have reported the suppressive function of androgens on autoimmunity through castration or supplementation of androgens in autoimmune-prone mouse models [16–18], the direct *in vivo* evidence that demonstrates T cells to be the central target of androgen signaling for protection from autoimmunity lacks. Therefore, we addressed whether androgen-AR signaling implicated in protection from T1D in NOD mice is operating at the level of T cells by performing an adoptive T cell transfer. To this end, peripheral T cells isolated from castrated or sham-operated 8-week-old male NOD mice were adoptively transferred into male NOD.SCID hosts for T1D observation. Recipients of T cells

from sham-operated donor males remained largely protected from T1D, recapitulating the T1D incidence rate in male NOD mice (<25%) housed in SPF condition **(Figure 3.7)**. In contrast, recipients of T cells from castrated donor males progressed to diabetes at a rate similar to that seen in SPF female NOD mice (>60%) **(Figure 3.7)**. Thus, the data corroborates the hypothesis that androgen-AR signaling acts at the level of T cells to reduce the autoreactive potential of T cells in NOD mice *in vivo*.

3.1.5 T cell intrinsic AR signaling is sufficient to attenuate T cell autoreactivity

Having established that androgen signaling works at the level of T cells, we next sought to investigate whether androgen-AR signaling is acting in a T cell-intrinsic or -extrinsic fashion to dampen T cell autoreactivity. First, we introduced a floxed AR allele on a NOD background (NOD.AR$^{f/y}$) through CRISPR/Cas9-assisted homology directed repair **(Figure 3.8)**. Subsequently, a mouse model with a T cell-specific deletion of AR was attained by crossing NOD.AR$^{f/f}$ mice to NOD.CD4Cre^{+} mice. When peripheral T cells from NOD.AR$^{wt/y}$CD4Cre^{+} or NOD.AR$^{f/y}$ donor males were adoptively transferred into male NOD.SCID hosts, the cumulative diabetes incidence rate recapitulated that observed in recipients of T cells from sham-operated male donors **(Figure 3.9)**. In contrast, transfer of peripheral T cells from NOD.AR$^{f/y}$CD4Cre^{+} donor males to male NOD.SCID hosts yielded a cumulative diabetes incidence rate mirroring that observed in recipients of T cells from castrated donor males (>60%) **(Figures 3.7 and 3.9)**. Therefore, T cell-intrinsic androgen-AR signaling is sufficient for attenuating T cell autoreactivity in NOD mice.

3.1.6 T cell intrinsic AR signaling in either CD4$^+$ or CD8$^+$ T cells is sufficient to yield a decrease in net T cell autoreactivity

The expression of CD4Cre$^+$ transgene peaks at the DP stage during T cell development in the thymus [32]. This suggests that T cell intrinsic AR signaling for attenuating T cell autoreactivity could be important in either CD4$^+$ T cell alone, CD8$^+$ T cell alone, or both CD4$^+$ and CD8$^+$ T cells. To identify which T cell compartment androgen-AR signaling is important in for attenuating T cell autoreactivity, CD4$^+$ T cells from NOD.AR$^{f/y}$CD4Cre$^+$ were mixed with CD8$^+$ T cells from AR$^{f/y}$ donors, or vice versa, followed by transfer into NOD.SCID hosts. As expected, recipients of AR-sufficient CD4$^+$ and CD8$^+$ T cells displayed low diabetogenic potential, while recipients of AR-deficient CD4$^+$ and CD8$^+$ T cells had high diabetogenicity. Interestingly, recipients of T cells sufficient in AR signaling in either CD4$^+$ or CD8$^+$ T cells alone displayed an attenuation in net T cell autoreactivity **(Figure 3.10)**. Given that the AR signaling in either CD4$^+$ or CD8$^+$ T cells alone is sufficient to dampen the autoreactivity of T cells overall, we entertain the possibility that T cell intrinsic AR signaling imprints T cells at the DP or earlier stage to impart low autoreactive potentials in the periphery.

3.2 Potential mechanisms of AR signaling mediated modulation of T cell autoreactivity

Having established that androgen-AR signaling has influence on modulating T cell autoreactivity, our next goal was to explore the potential mechanisms by which androgen-AR signaling can regulate T cell autoreactivity. The data presented thus far indicate that T cell intrinsic AR signaling dampens T cell autoreactivity in the context of adoptive T cell transfer experiments. However, considering that AR expression is widely distributed across different cell types and tissues, the potential of T cell extrinsic AR signaling influencing T

cell autoreactivity cannot be excluded. T cell-intrinsic and/or -extrinsic AR signaling can influence T cells at 2 stages: i) at the level of T cell selection in the thymus and/or 2) at the level of T cell function in the periphery.

3.2.1 T cell-intrinsic AR signaling suppresses antigen-specific CD8$^+$ T cell proliferation

First, we sought to characterize the functional consequence of T cell-intrinsic androgen-AR signaling in T cells. To this end, NOD.G9C8 and NOD.BDC2.5 TCR transgenic mice were utilized to test the antigen-specific T cell proliferation capacity *in vitro*. NOD.G9C8 mice bear the transgenic TCR derived from a diabetogenic CD8$^+$ T cell clone with a specificity towards an islet-specific antigen, Insulin $B_{15\text{-}23}$ [33]. NOD.BDC2.5 transgenic TCR is derived from a diabetogenic CD4$^+$ T cell clone with a specificity towards an islet-specific antigen, chromogranin A [34]. CD8$^+$ or CD4$^+$ transgenic TCR bearing mouse model was used separately to assess the role of androgen signaling on CD8$^+$ or CD4$^+$ T cells, respectively. Peripheral T cells isolated from transgenic TCR allele bearing mice that are either sufficient or deficient in T cell-intrinsic AR signaling were labeled with CellTrace Violet (CTV) and cultured with cognate antigens to measure antigen-specific T cell proliferation capacity. G9C8$^+$ CD8$^+$ T cells sufficient in AR signaling displayed reduced antigen-specific T cell proliferation compared to T cells deficient in AR signaling **(Figure 3.11.A)**. Importantly, the same trend of phenotypes was recapitulated with NOD.8.3 TCR bearing donor T cells, another CD8$^+$ TCR transgenic line with a TCR specificity towards an islet-specific antigen, $IGRP_{206\text{-}214}$ **(Figure 3.11.B)** [35]. On the other hand, BDC2.5$^+$ CD4$^+$ T cells exhibited an opposite trend with AR signaling sufficient T cells displaying increased T cell proliferation in comparison to T cells deficient in AR signaling **(Figure 3.11.C)**.

To validate our *in vitro* findings *in vivo*, we performed an *in vivo* T cell proliferation assay. Similar to the *in vitro* T cell proliferation assay, peripheral T cells were isolated and

stained with CTV, followed by adoptive transfer into NOD hosts for antigen-specific T cell proliferation in the pancreatic lymph nodes (PLNs) for 72 hours. Consistent with the *in vitro* findings, 8.3^+ $CD8^+$ T cells sufficient in AR signaling demonstrated a reduced capacity to proliferate in the PLNs compared to 8.3^+ $CD8^+$ T cells deficient in AR signaling **(Figure 3.12.A)**. In contrast, T cell-intrinsic AR signaling did not appear to influence the proliferative potentials of $BDC2.5^+$ $CD4^+$ T cells *in vivo* **(Figure 3.12.B)**. Functional influence of AR signaling in $CD8^+$ T cells, but not in $CD4^+$ T cells, is consistent with the finding that $CD8^+$ T cells have higher *Ar* expression compared to $CD4^+$ T cells ((**Figure 3.6.B and Figure 3.7.C)**. The findings demonstrate that the suppressive pressure exerted on $CD8^+$ T cell proliferation in response to cognate antigen recognition represents one potential mechanism by which T cell-intrinsic androgen signaling curtails T cell autoreactivity in NOD males.

3.2.2 T cell-intrinsic AR signaling enhances antigen-specific IFNγ secretion by CD8⁺ T cells

Previously, we have shown that macrophages isolated from sham-operated NOD males, compared to ones derived from castrated NOD males or NOD females, elicit enhanced IFNγ secretion by T cells [7]. This finding indicates that androgen-mediated influence on macrophages can regulate the level of IFNγ secretion by T cells. Considering that autocrine signaling of IFNγ/IFNγR in T cells may have proapoptotic effects on T cells [36], we hypothesized that increased IFNγ secretion by T cells serves as one potential mechanism by which androgens contribute to dampened T cell autoreactivity. Therefore, we measured the level of IFNγ in the supernatant of *in vitro* proliferation assays described above. Interestingly, despite T cell-intrinsic AR signaling reducing T cell proliferation, T cells from NOD.G9C8$^+$AR$^{f/y}$ donors secreted much higher levels of IFNγ in response to stimulation by the cognate peptide compared to AR deficient controls (NOD.G9C8$^+$AR$^{f/y}$CD4Cre$^+$) **(Fig-**

ure 3.13.A). In contrast, similar to no striking difference observed for T cell proliferation, BDC2.5^{+} CD4^{+} T cells sufficient or deficient in AR did not exhibit a major difference in the ability to secrete IFNγ after stimulation by cognate peptide **(Figure 3.13.B)**. Therefore, we conclude that T cell intrinsic androgen-AR signaling influences the capacity of CD8^{+} T cell's to proliferate and secrete IFNγ in response to cognate antigen stimulation.

3.2.3 Androgens regulate shaping of the TCR repertoire in the thymus

To elucidate whether androgen signaling orchestrates T cell development in the thymus as a mechanism to contribute to male protection from T1D, we performed a comparative analysis of thymic TCR repertoires (CD4SP, CD8SP, and CD4^{+}Foxp3^{+} Tregs) of castrated and sham-operated male TCR$\alpha^{+/-}$Foxp3^{GFP} mice on NOD and B6 background (a heterozygosity at the TCRα allele was used to prevent expression of dual α-chains by a given T cell clone [37–40]). A comparative analysis of the thymic TCR repertoires between castrated and sham-operated NOD.TCR$\alpha^{+/-}$Foxp3^{GFP} mice revealed CD4^{+} T cell compartment to be the most significantly influenced by androgens, where CD4^{+} T cells of castrated origin tended to have an increase in CDR3α strength, volume, and CDR3α/β charge compared to CD4^{+} T cells of sham-operated origin **(Figure 3.14)**. To understand whether the observed influence of androgen signaling on CD4^{+} T cell compartment was specific to the NOD background, we subsequently compared the thymic TCR repertoires of castrated and sham-operated mice on the NOD background against those on the B6 background. The changes detected in the thymic TCR repertoire resulting from the loss of androgens on the NOD background also manifested on the B6 counterparts, supporting the general role of androgens in modulating the thymic TCR repertoire shaping of the CD4^{+} T cell compartment (Figure). It is important to note that the differences detected in the TCR sequences of sham-operated vs. castrated mice could arise from androgens modulating TCR repertoire shaping in T cell-intrinsic and/or -extrinsic androgen signaling.

3.2.4 Androgen-AR mediated regulation of AIRE in modulation of T cell autoreactivity

To have a comprehensive understanding of the mechanisms by which androgen-AR signaling influences T cells, we next examined the role of T cell-extrinsic AR signaling. In support of T cell extrinsic AR signaling potentially influencing T cell autoreactivity, we found that T cells derived from NOD males exhibited different levels of autoreactivity following transfer into androgen-sufficient or -deficient background: T cells transferred into sham-operated SCID hosts remained low in their autoreactivity, in contrast to T cells transferred into castrated SCID hosts, which were highly aggressive **(Figure 3.15)**. Two hypotheses explain this data: it is possible that a continuous exposure to androgens is required for T cells to remain low in their autoreactivity; alternatively, non-T cells are targets of androgen signaling that contribute to T cell-extrinsic mechanism of AR signaling mediated regulation of T cell autoreactivity. Considering the wide distribution of AR expression in different types of cells and tissues [26], we tackled the 2^{nd} hypothesis by focusing on autoimmune regulator (AIRE)-expressing cells. $AIRE^{+}$ cells represent an interesting category of candidates that may be subjected to T cell extrinsic AR signaling, as they are not only involved in shaping the T cell repertoire [41, 42], but also transcriptionally regulated in an AR dependent manner [43]. AIRE is a transcription factor primarily expressed in thymic medullary epithelial cells (mTECs) for promoting promiscuous presentation of tissue-specific antigens (TSAs) on major histocompatibility (MHC) class II molecules, allowing negative selection of autoreactive TCR-bearing thymocytes in the thymus. Interestingly, several groups have reported that a fraction (5-20%) of T cells found in the thymus are of peripheral origin [44]. Peripheral T cells that recirculate to the thymus have been proposed to undergo another round of filtering of autoreactive T cell clones, whereby autoreactive T cells may be deleted after an encounter with a cognate antigen expressed by $AIRE^{+}$ mTECs [45–47]. Albeit to a lower degree than in mTECs, AIRE expression is also found on extra-thymic AIRE expressing cells

(eTACs) residing in secondary lymphoid organs. In the periphery, eTACs complement the role of mTECs in negative selection by inducing expression of distinct TSAs not regulated by mTECs and subject autoreactive clones that escaped the central tolerance in the thymus to functional inactivation or deletion [48, 49].

In a study published in 2016, androgen-AR signaling was shown to directly upregulate *Aire*, resulting in an increased negative selection of autoreactive T cells in a male-dependent fashion [43]. The study highlighted the contribution of ligand-dependent AR mediated transcriptional regulation of *Aire* to protection from experimental autoimmune encephalitis (EAE), a mouse model for MS [43]. In light of these findings, we tested the involvement of AIRE in T cell-extrinsic suppression of peripheral T cell autoreactivity by transferring peripheral T cells from NOD donors to NOD.SCID.AIRE$^{+/-}$ or NOD.SCID.AIRE$^{-/-}$ recipients. We hypothesized that if AR-mediated regulation of *Aire* is involved in modulating T cell autoreactivity in NOD mice, T cells derived from female donors should be equally aggressive in AIRE$^{+/-}$ and AIRE$^{-/-}$ hosts. However, T cells from male donors should be more aggressive in AIRE$^{-/-}$ hosts than in AIRE$^{+/-}$ hosts. As expected, we observed no difference in the overall diabetogenic potential of T cells when T cells from female donors were transferred into AIRE$^{+/-}$ or AIRE$^{-/-}$ female hosts **(Figure 3.16)**. However, T cells isolated from male donors showed a striking difference: T cells were highly autoreactive when they were exposed to AIRE$^{-/-}$ background compared to AIRE$^{+/-}$ background **(Figure 3.16)**. We therefore conclude that AIRE-deficiency enhances autoreactivity of donor T cells in a male-specific fashion. Three hypotheses can explain these results: i) AIRE^{+} mTECs in the thymus are subjecting recirculating peripheral T cells to another round of negative selection. In male hosts, androgen-AR signaling enhances AIRE expression on mTECs, and therefore, male AIRE$^{+/-}$ hosts experience decreased autoreactivity compared to male AIRE$^{-/-}$ hosts; ii) androgen-AR signaling increases AIRE expression on eTACs and the resulting sequestration of autoreactive T cell clones that recognize self-peptides presented by eTACs in

secondary lymphoid organs is another mechanism by which AIRE$^{+/-}$ male hosts yield attenuated autoreactivity compared to AIRE$^{-/-}$ male hosts; iii) AIRE influences autoreactivity of transferred T cells in a manner independent of androgen-AR signaling mediated direct control of *Aire*.

3.2.5 Androgen-AR signaling primarily acts as a transcription factor in thymocytes

To identify the genes that may associate into regulatory networks driven by AR, we subjected DN and CD8SP thymocytes from prepubescent NOD males to ChIP-seq analysis with AR-specific antibodies following *ex vivo* stimulation by DHT. This genome-wide analysis revealed DHT-dependent AR bindings to be the most prevalent in the regulatory regions of the AR target genes – promoter regions (5K upstream of transcription start, 32%), 5'UTR (20%), and intergenic regions (15%)] **(Figure 3.17.A)**. That was expected given the role of AR in transcriptional regulation of gene expression. Utilizing the list of significant ($p<0.05$) DHT-dependent AR target genes, gene set enrichment analysis was performed using Metascape [24]. Among the top enriched terms, formation of beta-catenin:TCF transactivating complex, a known AR target [50, 51], and TCR signaling related pathways including Ca^{2+}-dependent events and phosphorylation of CD3 and TCR ζ chains **(Figure 3.17.B)** were found. A quantitative RT-PCR analysis of genes from the top enriched term (formation of beta-catenin:TCF transactivating complex) detected reduction of expression of *Axin2* (a prototypic β-catenin regulated gene), of *Ctnnb1* (encoding β-catenin itself) and induction of expression of *Nur77* (a negative regulator of β-catenin) in castrated male mice **(Figures 3.17.C and 3.17.D)**.

3.2.6 Androgen-AR signaling regulates expression of Ptpn22 in T cells

Analyzing the set of genes under 'phosphorylation of CD3 and TCR zeta chains' **(Figure 3.17.B)**, we found that one of the most significant genes among the top enriched in the ChIP-seq analysis was *Ptpn22*, which encodes for Protein Tyrosine Phosphatase Non-receptor Type 22 (PTPN22), a phosphatase preferentially expressed in leukocytes **(Figure 3.18.A)**. In T cells, PTPN22 is known to regulate proximal TCR signaling events that hinge on phosphorylation for tuning TCR signaling strength upon T cell activation (Bottini and Peterson, 2014; Stanford and Bottini, 2014). In several genome-wide association studies (GWAS), the mutant PTPN22 locus has been identified as the top major risk locus, aside from the human leukocyte antigen (HLA) region, associated with multiple display gender bias, including RA, T1D, SLE, and Graves' disease [52–55]. To understand whether AR transcriptionally regulates *Ptpn22* expression, we subjected DN and CD8SP thymocytes from castrated or sham-operated B6J and NOD mice to qPCR analysis. Expression of *Ptpn22* was consistently higher in mice sufficient in androgen signaling compared to the androgen deficient mice, supporting the direct transcriptional control of *Ptpn22* by androgen-AR signaling **(Figure 3.18.B and 3.19)**. Furthermore, when Jurkat cells (immortalized human T cell line) were transduced with human androgen receptor encoding construct followed by stimulation with an AR agonist R1881, expression of *Ptpn22* in the presence of the AR agonist was increased **(Figure 3.18.C)**.

3.2.7 Involvement of PTPN22 in sexual dimorphism of SLE

We hypothesized that AR mediated regulation of *Ptpn22* leading to modulation of TCR signaling cascade represents a potential mechanism by which androgens confer protection against autoimmunity in males. To test this hypothesis in the context of systemic gender-biased autoimmunity, we used the B6.NZM model, a tri-congenic mouse line of SLE generated by the transfer of three lupus susceptibility loci (*Sle1*, *Sle2*, and *Sle3*) from the

New Zealand Mixed 2410 (NZM2410) mice onto the B6 genetic background [56]. B6.NZM mice were crossed to B6.PTPN22-negative mice [57] and bred to homozygosity for all *Sle* loci. When B6.NZM mice were analyzed for various SLE parameters characteristic of disease progression, sex bias with lower disease penetrance in males was clearly present in agreement with previous reports [9, 56] **(Figure 3.18.D)**. The loss of PTPN22 **(Figure 3.20.A)** coincided with a loss of the gender bias of the same phenotypes as evidenced by analyses of splenomegaly, anti-nuclear antibodies, and kidney C3 immune complex deposits: disease severity increased in B6.NZM.PTPN22$^{-/-}$ males, whereas the severity in females was largely unaffected by the deficiency in PTPN22 **(Figure 3.18.D)**. The sex dependent effect of PTPN22 deficiency was also evident in the increased frequency of CD4^{+} and CD8^{+} effector and effector/memory T cell populations (defined as CD4^{+}CD44$^{\text{hi}}$CD62L$^{\text{lo}}$ and CD8^{+}CD44$^{\text{hi}}$CD62Llo) in B6.NZM.PTPN22$^{-/-}$ males **(Figure 3.18.E)**. At the same time, it did not affect the B cell subpopulation frequencies **(Figure 3.18.F)**. Thus, sexual dimorphism of many SLE associated phenotypes was found to be sensitive to PTPN22 deficiency.

3.2.8 Identification of a putative ARE motif within the upstream regulatory region of Ptpn22

To further support the finding that androgen-dependent AR signaling may directly regulate transcription of *Ptpn22*, we analyzed H3K27ac and H3K4me3 epigenetic marks for open and active chromatin in the AR binding locus of*Ptpn22* identified by our ChIP seq analysis. The results were in line with transcriptional regulation of *Ptpn22* by androgen-dependent AR binding as H3K27ac and H3K4me3 marks coincided with AR binding region **(Figure 3.21.A)**. Interestingly, the chromatin remained largely closed in B cells in both mice and humans, coinciding with the lack of AR expression in mature peripheral B cells **(Figure 3.5)** and the lack of sex differences in B cell-associated phenotypes in B6.NZM

mice **(Figure 3.18.F)**. Based on these findings, we aimed to identify the precise *androgen response element* (*ARE*) motif within the AR binding site in the upstream regulatory region of *Ptpn22* using a functional luciferase reporter expression assay in human embryonic kidney 293T (HEK293T) cells. In the classical mode of AR action, AR translocates to the nucleus upon ligand binding followed by the recognition of *ARE* – short sequences derived from the regulatory elements of target genes. Thus, HEK293T cells were co-transfected with an AR encoding construct and a luciferase encoding construct driven by a minimal promoter, in which varying segments of the putative upstream regulatory region of *Ptpn22* were inserted 5' of luciferase encoding gene **(Figure 3.21.B)**. The DNA segment including 1kb promoter and 5'UTR region of *Ptpn22* induced luciferase expression in response to R1881 treatment, with a 56bp region near the 3' end yielding the strongest induction of luciferase expression **(Figure 3.21.B)**. These results indicated that the 56bp sequence likely contained a functional *ARE*. Importantly, this 56bp sequence is found within the region that is significantly conserved across 60 vertebrate species, implying a presence of a potential critical regulatory function within this region **(Figure 3.21.A)**. Accordingly, the corresponding 56bp region from human *PTPN22* yielded a high induction of promoter activity following stimulation with R1881 **(Figure 3.21.B)**. The critical sequence was subsequently determined by transfecting human and mouse *Ptpn22* constructs bearing either truncations or mutations of the 56bp region. As a result, 5'-GCTnnGCT-3' sequence in the 5'UTR region was determined to be critical for androgen-AR signaling-dependent *Ptpn22* expression **(Figure 3.21.C)**. Collectively, these findings suggest that the direct binding of the androgen-AR complex on the 5'-GCTnnGCT-3' motif in the 5'UTR of *Ptpn22* mediates the transcriptional regulation of *Ptpn22*.

3.2.9 Disruption of the ARE motif in the 5'UTR of Ptpn22 results in modulation of T cell activity in males

To test the physiological relevance of the *Ptpn22 ARE* motif identified *in vitro*, we introduced mutations into the putative *ARE* motif of the 5'UTR of *Ptpn22* on the NOD genetic background (NOD.PTPN22^{AREmut}) using the CRISPR/Cas9 approach **(Figure 3.22.A)**. The NOD.PTPN22^{AREmut} mouse line has 5'-GCTnnGCT-3' *ARE* motif mutated to 5'-TAGnnTAG-3'. First, we confirmed that regulation of *Ptpn22* transcription through the putative *ARE* motif was sex dependent. We measured *Ptpn22* expression in CD4SP and CD8SP thymocytes of mutant males and females and found it to be relatively dampened in male cells only **(Figure 3.23.A)**. At the same time, no gross difference in the composition of the thymocyte subpopulations was observed except for an increase in the FoxP3^{+} Treg compartment in NOD.PTPN22^{AREmut} males, indicative of a change in the TCR signaling strength in males [58, 59] **(Figure 3.22.B)**. However, increased frequencies of effector/effector memory (CD44$^{\text{hi}}$CD62L$^{\text{lo}}$) CD8^{+} T cell populations were detected in the spleen of NOD.PTPN22^{AREmut} males, a phenotype that was absent in females **(Figure 3.22.C)**. Since chronic dysregulation of TCR signaling affects autoreactivity, we tested the autoreactive potential of T cells by their transfer into NOD.SCID recipients. As expected, no difference in the overall incidence of T1D was observed in the female NOD.SCID recipients of T cells from wild-type (NOD.PTPN22^{AREwt}) or NOD.PTPN22^{AREmut} females. However, T cells from NOD.PTPN22^{AREmut} males were highly autoreactive in comparison to T cells from wild-type controls when transferred into male NOD.SCID recipients **(Figure 3.22.B)**. This data provides strong evidence for the in vivo functionality of the identified *ARE* motif in mediating androgen-dependent regulation of T cell autoreactivity. Next, we examined whether the disruption of the *ARE* motif alters the antigen-specific proliferative capacity of T cells. For this, CTV-labeled insulin-specific T cells from G9C8 TCR transgenic NOD.G9C8.PTPN22^{AREmut} mice of either sex were transferred into NOD hosts to track the

proliferation of T cells in the PLN. Only male T cells were affected by the disruption of ARE and displayed higher capacity to proliferate in response to the stimulation by the cognate antigen compared to T cells from wild-type controls **(Figure 3.23.C)**. The lack of a discernible phenotype in T cells from NOD.G9C8.PTPN22^{AREmut} females indicates that the mutation did not dysregulate AR-independent PTPN22 expression.

3.2.10 T cell-intrinsic AR signaling and Ptpn22 regulation are not sufficient to establish male protection from T1D in NOD males

Based on these findings, we asked whether the disruption of *ARE* in the upstream regulatory region of *Ptpn22* was sufficient to reverse the protection from T1D in male NOD mice. There were several important observations. As expected, wild-type animals developed T1D in a gender biased fashion, where females had higher overall incidence than males ($p<0.0001$, hazard ratio=8.83) **(Figure 3.23.D)**. In their littermate mutants, females were still more prone to diabetes, but the difference between genders became similar ($p=0.04$, hazard ratio=2.32) **(Figure 3.23.D)**. A similar observation was made with NOD.AR$^{f/y}$CD4Cre^{+} lines of mice: gender bias was evident in wild-type animals ($p<0.0001$, hazard ratio=4.16) and littermate, T cell-specific AR-deficient males did not lose protection, albeit displayed a reduction in the degree of gender bias ($p=0.0003$, hazard ratio=3.52) **(Figure 3.24)**. These results fit into a scheme in which T cell-intrinsic AR signaling and its regulation of *Ptpn22* in males make T cells less autoreactive. However, other factors involved in T1D protection of males are likely to synergize with T cell-intrinsic AR signaling and its modulation of *Ptpn22*. It is important to keep in mind that NOD males are protected from T1D due to the presence of commensal microbiota [20]. Integration of microbial signals with signals provided by AR likely goes beyond T cell-intrinsic AR signaling and its regulation of *Ptpn22*. Furthermore, considering the widely distributed expression of AR across various types of cells and tissues, cell types other than T cells are likely involved in regulation by androgens to contribute to

male protection from T1D in NOD males.

3.2.11 Regulation of PTPN22 by sex hormones may contribute to the gender bias of autoimmunity in humans

Our findings regarding androgen-AR signaling-mediated regulation of *Ptpn22* clearly show its effect on some features of the gender bias in the two animal models of autoimmunity – T1D and SLE development in NOD mice and B6.NZM mice, respectively. What is the relevance of these findings to human autoimmunity where a single coding SNP that encodes a R620W nonsynonymous mutation in PTPN22 (C1858T) is associated with an increased susceptibility to several autoimmune disorders? We hypothesized that this mutation that changes the property of the phosphatase is likely not dependent on sex hormone regulation and, thus, should not directly correlate with the sexual dimorphism of a given autoimmune disease. Thus, we analyzed the available results of GWAS of PTPN22R620W contribution to autoimmunity [54, 60, 61]. We plotted the association of the mutation with disease development (odds ratio) vs. the 'degree of the gender bias' (percent of affected females among the total number of patients with a given nosology) **(Figure 3.26.A)**. It became obvious that the relationship was inverse: the more sexually biased was a disease, the less was the reported contribution of $PTPN22^{R620W}$ allele. This finding argues that due to the sensitivity of PTPN22 to hormonal regulation, its wild-type (most common) allele could control the gender sensitivity in human diseases with a stronger gender bias. Another prediction was that there should be no gender bias in patients carrying C1858T mutation regardless of the sexual dimorphism of the disorder. For that, previously published studies of the input of PTPN22 C1858T mutation on autoimmune diseases [23, 62, 63], were reanalyzed to detect the gender representation in the carriers of the mutation. **Figure 3.26.B** demonstrates that although the frequency of the mutation was higher in patients than in healthy controls, there were no visible differences in the mutation distribution between sexes. Importantly,

such equal distribution was found in both sexually dimorphic (Autoimmune Thyroid Diseases, AITD and Polyglandular Autoimmunity represented by AITD+T1D, PGA) and in a non-dimorphic disease (non-PGA T1D).

3.3 Involvement of microbes in pathogenesis of gender biased systemic autoimmunity, systemic lupus erythematosus (SLE)

3.3.1 SPF B6.NZM model of SLE presents different severity of SLE depending on institution

As demonstrated in our work published in 2013 [7], signals from the microbiota and androgens are required to establish male protection from T1D, an organ-specific autoimmune disorder, in NOD males. We sought to test the relevancy of these findings in a mouse model of systemic autoimmunity, systemic lupus erythematosus (SLE). We chose the B6.NZM mouse model of spontaneous lupus, because the model has been shown to develop gender biased autoimmunity with 100% mortality in both sexes by 12 month of age [56]. However, interestingly, B6.NZM housed in our institution—University of Chicago (U of C)—presented significantly attenuated level of autoimmunity in various classic SLE parameters measured, albeit with an expected gender bias **(Figure 3.28)**. Strikingly, the incidence of fatal SLE was significantly decreased **(Figure 3.28 A)**. The attenuation in the overall severity of SLE in B6.NZM mice housed at U of C is in marked contrast to the fully penetrant SLE reported in B6.NZM mice housed at the University of Florida (U of F) (Dr. Morel, University of Florida, personal communication) and University of Texas Southwestern [56].

3.3.2 GF B6.NZM mice present moderate level of autoimmunity

The difference in the degree of SLE severity between B6.NZM mice housed at different institutions (U of F vs. U of C) is reminiscent of the well-established influence of the

microbiota in modulating sex bias and disease severity in T1D of NOD mice [7]. Therefore, we tested the potential involvement of the microbiota in dictating the degree of severity and presentation of gender bias in various lupus parameters of B6.NZM mice by rederiving B6.NZM mice into a GF setting. We hypothesized that if the microbiota has a role in modulating the severity or gender bias of SLE in B6.NZM mice, GF B6.NZM mice should display a different degree of SLE severity or sex bias compared to that of SPF B6.NZM mice. Interestingly, while the severity of SLE in GF B6.NZM mice was overall still attenuated compared to that of mice housed at U of F [56], it was elevated compared to SPF B6.NZM mice housed at the U of C **(Figure 3.29 and 3.30)**.

Moreover, absence of the microbiota coincided with a change in gender bias in a subset of SLE parameters. Collectively, these results led us to hypothesize that the severity and gender bias of SLE in B6.NZM mice could be influenced either in a microbiota-dependent or -independent manner: in a microbiota-dependent scenario, the difference in the composition of the microbiota is driving the variation in the severity of SLE in B6.NZM mice; alternatively, in a microbiota-independent context, the variations in the genetic composition of B6.NZM mice in different institutions underlie the change in SLE severity in B6.NZM mice. The plausibility of the 2nd hypothesis is based on the characteristic that B6.NZM mice are poor breeders that usually produce and nurse successfully only 1-2 pups at a time. With poor breeding capabilities, the likelihood of a genetic drift occurring over time in a given mouse colony increases [64], which may result in genetic differences in mice housed at different settings that could affect the course of SLE pathogenesis.

3.3.3 Is the microbiota driving the difference in the severity of SLE in B6.NZM mice housed in different institutions?

In order to address whether the differences in the composition of the microbiota is underlying the variation in the degree of SLE pathogenesis in B6.NZM mice at U of C vs U of

F, we performed a colonization study. Based on the degree of SLE severity observed in SPF B6.NZM at U of C, at U of F, and GF B6.NZM mice, we hypothesized that disease-promoting microbes are present in B6.NZM mice housed at U of F, whereas disease-suppressing microbes are present in B6.NZM mice housed at U of C. To test this hypothesis, GF B6.NZM females were gavaged with cecal contents of SPF B6.NZM females of either U of C or U of F origin and were kept in isolators to breed with GF B6.NZM males. This strategy allows generation of G_1 progenies, which would have exposure to the microbiota from birth to circumvent confounding issues associated with animals raised in GF conditions during critical developmental windows [65]. Overall, we found that the degree of SLE severity in G_1 mice did not reflect that of donor mice from either origin (U of C vs. U of F) **(Figure 3.31)**. Therefore, the collective data argue that the microbiota is not the main driver that dictates the severity or gender bias of B6.NZM mice housed in different institutions.

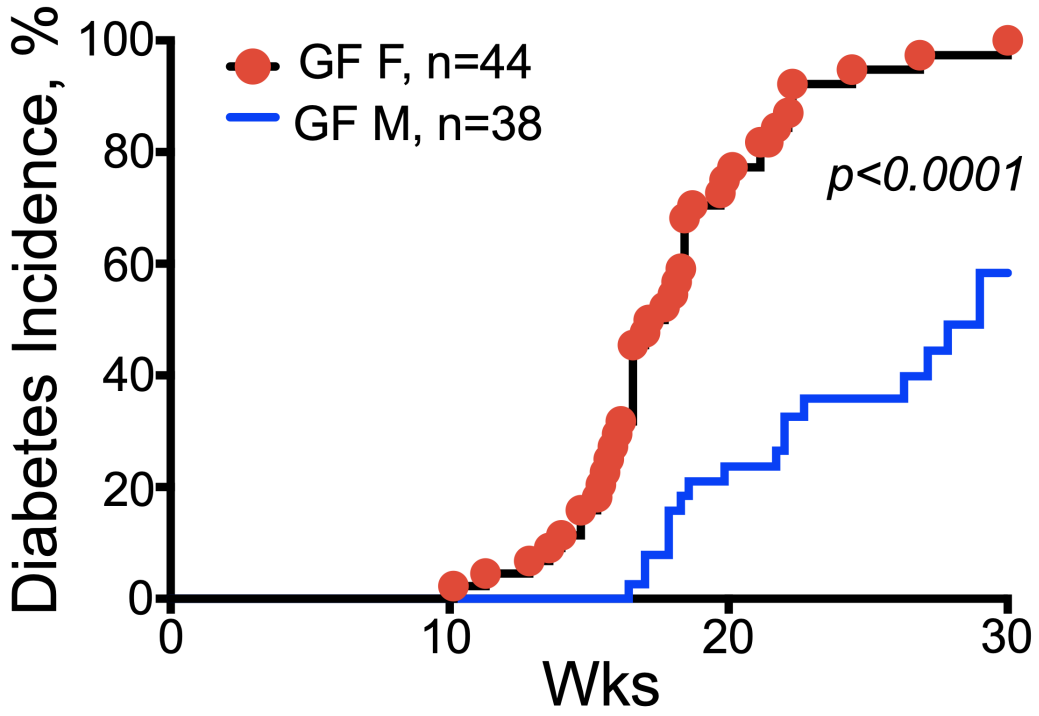

Figure 3.1: Androgens alone, in the absence of the microbial signal, can protect NOD males from T1D. T1D incidence in male (M) and female (F) GF NOD mice in 2019. n=number of animals per group. p values were calculated using Mantel-Cox log-rank test.

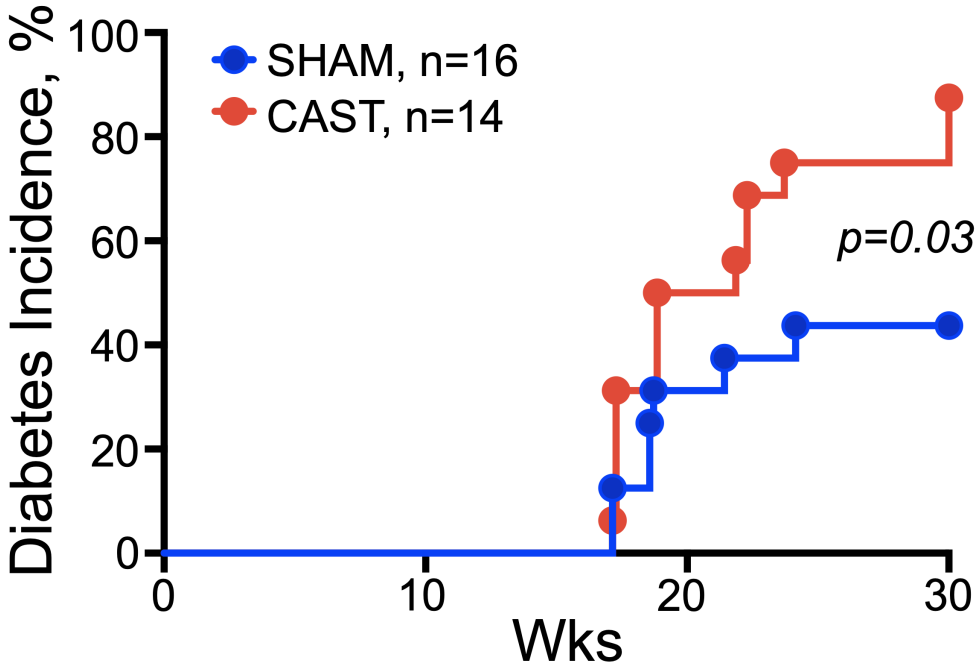

Figure 3.2: Surgical castration reverses protection from T1D in NOD males. T1D incidence in sham-operated and castrated NOD males. n=number of animals per group. p values were calculated using Mantel-Cox log-rank test.

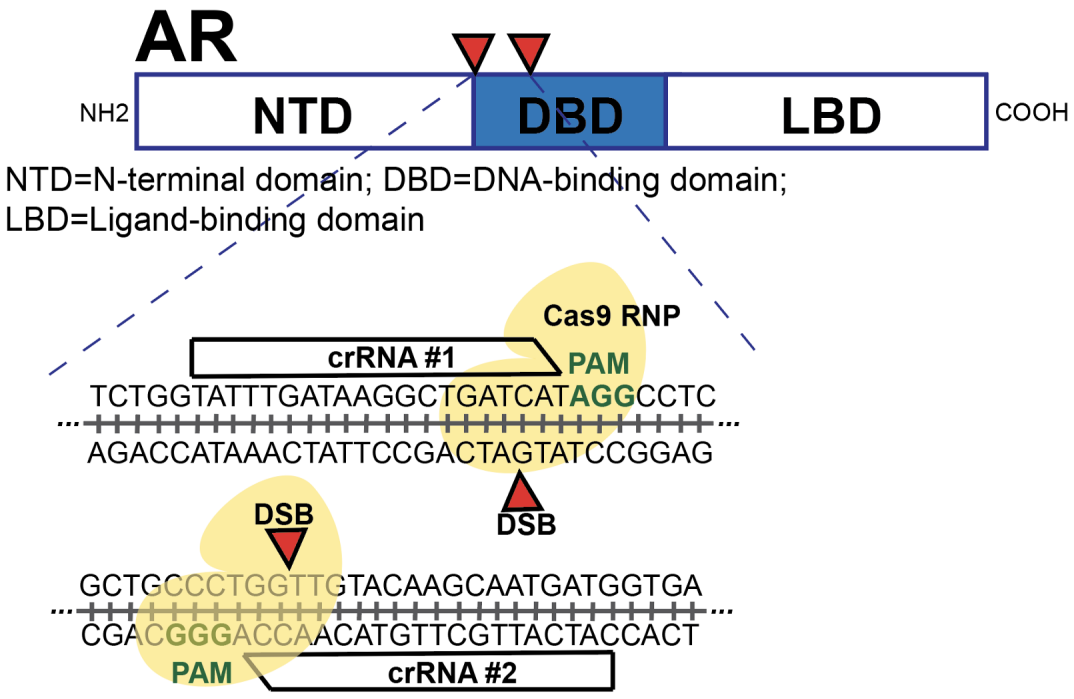

Figure 3.3: Generation of NOD.ARKO mice using CRISPR/Cas9. Targeting strategy for generating NOD.ARKO mice using CRISPR/Cas9.

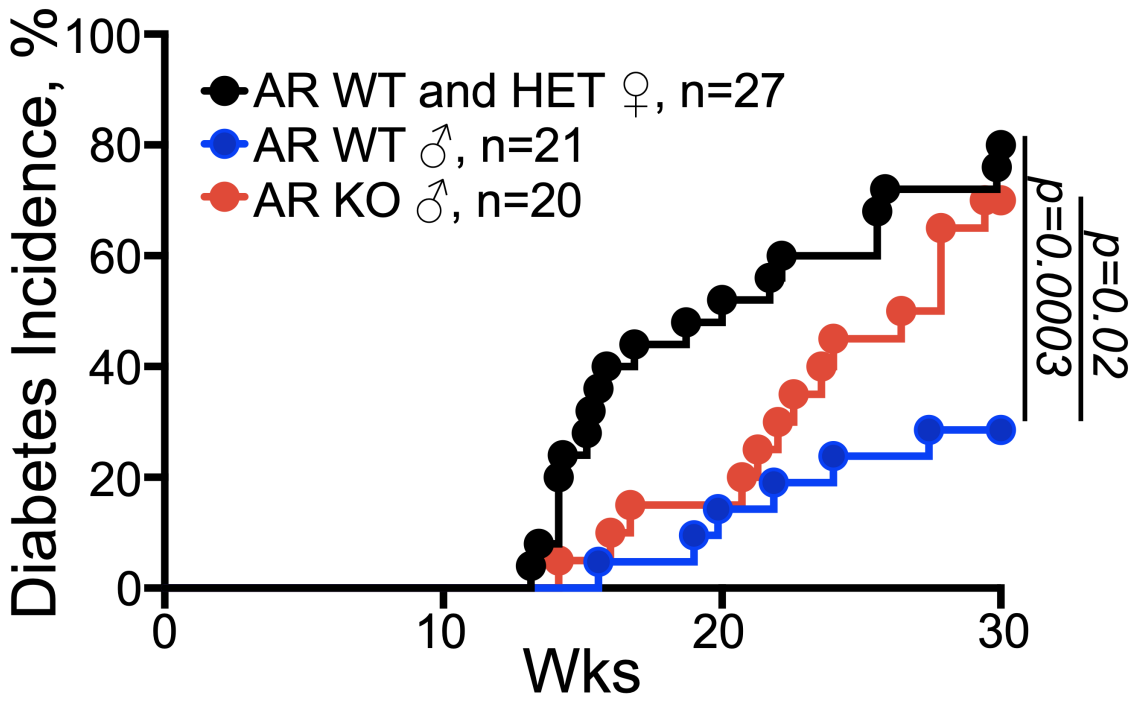

Figure 3.4: AR deficiency reverses protection from T1D in NOD males. T1D incidence in control females (NOD.ARWT and NOD.ARHET), control males (NOD.ARWT), and NOD.ARKO males. n=number of animals per group. p values were calculated using Mantel-Cox log-rank test.

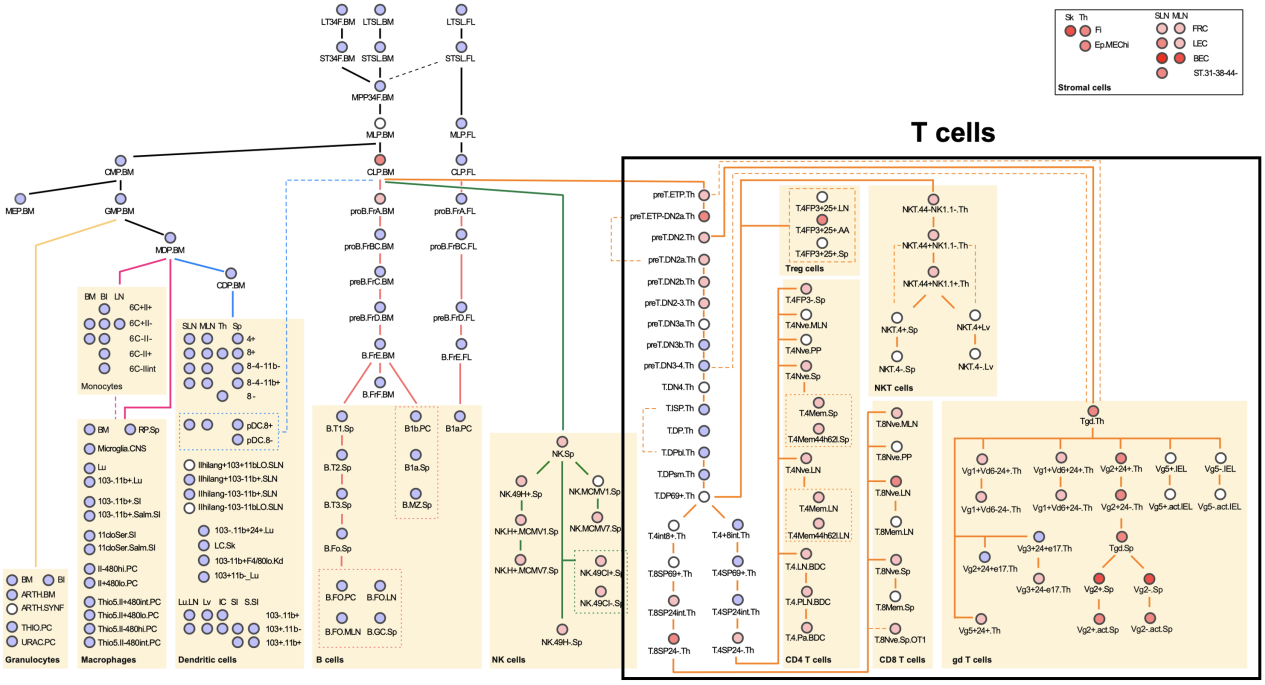

Figure 3.5: *Ar* expression in hematopoietic cells. Analysis of relative *Ar* expression in hematopoietic lineage cells using the ImmGen database. Blue—low expression, red—high expression.

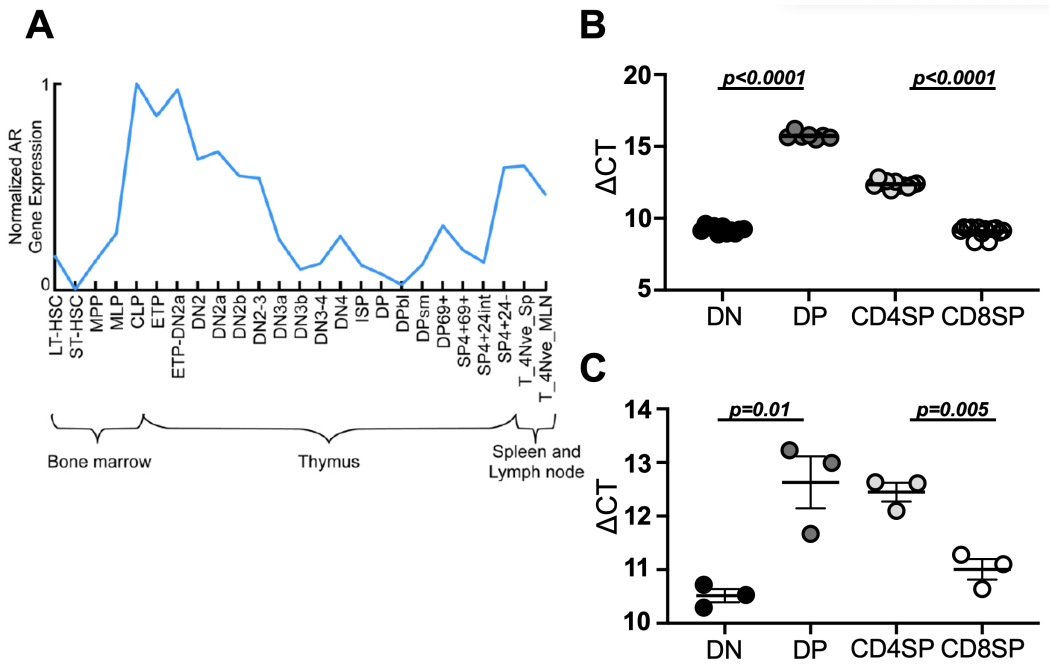

Figure 3.6: T cell-specific expression of nuclear androgen receptor *Ar*. **(A)** Dynamics of *Ar* gene expression during T cell differentiation; **(B-C)** RT-PCR quantification of *Ar* transcript levels in DN, DP, CD4SP, CD8SP thymocytes from 8-week-old B6 males **(B)** and NOD males **(C)**. Delta CT inversely correlates with the strength of expression. Symbols — individual mice. Mean± sem. Significance was calculated using an unpaired t-test.

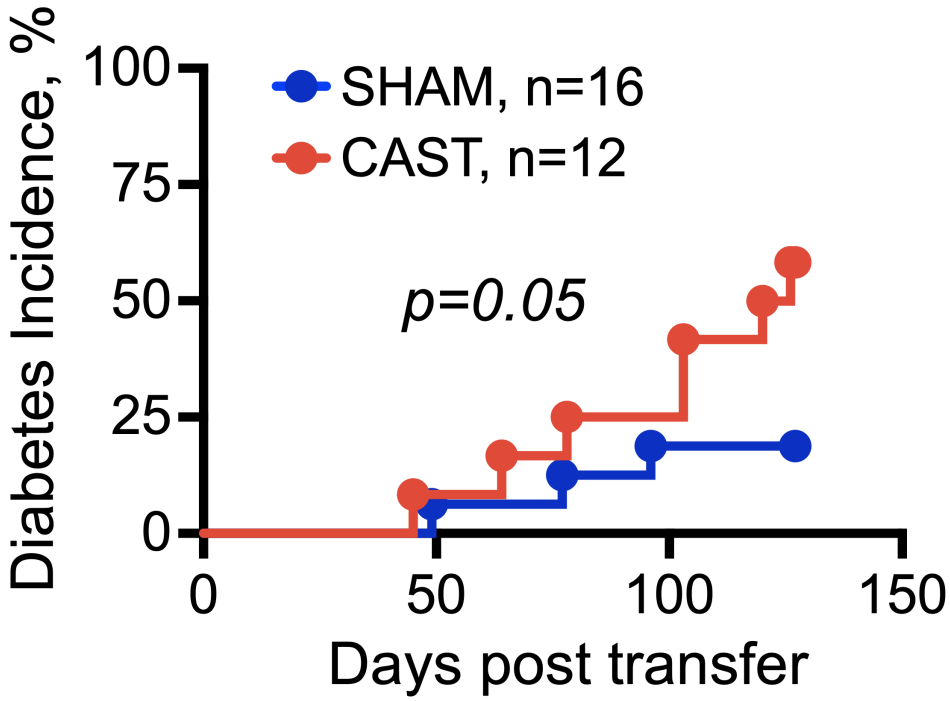

Figure 3.7: Androgens influence T cell autoreactivity. T1D incidence in male NOD.SCID recipients of T cells from sham-operated or castrated NOD donors. n=number of animals per group. p values were calculated using Mantel-Cox log-rank test.

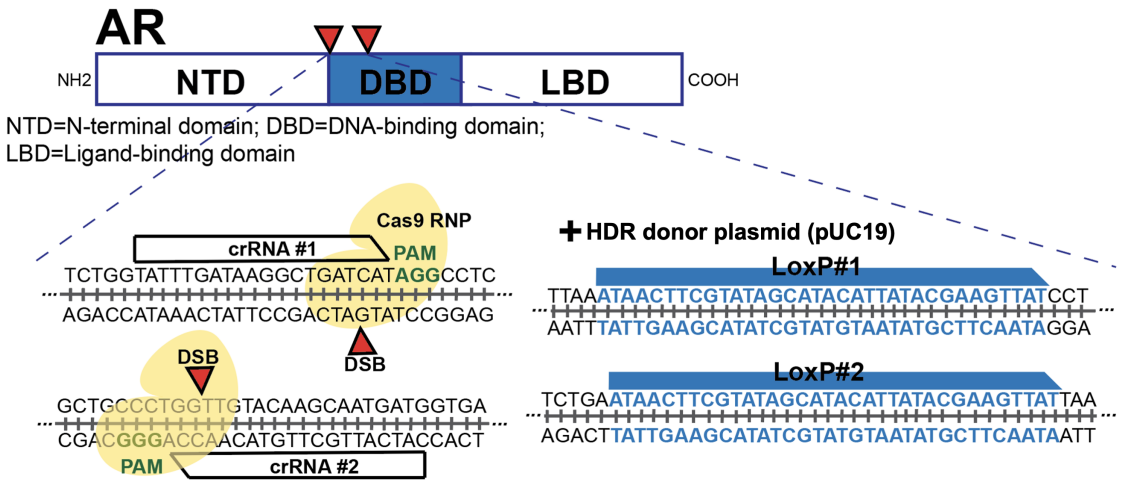

Figure 3.8: Generation of NOD.AR$^{f/y}$ mice using CRISPR/Cas9. Targeting strategy for generating NOD.AR$^{f/y}$ mice using CRISPR/Cas9.

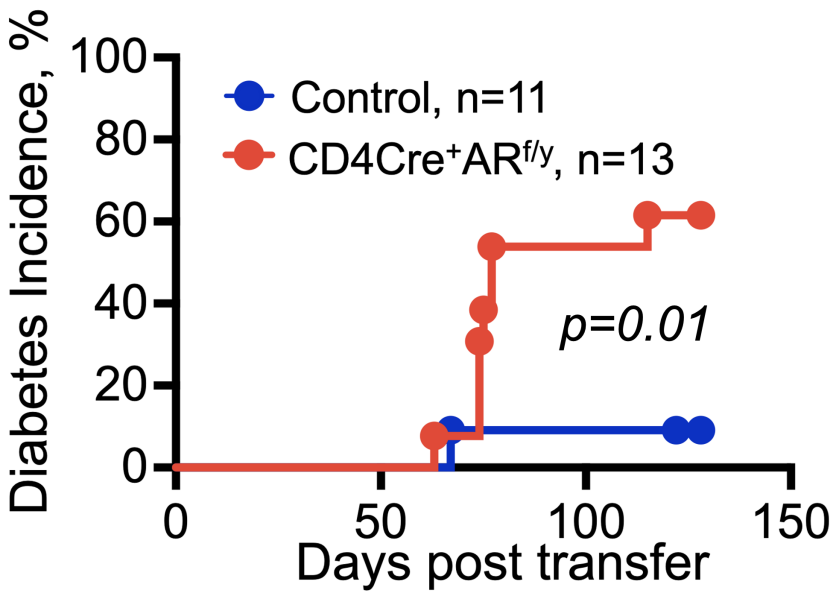

Figure 3.9: T cell-intrinsic AR signaling is sufficient to attenuate T cell autoreactivity. T1D incidence in male NOD.SCID recipients of T cells from control (NOD.AR$^{f/y}$ or NOD.CD4Cre^{+}) or NOD.AR$^{f/y}$CD4Cre^{+} donors. n=number of animals per group. p values were calculated using Mantel-Cox log-rank test.

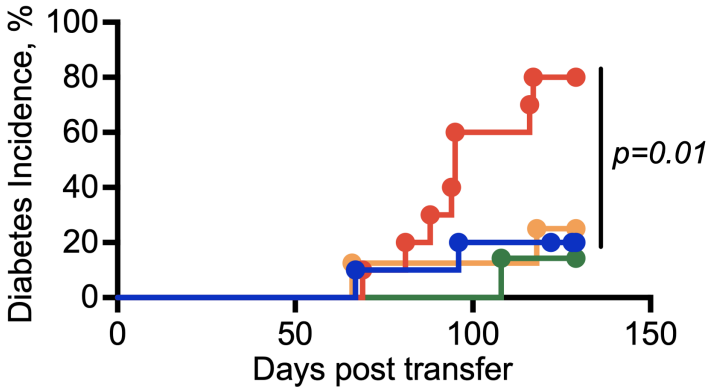

Donor cell combination	AR in CD4	AR in CD8	n
group 1	+	+	10
group 2	-	-	10
group 3	-	+	7
group 4	+	-	8

Figure 3.10: T cell-intrinsic AR signaling in either CD4$^+$ or CD8$^+$ T cells is sufficient to attenuate net T cell autoreactivity. T1D incidence in male NOD.SCID recipients of CD4$^+$ and CD8$^+$ T cell combination from control (NOD.AR$^{f/y}$ or NOD.CD4Cre$^+$) or NOD.AR$^{f/y}$CD4Cre$^+$ donors as indicated in the table. n=number of animals per group. p values were calculated using Mantel-Cox log-rank test.

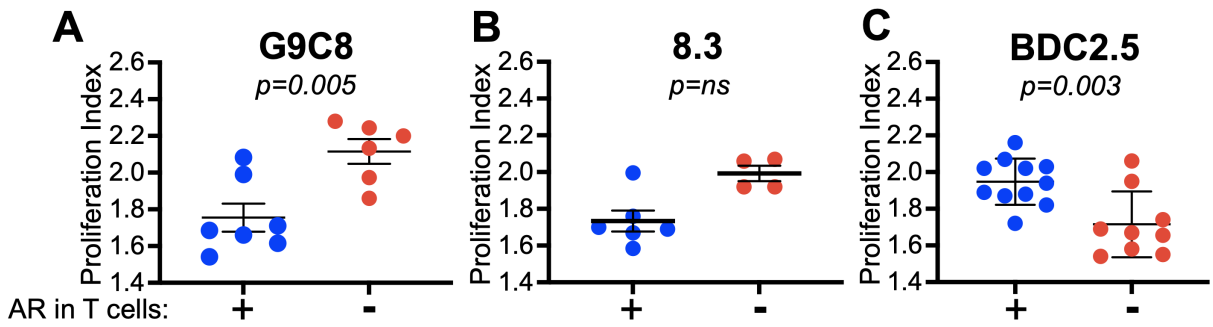

Figure 3.11: *In vitro* proliferation of T cells from TCR transgenic male NOD mice that are either wild-type or lack AR. *In vitro* proliferation of G9C8^{+}**(A)**, 8.3^{+}**(B)**, and BDC2.5^{+}**(C)** T cells labeled with CTV and stimulated with cognate peptides presented by irradiated splenocytes. Symbols — individual mice. p values were calculated using unpaired t-test.

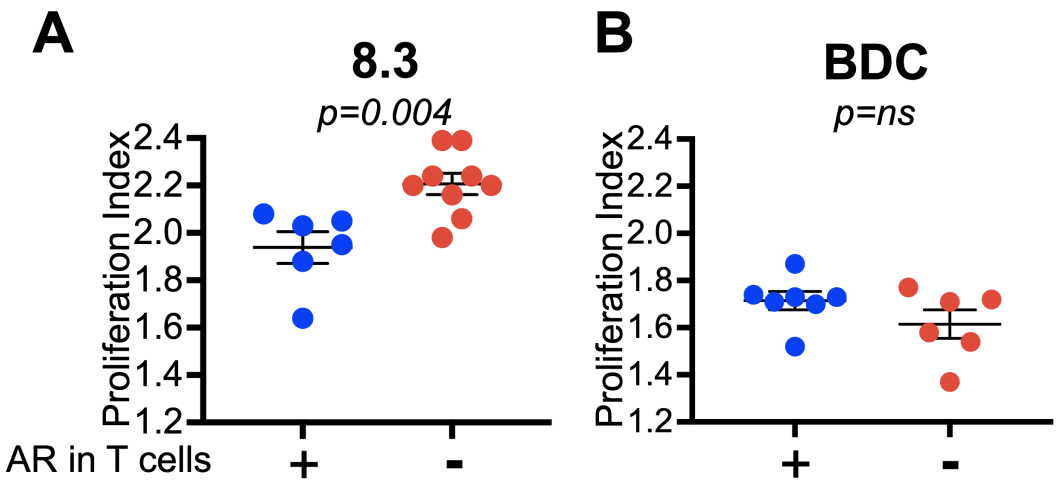

Figure 3.12: *In vivo* proliferation of T cells from TCR transgenic male NOD mice that are either wild-type or lack AR. *In vivo* proliferation of CTV labeled 8.3^{+}**(A)** or BDC2.5^{+}**(B)** T cells in PLNs after adoptive transfer into male NOD hosts. Symbols — individual mice. p values were calculated using unpaired t-test.

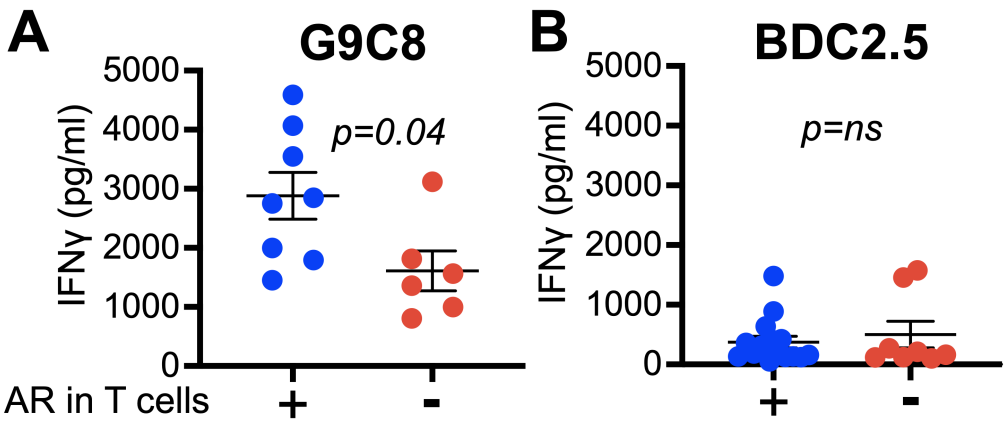

Figure 3.13: Measurement of antigen-specific IFNγ secretion by T cells. IFNγ secretion by G9C8$^+$ **(A)** or BDC2.5$^+$ **(B)** T cells following stimulation with the cognate peptide *in vitro*. Symbols — individual mice. p values were calculated using unpaired t-test.

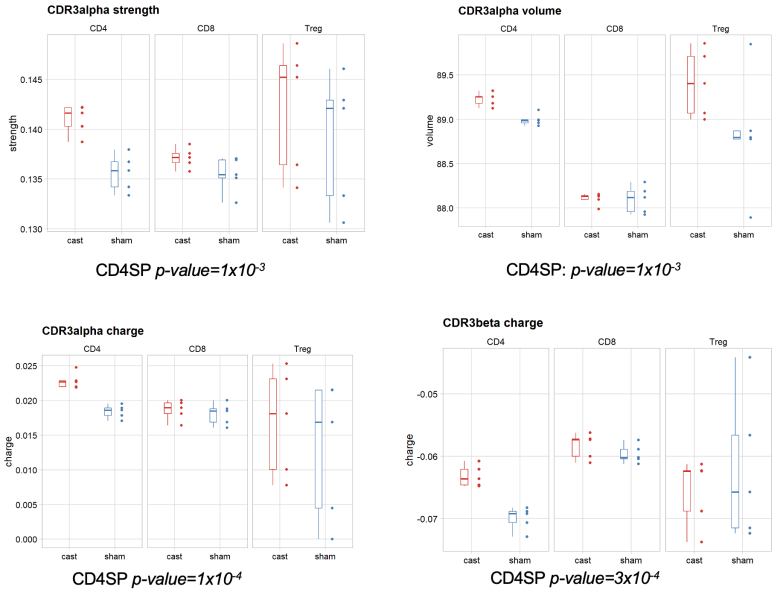

CD4 compartment:

Parameter	
CDR3α strength	CASTRATED > SHAM-OPERATED
CDR3α volume	CASTRATED > SHAM-OPERATED
CDR3α&β charge	CASTRATED > SHAM-OPERATED

Figure 3.14: Analysis of androgen-dependent TCRα and TCRβ CDR3 sequence characteristics in thymocytes of NOD mice. Comparison of TCRα and TCRβ CDR3 sequence characteristics from CD4SP, CD8SP, and Treg thymocytes isolated from the thymi of sham-operated or castrated NOD males. Significant differences for alpha and beta CDR3 regions are listed in the table. Symbols — individual mice. p values were calculated using unpaired t-test.

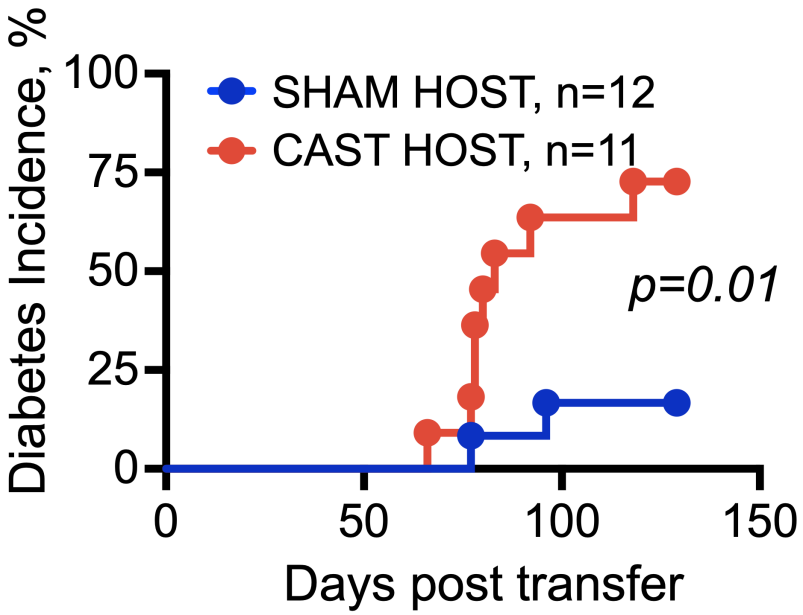

Figure 3.15: Androgens in T cell host influence T cell autoreactivity. T1D incidence in sham-operated or castrated male NOD.SCID recipients of T cells from NOD male donors. n=number of animals per group. p values were calculated using Mantel-Cox log-rank test.

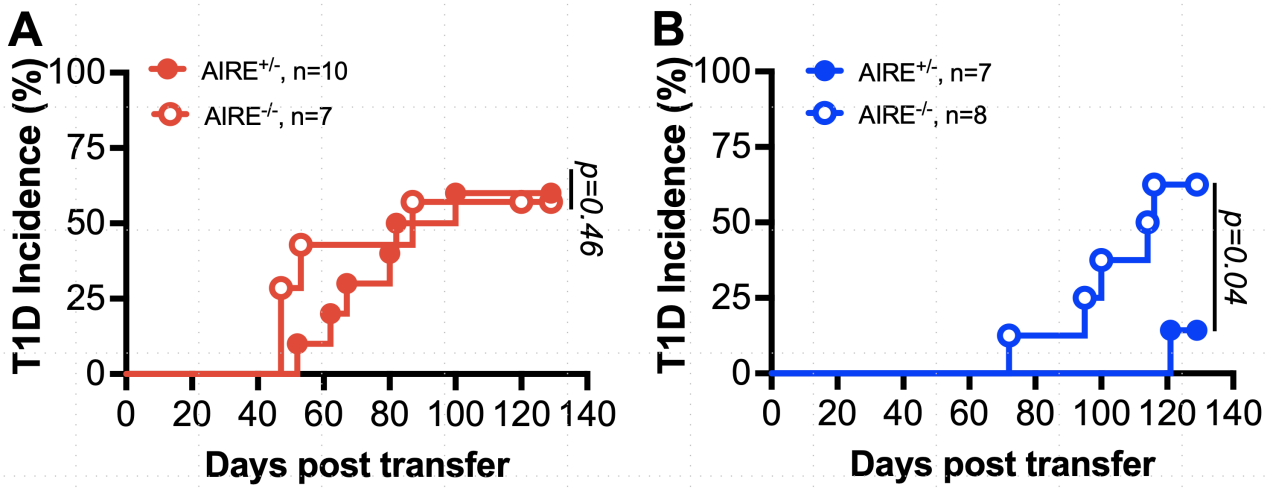

Figure 3.16: AIRE$^{-/-}$ enhances donor T cell autoreactivity in male-specific manner. T1D incidence in female **(A)** or male **(B)** NOD.SCID recipients of T cells from control (NOD.AIRE$^{+/-}$) or NOD.AIRE$^{-/-}$ donors. n=number of animals per group. p values were calculated using Mantel-Cox log-rank test.

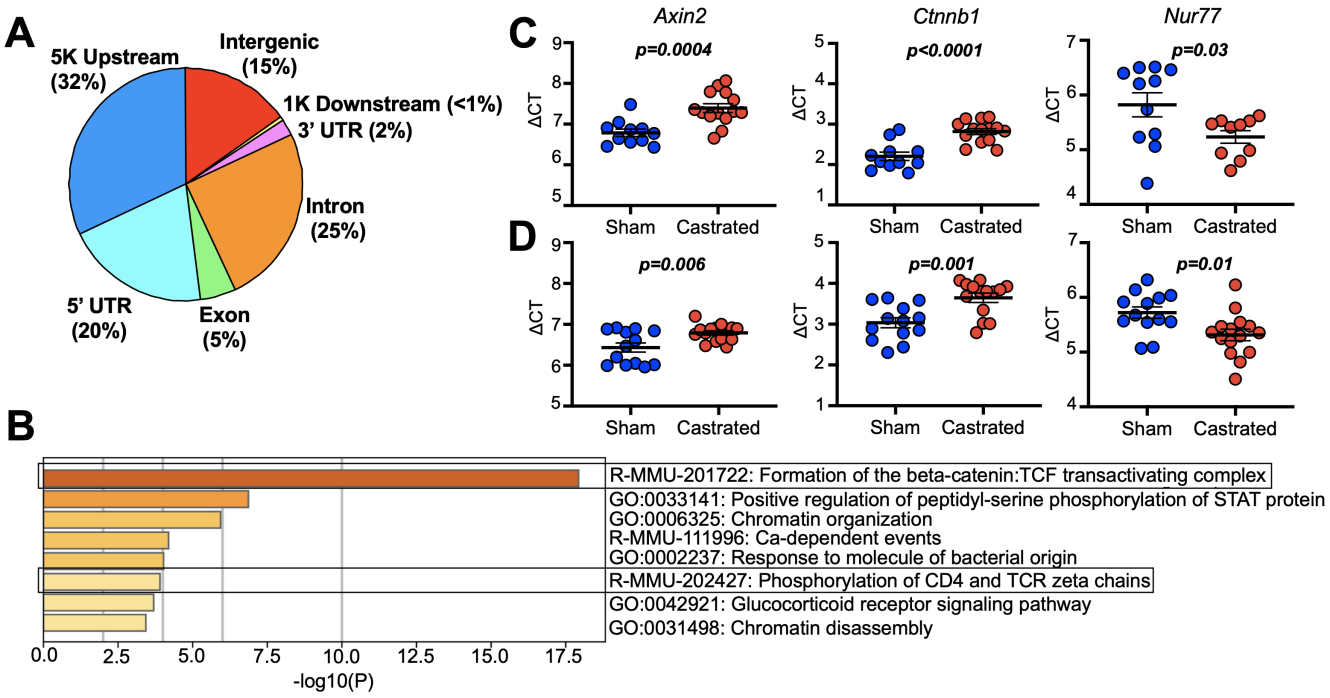

Figure 3.17: Identification of AR target genes and signaling pathways in the androgen-activated thymocytes. **(A)** Genome-wide distribution of AR binding sites identified by ChIP-seq analysis; **(B)** Top terms of Metascape gene set enrichment analysis of significantly ($p<0.05$) AR targeted genes; **(C, D)** RT-PCR quantification of genes regulated by beta-catenin in DN **(C)** and CD8SP **(D)** thymocytes from 8-week-old B6J males that were either sham-operated or castrated as 4-week-olds. Delta CT is shown, which is inversely correlated with the strength of expression. Symbols – individual mice. Mean±sem. Significance was calculated using an unpaired t-test.

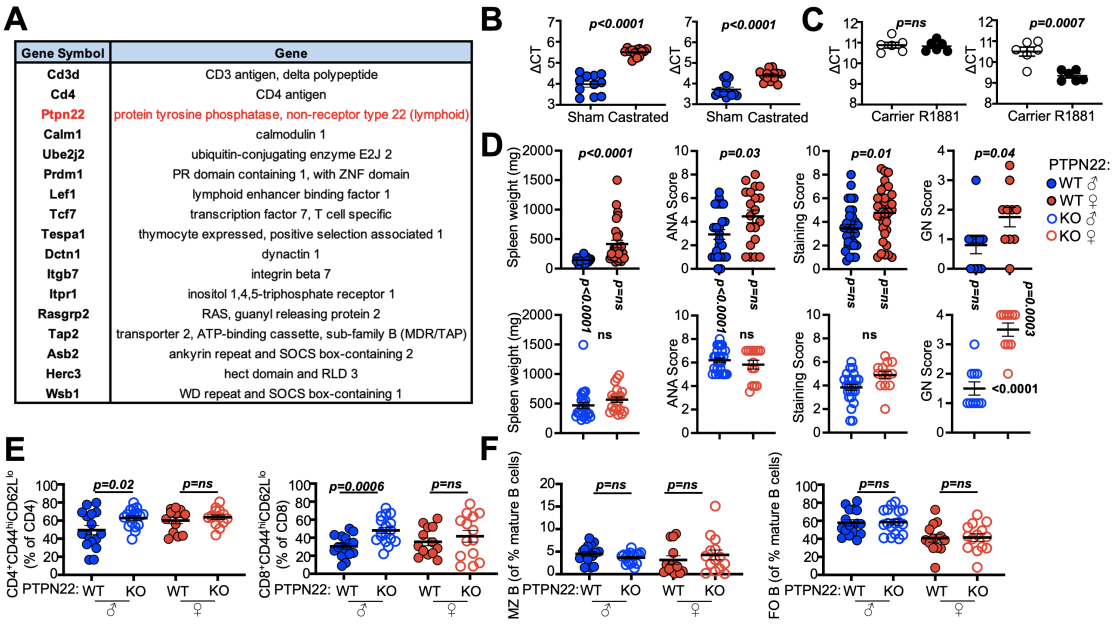

Figure 3.18: Androgen regulates *Ptpn22* in T cells. **(A)** A list of genes in the 'Phosphorylation of CD3 and TCR ζ chains' category from Metascape gene set enrichment analysis with *Ptpn22* highlighted in red; **(B)** RT-PCR quantification of *Ptpn22* transcript levels in DN (left) and CD8SP (right) thymocytes from 8-week-old B6J males that were subjected to sham-operation or castration as 4-week-olds; **(C)** RT-PCR quantification of *Ptpn22* transcript level in Jurkat T cells transduced with either an AR encoding plasmid (left) or an empty vector (right), and treated with R1881 (5nM) or carrier (0.1% EtOH) for 16h; **(D-F)** Pathophysiological parameters of SLE measured in 8-10-month-old B6.NZM wild-type and B6.NZM.PTPN22KO male and female mice. Spleen weights, anti-nuclear antibodies (ANA) scores measured by immunofluorescence of HEp-2 cells with sera diluted 1:100, complement C3 deposits measured in kidneys using immunofluorescence, and glomerulonephritis (GN) scores determined on Hematoxylin Eosin (HE) and periodic acid Schiff (PAS) stained kidneys by light microscopy determined at terminal observation point **(D)**. p values between males and females reflecting gender bias are shown horizontally, values estimating differences between wild-type and KO mice are shown vertically; FACS analyses performed on splenocytes measuring effector/effector memory T cells. Gating strategies are shown in **Fig3.20B**. Effector/effector memory $CD4^+$ (left) and $CD8^+$ (right) T cells were defined as $CD4^+CD44^{hi}CD62L^{lo}$ and $CD8^+CD44^{hi}CD62L^{lo}$, respectively. $CD4^+$ and $CD8^+$ T cell subsets are shown as percentage of the total $CD4^+$ and $CD8^+$ T cell populations, respectively. All samples were collected from 7 to 9-mo-old mice **(E)**; and FACS analyses performed on splenocytes measuring marginal zone B cells (MZ B) and follicular B cells (FO B). Gating strategies are shown in **Fig3.20C**. MZ B (left) and FO B (right) were defined as $CD93^-B220^+IgM^{hi}CD23^-CD21^+CD1d^+$ and $CD93^-B220^+IgM^{lo}CD23^+$, respectively. All B cell subsets are shown as percentage of the total $CD93^-B220^+$ B cell population. All samples were collected from 7 to 9-mo-old mice **(F)**. Symbols – individual mice. Mean±sem. Significance was calculated using an unpaired t-test.

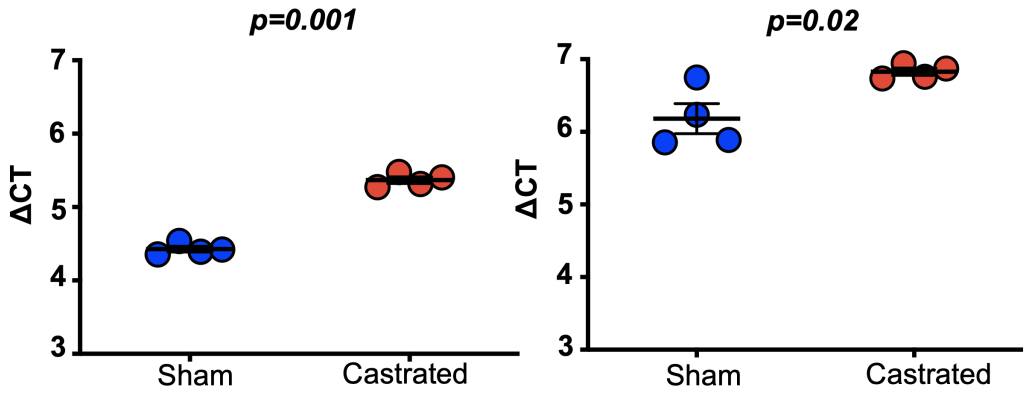

Figure 3.19: *Ptpn22* expression in thymocytes of sham-operated vs. castrated NOD mice. RT-PCR quantification of *Ptpn22* transcript levels in DN (left) and CD8SP (right) thymocytes from 8-week-old NOD males that were either sham-operated or castrated as 4-week-olds. Mean±sem. Significance was calculated using an unpaired t-test.

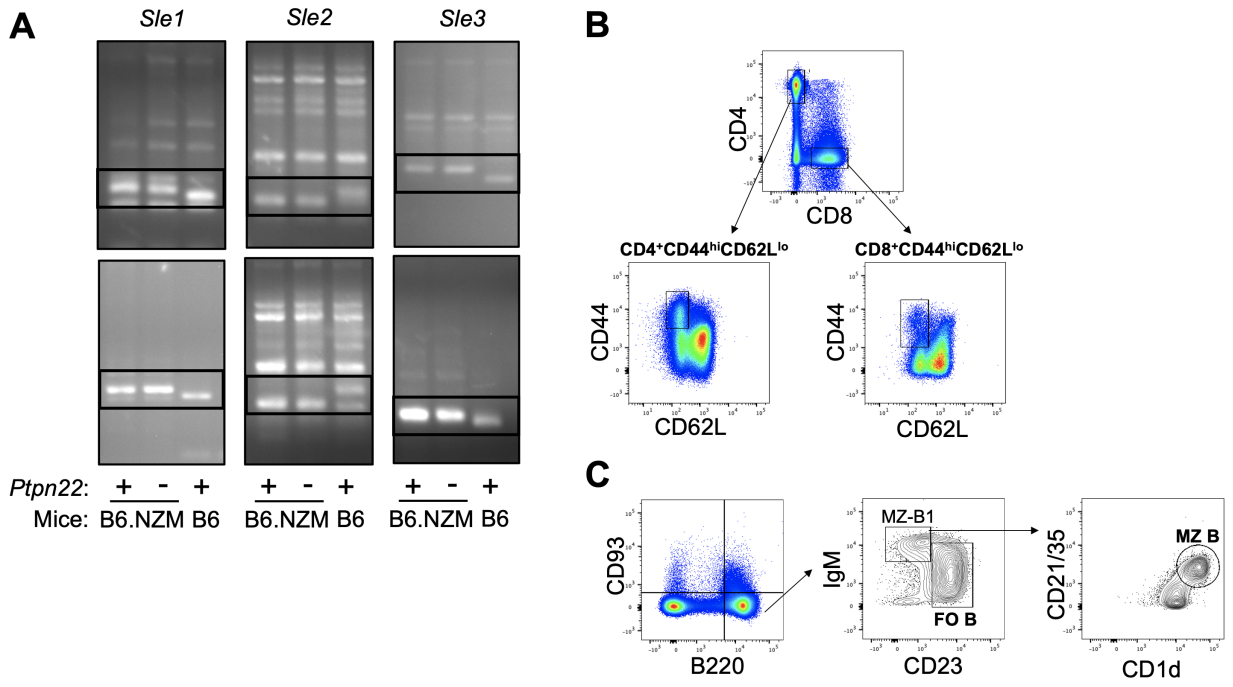

Figure 3.20: Generation of B6.NZM.PTPN22$^{-/-}$ mice and gating strategies for flow cytometric analysis of effector/effector memory T cell populations and B cell subpopulations. **(A)** Validation of the presence of *Sle1*, *Sle2*, *Sle3* in B6.NZM.PTPN22$^{-/-}$ mice. Proximal and distal regions of *Sle1*, *Sle2*, and *Sle3* loci were amplified via PCR and analyzed by gel electrophoresis. Specific PCR products are framed; **(B)** For analysis of CD4^{+} and CD8^{+} effector/effector memory T cell populations, red blood cell lysed, single cell suspensions of spleen or PLN were stained with mAbs specific for CD4, CD8a, CD44, CD62L, and Fc Block. Propidium iodide was used to discriminate dead cells. Shown are representative plots. Live and single lymphocytes were plotted as CD4 vs CD8 (top) to identify CD4^{+} and CD8^{+} T cells (PI^{-}CD4^{+}CD8^{-} or PI^{-}CD4^{-}CD8^{+}). CD4^{+} or CD8^{+} T cells were plotted as CD44 vs CD62L to identify effector/effector memory T cells (bottom; CD44^{hi}CD62L^{lo}); **(C)** For analysis of MZB and FO B cell populations, red blood cell lysed, single cell suspensions of spleen were stained with mAbs specific for CD93, B220, IgM, CD23, CD21/35, CD1d, and Fc Block. Propidium iodide was used to discriminate dead cells. Shown are representative plots. Live and single lymphocytes were plotted as CD93 vs B220 to identify CD93^{-}B220^{+} cells (PI^{-}CD93^{-}B220^{+}). CD93^{-}B220^{+} cells were plotted as IgM vs CD23 to identify follicular (FO) B cells (PI^{-}CD93^{-}B220^{+}IgM^{lo}CD23^{hi}) and MZ-B1 cells (PI^{-}CD93^{-}B220^{+}IgM^{hi}CD23^{lo}). MZ-B1 cells were plotted as CD21/35 vs CD1d to identify marginal zone (MZ) B cells (PI^{-}CD93^{-}B220^{+}IgM^{hi}CD23^{lo}CD21/35^{hi}CD1d^{hi}).

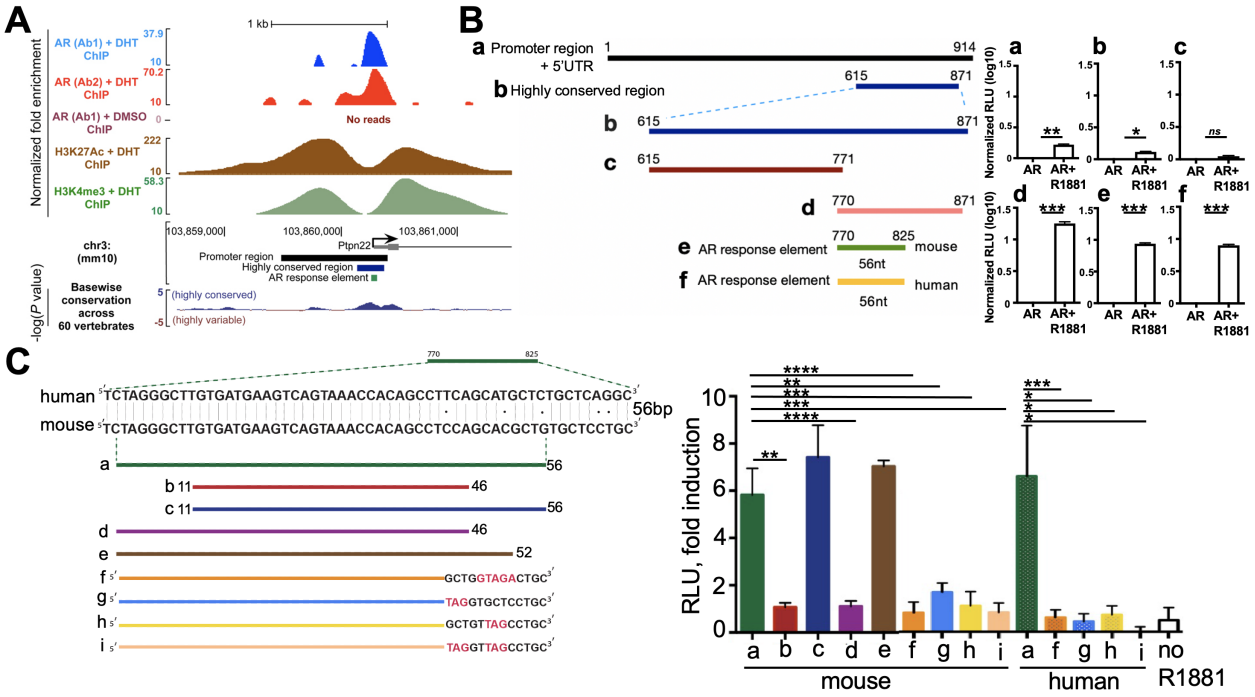

Figure 3.21: Characterization of *Androgen Response Element* (*ARE*) in the upstream regulatory region of *Ptpn22*. **(A)** Normalized fold enrichment of AR based on ChIP-seq experiment in the upstream regulatory region of *Ptpn22* (top) including the state of the chromatin and base-wise conservation across 60 vertebrate species; **(B)** Schematic diagram of regions tested for AR-mediated *Ptpn22* promoter activity, encompassing 1kb upstream regulatory site (left) and their respective *Ptpn22* promoter activity measured by luciferase (right); **(C)** Precise delineation of ARE within the conserved 56nt sequence. RLU - relative luciferase units. In all expression tests, HEK293T cells were transiently transfected with mouse or human, wild-type or mutant *Ptpn22* promoter-luciferase reporter plasmid pGL4.23 and pIRES2-zsGreen-1-AR in the presence or absence of 0.01uM R1881 for 48 h. pRL-CMV was used to control for transfection efficiency. Firefly luciferase levels were normalized to *Renilla* luciferase levels. Significance was calculated using an unpaired t-test.

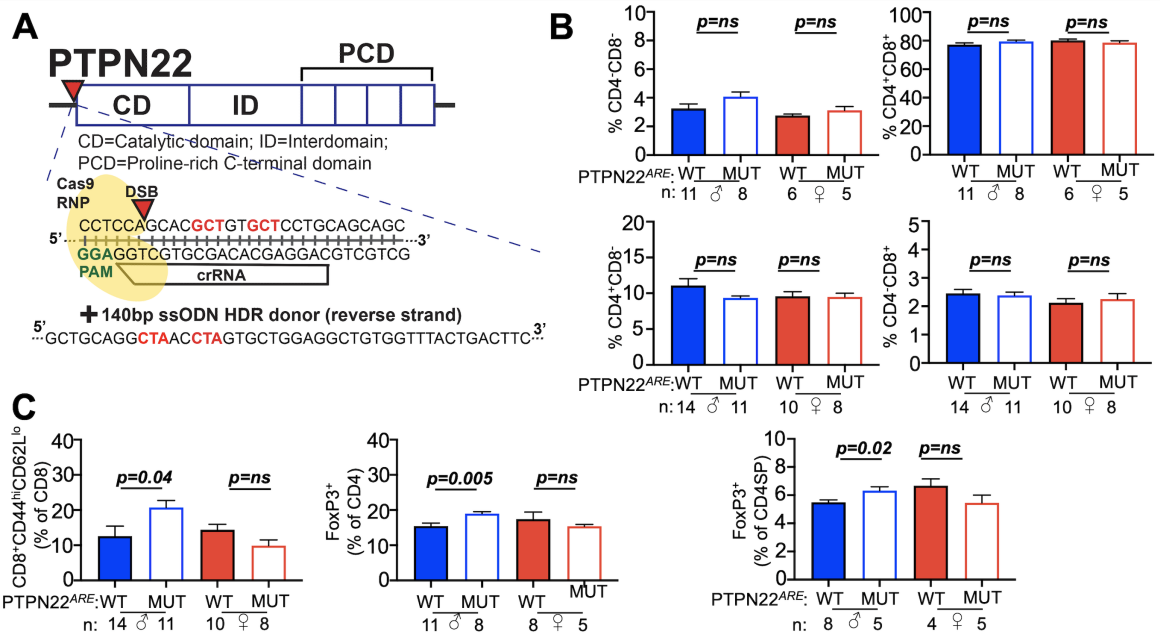

Figure 3.22: Generation of NOD.PTPN22^{AREmut} mice and flow cytometric characterization of thymic and peripheral T cell profiles. **(A)** CRISPR/Cas9 targeting strategy for generation of NOD.PTPN22^{AREmut} mice; **(B)** Frequencies of DN (CD4$^-$CD8$^-$), DP (CD4$^+$CD8$^+$), CD4SP (CD4$^+$CD8$^-$), and CD8SP (CD4$^-$CD8$^+$) thymocytes in PI$^-$Ter119$^-$CD19$^-$CD11c$^-$CD11b$^-$ cells of the thymi of 8-week-old NOD.PTPN22^{ARE} wild-type or mutant male and female mice. Mean±sem. Significance was calculated using an unpaired t-test; **(C)** Frequencies of CD8$^+$CD44^{hi}CD62L^{lo} T cells (left), and CD4$^+$FoxP3$^+$ T cells (right) in the spleen of 8-week-old NOD.PTPN22^{ARE} wild-type or mutant male and female mice. Gating strategies are shown in **Fig3.20B** and **Fig3.25**. Mean±sem. Significance was calculated using an unpaired t-test.

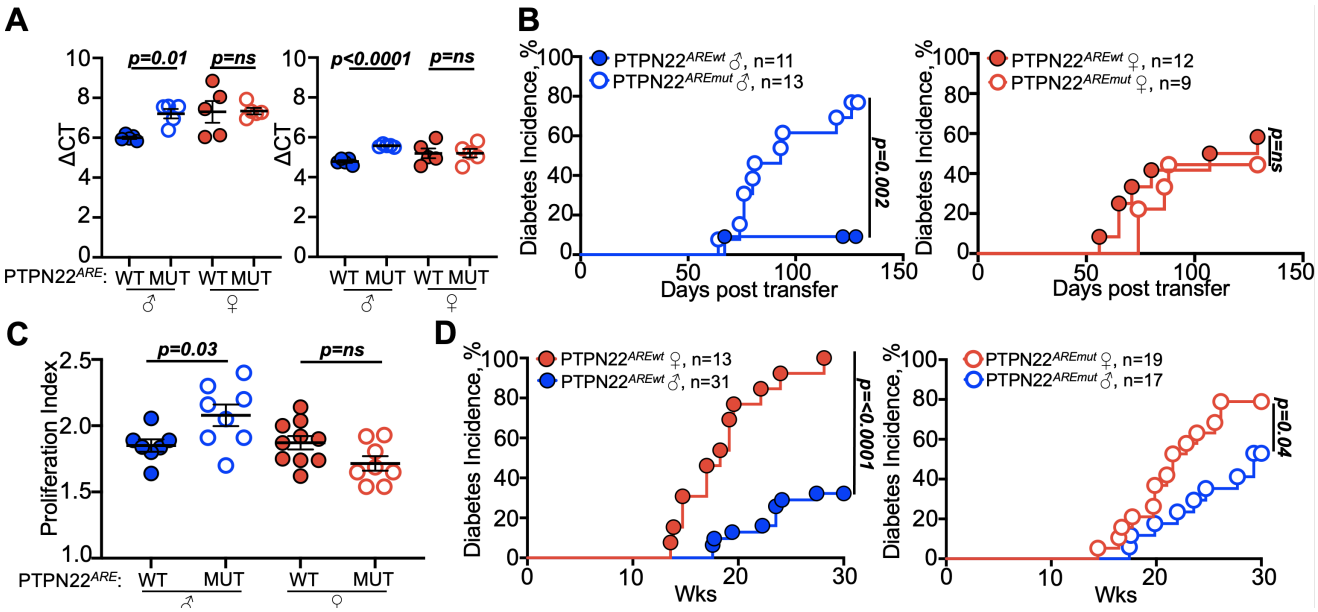

Figure 3.23: Disruption of the *ARE* motif in the 5'UTR of *Ptpn22* modulates T cell activity *in vivo*. **(A)** RT-PCR quantification of *Ptpn22* in CD4SP (left) and CD8SP (right) thymocytes from 8 to 9-week-old NOD.PTPN22^{ARE} wild-type and mutant males and females. Delta CT inversely correlates with the strength of expression. Symbols – individual mice. Mean±sem; **(B)** Cumulative T1D incidence in male (left) and female (right) NOD.SCID recipients of T cells from 8-week-old NOD.PTPN22^{ARE} wild-type or mutant male or female mice. Significance was calculated using log-rank Mantel-Cox test; **(C)** Proliferation of CTV-labeled G9C8 CD8^{+} T cells from 8-week-old NOD.PTPN22^{ARE} wild-type or mutant male or female mice in the PLNs of NOD male or female hosts 3 days post transfer. Significance was calculated using an unpaired t-test. Symbols – individual mice. Mean±sem; **(D)** Cumulative T1D incidence in PTPN22^{ARE} wild-type (left) or mutant (right) littermate males and females. Significance was calculated using log-rank Mantel-Cox test.

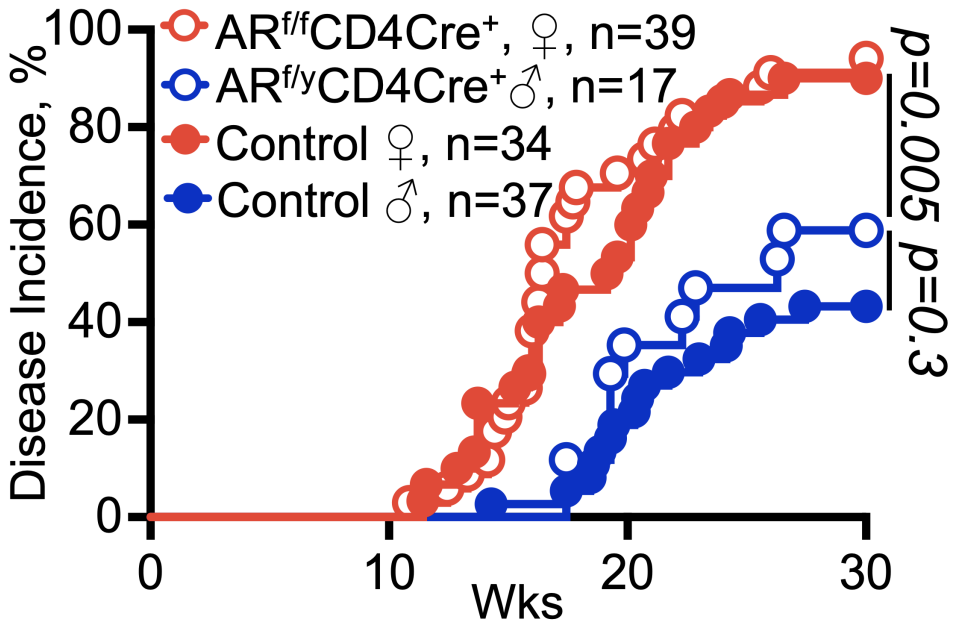

Figure 3.24: T cell intrinsic AR signaling is not sufficient for protection from T1D in NOD males. Cumulative T1D incidence in control (NOD.AR$^{f/y}$, NOD.AR$^{f/f}$, or CD4Cre^{+}) or NOD.AR$^{f/f}$CD4Cre^{+} females or NOD.AR$^{f/y}$CD4Cre^{+} males. n=number of animals per group. p values were calculated using Mantel-Cox log-rank test.

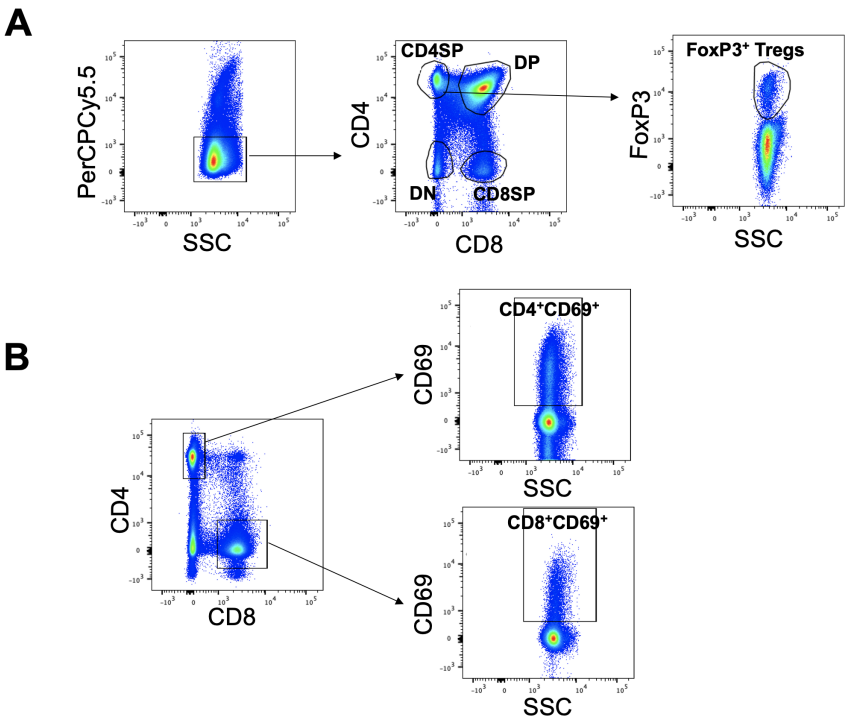

Figure 3.25: Gating strategies for flow cytometric analysis of thymic T cell subpopulations and peripheral CD69$^+$ CD4$^+$ and CD8$^+$ T cell frequencies. (A) For analysis of thymic T cell subpopulations, single cell suspensions of thymi were stained with mAb specific for CD4, CD8a, CD11a-biotin, CD11b-biotin, CD11c-biotin, CD19-biotin, Ter119-biotin, and Fc Block. Cells were subsequently stained with Streptavidin-PerCPCy5.5. Cells were fixed and stained with mAb specific for FoxP3 to identify Tregs. Zombie Aqua was used to discriminate dead cells. Shown are representative plots. Live and single lymphocytes were plotted as PerCPCy5.5 vs SSC to identify CD11a$^-$CD11b$^-$CD11c$^-$CD19$^-$Ter119$^-$ (PerCPCy5.5$^-$) cells. ZA$^-$CD11a$^-$CD11b$^-$CD11c$^-$CD19$^-$Ter119$^-$ cells were plotted as CD4 vs CD8 to identify DN (CD4$^-$CD8$^-$), DP (CD4$^+$CD8$^+$), CD4SP (CD4$^+$CD8$^-$), and CD8SP (CD4$^-$CD8$^+$) cells. CD4SP cells were plotted as FoxP3 vs SSC to identify FoxP3$^+$ Tregs; **(B)** For analysis of CD69$^+$ CD4$^+$ and CD8$^+$ T cells, single cell suspensions of PLN or red blood cell lysed spleen were stained with mAbs specific for CD4, CD8a, CD69, and Fc Block. Propidium iodide was used to discriminate dead cells. Shown are representative plots. Live and single lymphocytes were plotted as CD4 vs CD8 to identify CD4$^+$ and CD8$^+$ T cells (PI$^-$CD4$^+$CD8$^-$ or PI$^-$CD4$^-$CD8$^+$). CD4$^+$ or CD8$^+$ T cells were plotted as CD69 vs SSC to identify activated T cells (PI$^-$CD4$^+$CD69$^+$ or PI$^-$CD8$^+$CD69$^+$).

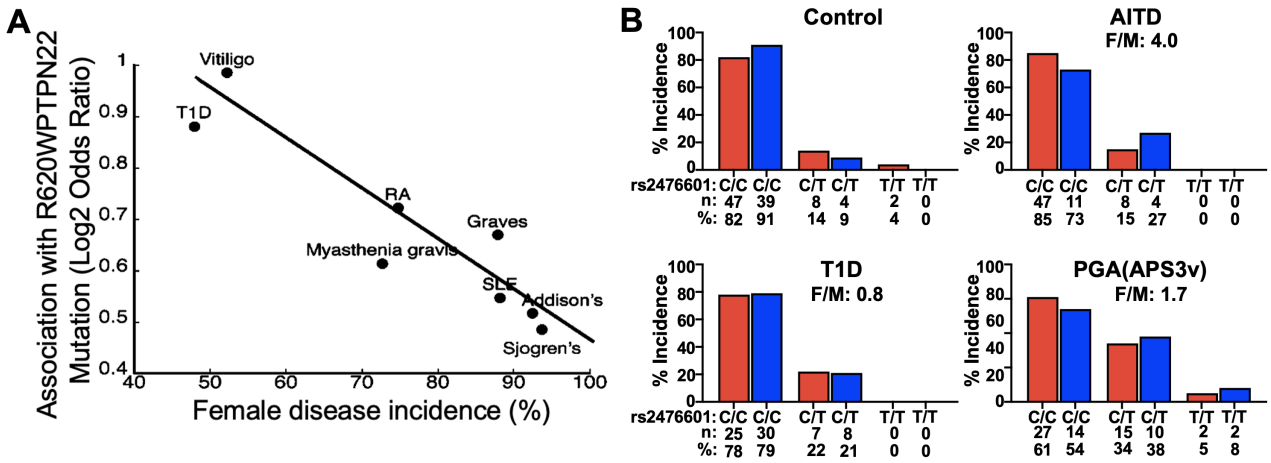

Figure 3.26: Contribution of the R620W (C1858T) mutation to human PTPN22 autoimmunity is independent of disease' gender bias. **(A)** Inverse correlation of the input of PTPN22 mutation associated with autoimmunity and the degree of sexual dimorphism in major human autoimmune diseases. Based on the compilation of published data; **(B)** Gender representation of C>T mutations in healthy individuals and patients with Autoimmune Thyroid Diseases (AITD), Type 1 Diabetes (T1D) and Polyglandular Autoimmunity (PGA) that manifests as both AITD and T1D in the same patients. Female to male patient ratio was 4.0 n AITG, 0.8 in T1D, and 1.7 in PGA.

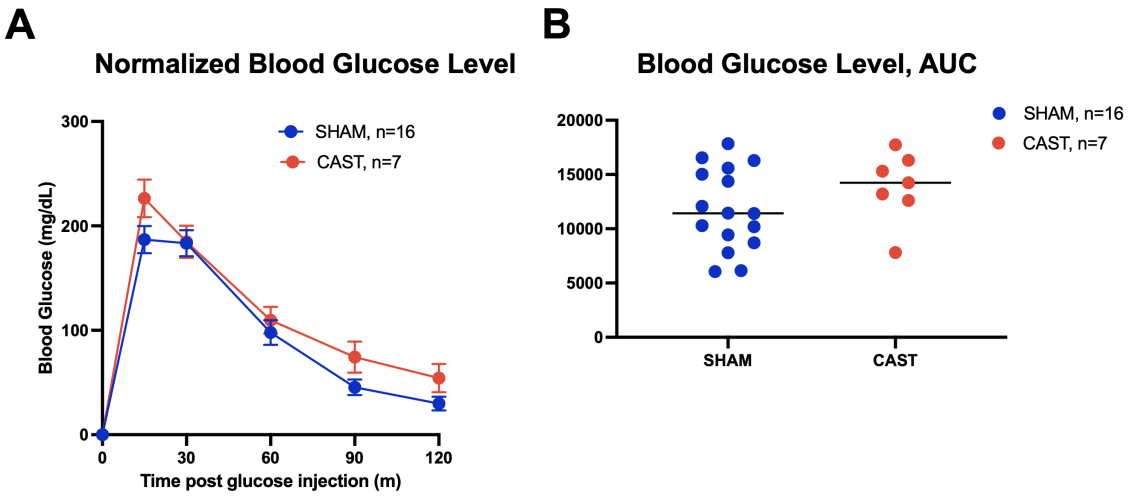

Figure 3.27: Glucose tolerance is not affected by androgens in NOD mice. (A) Intraperitoneal glucose tolerance test in 8-10 week-old NOD males that have undergone either sham-operation or castration at 4 weeks of age; **(B)** Analysis of area under the curve. n=number of animals per group.

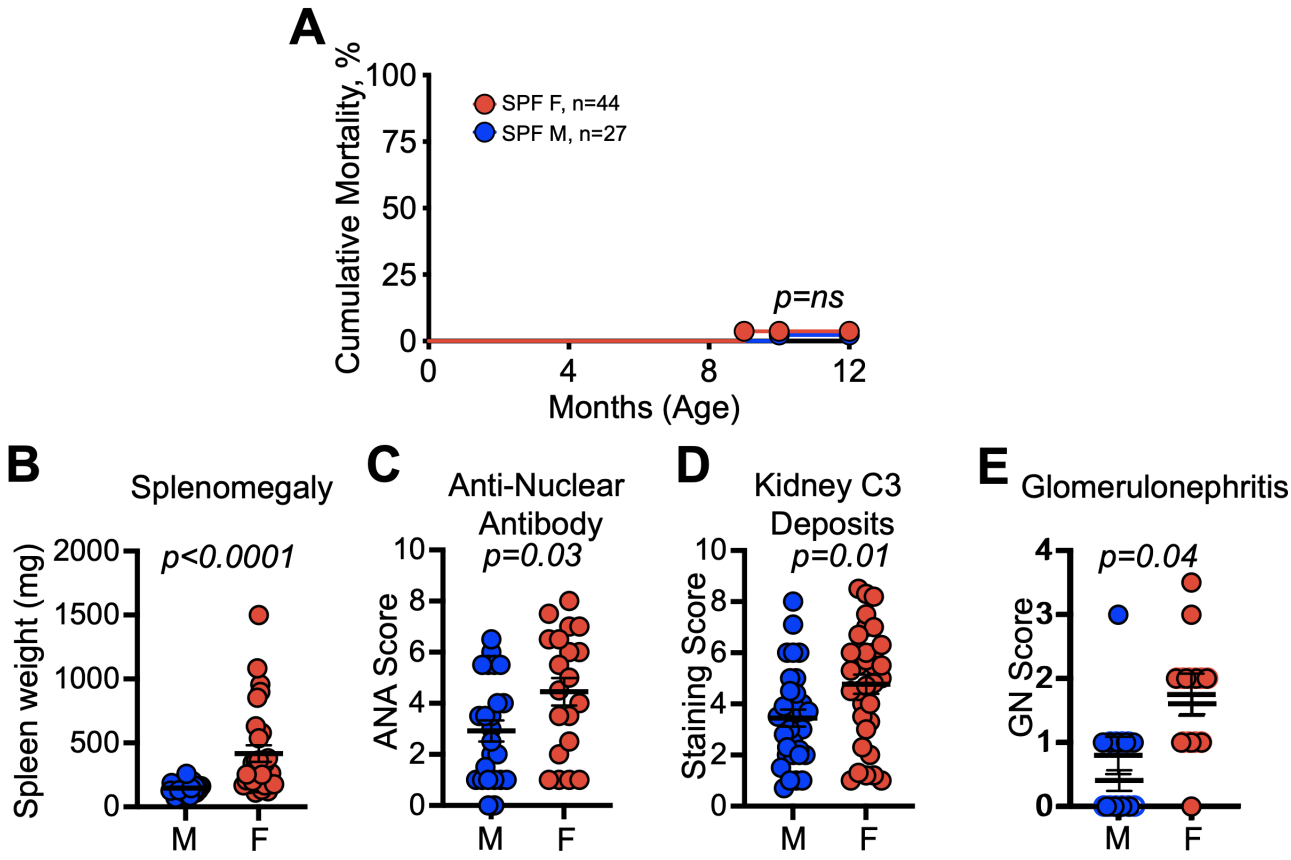

Figure 3.28: B6.NZM mice housed at U of C have gender bias but attenuated severity of SLE. **(A)** Cumulative mortality of B6.NZM mice over the course of 12-months. n=number of animals per group. Significance was calculated using log-rank Mantel-Cox test; **(B)** splenomegaly; **(C)** ANA scores measured by immunofluorescence of HEp-2 slides with sera diluted 1:100 **(D)** complement C3 deposits measured in kidneys using immunofluorescence; **(E)** GN scores. **(B-E)** Significance was calculated using an unpaired t-test. All parameters were measured with samples collected from 8- to 10-mo-old mice.

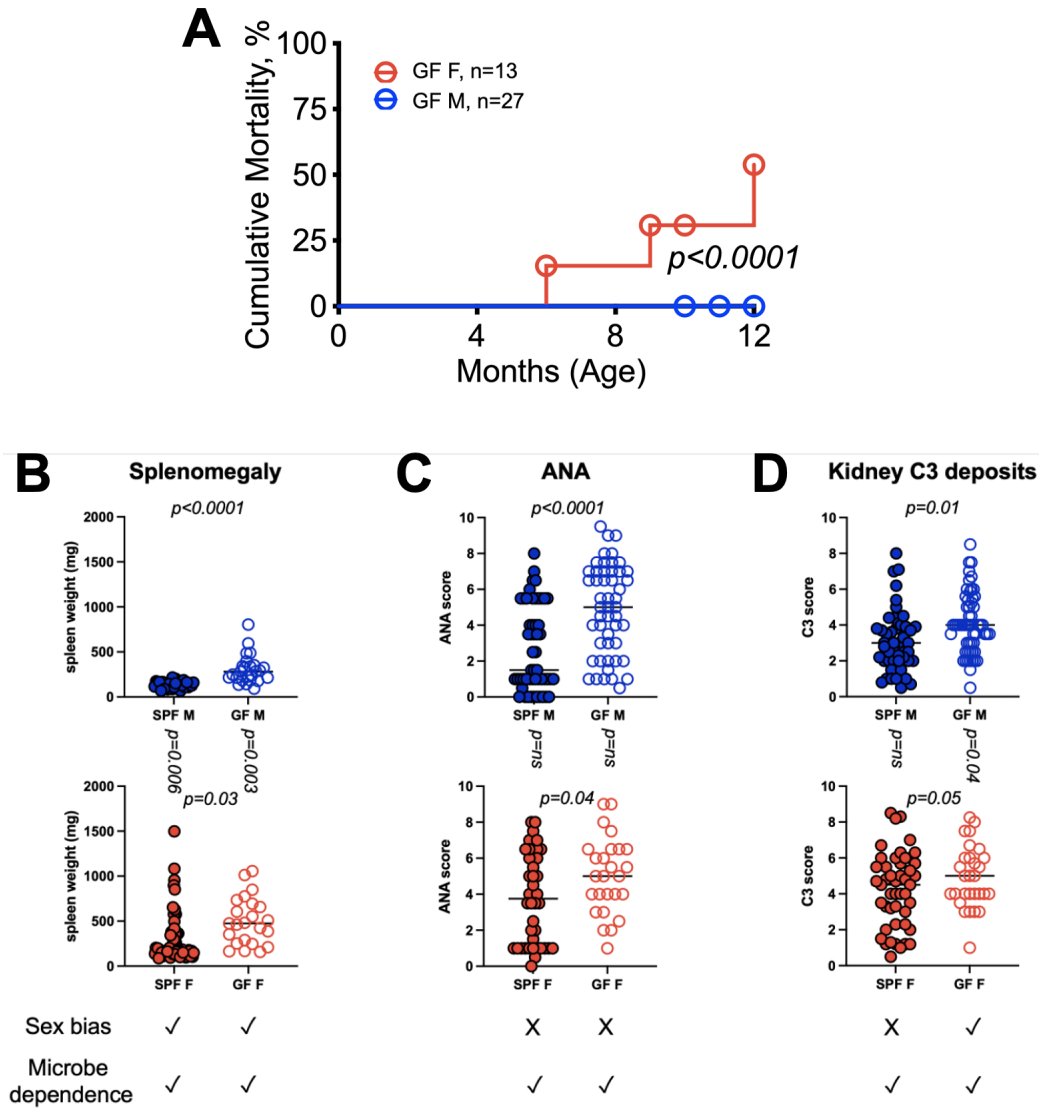

Figure 3.29: GF B6.NZM mice have moderate severity of SLE. **(A)** Cumulative mortality of GF B6.NZM mice over the course of 12-months. n=number of animals per group. Significance was calculated using log-rank Mantel-Cox test; **(B)** splenomegaly; **(C)** ANA scores measured by immunofluorescence of HEp-2 slides with sera diluted 1:100 **(D)** complement C3 deposits measured in kidneys using immunofluorescence. **(B-D)** Significance was calculated using an unpaired t-test. All parameters were measured with samples collected from 8- to 10-mo-old mice.

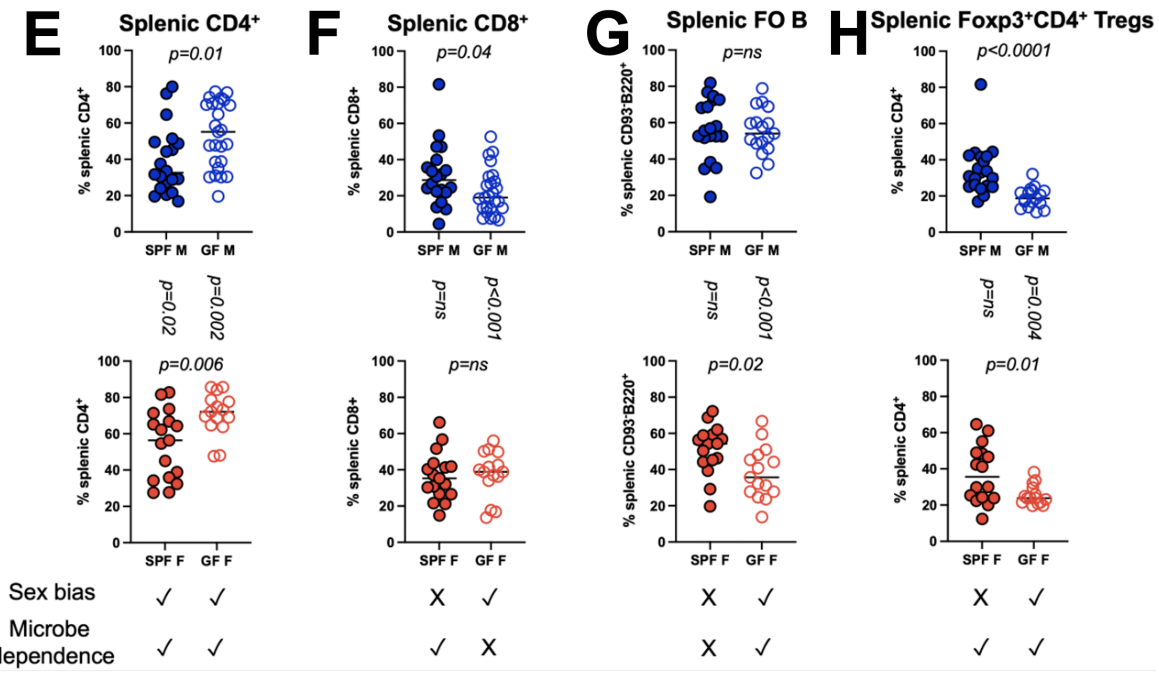

Figure 3.30: GF B6.NZM mice have moderate severity of SLE. (E-H) FACS analyses performed on splenocytes measuring populations indicated on the ordinates of the graphs. Follicular B cells (FO B) were defined as $CD93^{-}B220^{+}IgM^{lo}CD23^{+}$. Gating strategy is shown in **Figure 3.20**. FO B cells are shown as percentage of total $CD93^{-}B220^{+}$ B cell population. Regulatory T cells (Tregs) were defined as $Foxp3^{+}CD4^{+}$. Tregs are shown as percentage of total $CD4^{+}$ T cell population. **(E-H)** Significance was calculated using an unpaired t-test. All parameters were measured with samples collected from 8- to 10-mo-old mice.

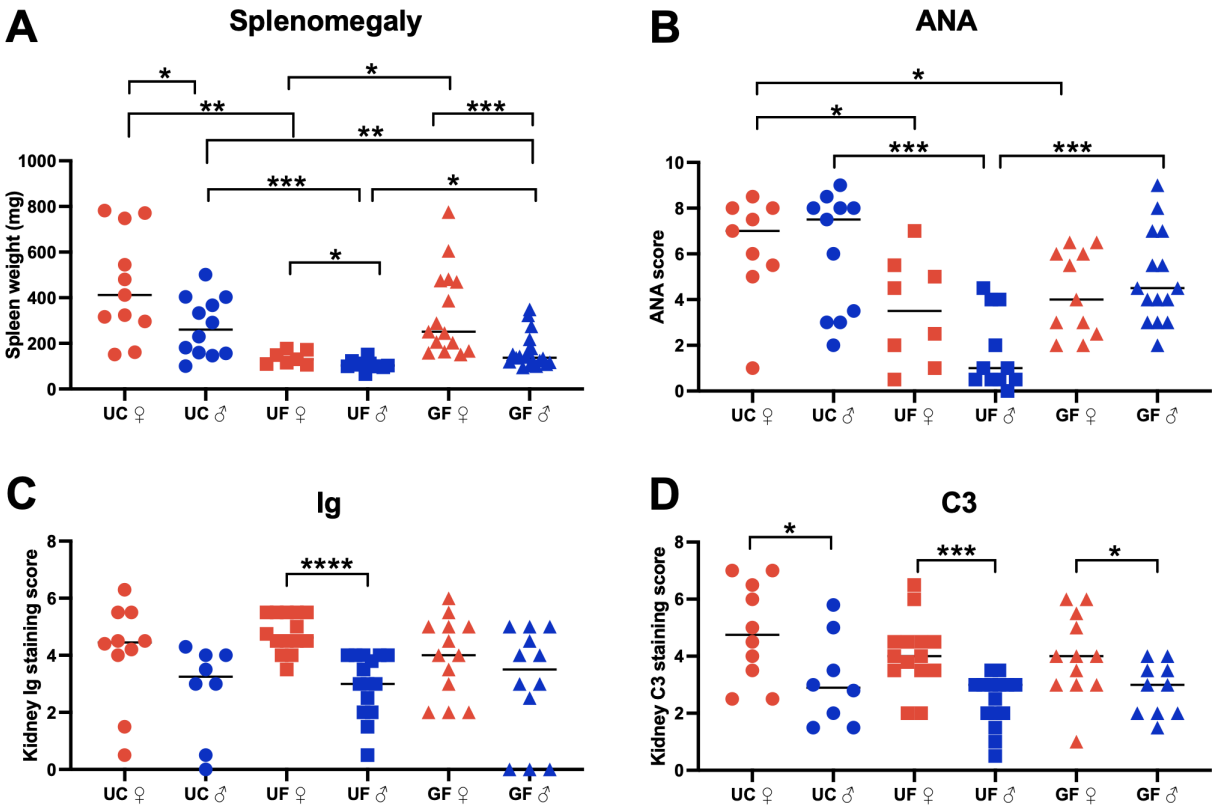

Figure 3.31: Severity of SLE in G_1 B6.NZM mice colonized with U of C or U of F microbiota. **(A)** splenomegaly; **(B)** ANA scores measured by immunofluorescence of HEp-2 slides with sera diluted 1:100; **(C)** Immunoglobulin G (IgG) deposits or **(D)** complement C3 deposits measured in kidneys using immunofluorescence. **(A-D)** Significance was calculated using an unpaired t-test. All parameters were measured with samples collected from 8- to 10-mo-old mice.

CHAPTER 4

DISCUSSION AND FUTURE DIRECTIONS

It has long been appreciated that androgens have a protective role against autoimmunity [16, 17], but the understanding of molecular and cellular mechanisms by which androgens establish protection against autoimmunity have not been fully understood. Our interest in uncovering the mechanisms by which androgens regulate autoimmunity was sparked by the finding that in NOD mice, gender bias of T1D is regulated both by hormonal and microbial signals [7]. Since *Ar* has a wide distribution pattern of expression across various tissues and cell types [26], we first needed to narrow down the cell type androgens target to mediate male protection from T1D in NOD males. Based on the computational analysis of ImmGen database and subsequent gene expression measurements for *Ar* both *in vitro* and *in vivo*, the highest expression level of *Ar* was found in the T cell compartment. T cells represented an interesting category of candidates considering that T1D is a chronic, T cell-mediated disorder. With our focus set on T cells, we uncovered through adoptive T cell transfer studies that T cell-intrinsic AR signaling alone is sufficient to dampen T cell autoreactivity.

Having established that T cell-intrinsic AR signaling has direct impact on modulating T cell autoreactivty, we investigated the downstream molecular consequences of T cell-intrinsic AR signaling that contribute to attenuated T cell autoreactivity. Using the well characterized diabetogenic TCR transgenic systems, we discovered that T cell-intrinsic AR signaling *in vivo* mediates increased IFNγ secretion despite decreased T cell proliferation following antigen-specific stimulation of peripheral $CD8^+$ T cells, but not so much peripheral $CD4^+$ T cells. While the finding that AR signaling has readily apparent phenotypes in $CD8^+$ T cells but not in $CD4^+$ T cells is consistent with our finding that $CD8^+$ T cells have higher *Ar* expression than $CD4^+$ T cells, we cannot exclude the possibility of different intrinsic signaling strength threshold for individual TCR [66–69] contributing to the discrepancies we observe between $BDC2.5^+$ $CD4^+$ T cell clones vs. $G9C8^+$ $CD8^+$ T cell clones. Whether

increased secretion of IFNγ by AR-sufficient CD8$^+$ T cells contribute to dampened T cell autoreactivity by acting as a proapoptotic signal in an autocrine manner is a subject for future investigation. To this end, G9C8$^+$ T cells from males will be treated with inhibitory IFNγ/IFNγR antibodies to measure the effect of IFNγ/IFNGγR signaling on T cell viability after stimulation with a cognate peptide. Alternatively, NOD.IFNGR$^{f/f}$ mice will be crossed to NOD.G9C8$^+$CD4Cre$^+$ to measure T cell viability following stimulation with a cognate peptide. To complement this data, NOD.IFNG$^{f/f}$ mice will be generated *via* CRISPR/Cas9 approach to perform the same experiment mentioned above. If AR signaling mediated induction of IFNγ secretion signals in an autocrine manner to curb T cell proliferation, we expect IFNγ/IFNγR-sufficient G9C8$^+$ T cells from males to have lower T cell viability than IFNγ/IFNγR-deficient G9C8$^+$ T cells from males.

To complement our finding that T cell-intrinsic AR signaling regulates peripheral T cell proliferation and IFNγ secretion following cognate antigen stimulation, we plan to further dissect the role of T cell intrinsic AR signaling mediated regulation of thymic T cell repertoire. To this end, TCRs of the thymocytes from NOD.AR$^{f/y}$CD4Cre$^+$ vs. control (NOD.AR$^{f/y}$) mice will be analyzed at a single cell level. In addition, thymocytes and peripheral T cells from the same groups of mice will be isolated for RNA sequencing to understand the influence of T cell-intrinsic AR signaling on T cell function and physiology.

Despite the sufficiency of T cell-intrinsic AR signaling in reducing T cell autoreactivity **(Figure 3.9)**, it alone was not sufficient to establish male protection from spontaneous T1D in NOD mice **(Figure 3.24)**. This is an important finding that warrants understanding the role of T cell-extrinsic AR signaling and AR signaling in non-T cells that contribute to protection from spontaneous T1D in NOD males. We have demonstrated that T cells transferred into AIRE$^{-/-}$ hosts become more autoreactive compared to T cells transferred into AIRE$^{+/-}$ hosts **(Figure 3.16)**. This data supports that AIRE expressing cells serve as one category of cells that participate in T cell-extrinsic AR signaling mediated regulation

of T cell autoreactivity. Three hypotheses can explain the data: i) AIRE^{+} mTECs in the thymus are subjecting recirculating peripheral T cells to another round of negative selection. In male hosts, androgen-AR signaling enhances AIRE expression on mTECs, and therefore, male AIRE$^{+/-}$ hosts have decreased T1D incidence compared to male AIRE$^{-/-}$ hosts. To address this hypothesis, an athymic mouse (NOD$^{nu/nu}$) on the NOD background could be generated with CRISPR/Cas9 and crossed to AIRE$^{-/-}$ allele to be used as hosts for T cell transfers. If athymic group of male AIRE$^{-/-}$ mice display the same degree of diabetogenicity as euthymic group of male AIRE$^{-/-}$ mice, we could conclude that AIRE in the periphery, rather than in the thymus, is controlling the autoreactivity of donor T cells; ii) AIRE^{+} eTACs in the periphery are acting on peripheral T cells to sequester autoreactive clones. In male hosts, androgen-AR signaling increases AIRE expression on eTACs and sequestration of autoreactive T cell clones that recognize self-peptides presented by eTACs in secondary lymphoid organs is one mechanism by which male AIRE$^{+/-}$ hosts are less autoreactive than AIRE$^{-/-}$ hosts. We hypothesize that if this hypothesis is true, an increased accumulation of T cells can be detected in the secondary lymphoid organs of male AIRE$^{+/-}$ hosts compared to those of male AIRE$^{-/-}$ hosts. Sequencing the TCRs of T cells accumulated in lymphoid organs will reveal whether autoreactive clones are preferentially building up in the secondary lymphoid organs, potentially due to AIRE^{+} eTACs; iii) AIRE influences autoreactivity of transferred T cells, but not through androgen-AR signaling mediated direct control of AIRE. The possibility of other sex-specific factors aside from androgen-AR signaling influencing AIRE to impact T cell autoreactivity remains open, and it can be addressed by generation of a mouse model on the NOD background that has a disruption of the *ARE* in the promoter of *Aire*. Given the broad expression pattern of AR, it is likely that AR signaling in non-T cells participate in establishing protection from T1D in NOD males. In support of this, we have shown that macrophages isolated from NOD males, in comparison to counterparts from NOD females or castrated males, can elicit increased levels of IFNγ

secretion from T cells [7]. Moreover, gene expression analysis revealed that genes implicated in monocyte-macrophage lineage may be regulated by androgens [7]. Lastly, T cells from donor males were more autoreactive following transfer into castrated NOD.SCID hosts than sham-operated hosts **(Figure 3.15)**. Therefore, we hypothesize that AR signaling in antigen-presenting cells (APCs) and/or cells of the islet serve as targets for AR signaling mediated protection from T1D. Because no gross difference in glucose clearance rate was detected in intraperitoneal glucose tolerance test (IPGTT) performed on castrated or sham-operated NOD.SCID mice **(Figure 3.27)**, we decided to start by formally testing the involvement of APCs as AR targets for protection from T1D in NOD mice. To this end, we generated mice deficient in AR signaling in either myeloid lineage cells or dendritic cells by using Lyz2Cre or CD11cCre allele, respectively, in the context of a floxed AR allele. We also generated double- (NOD.Lyz2Cre^{+}CD11cCre^{+}AR$^{f/y}$, and NOD.Lyz2Cre^{+}CD4Cre^{+}AR$^{f/y}$, and CD11cCre^{+}CD4Cre^{+}AR$^{f/y}$) or triple-Cre (NOD.Lyz2Cre^{+}CD11cCre^{+}CD4Cre^{+}AR$^{f/y}$) expressing lines of mice. Single-, double-, triple-Cre expressing mice are currently under observation for spontaneous T1D rates in order to understand the contribution of AR signaling in different cell types to protection from spontaneous T1D in NOD males. At the same time, T cells from male NOD donors are transferred into NOD.Lyz2Cre.AR$^{f/y}$.SCID, NOD.CD11cCre.AR$^{f/y}$.SCID, and NOD.Lyz2Cre.CD11cCre.AR$^{f/y}$.SCID hosts to test T cell-extrinsic AR signaling mediated regulation of T cell autoreactivity. It is possible that the range of cell types involved in AR signaling for establishing protection from T1D in NOD males could be broad. In order to delineate the types of cells that serve as AR targets for AR-mediated protection from T1D in NOD males, we plan to generate bone marrow chimera using the congenic NOD.CD45.2 (AR wild-type) mice and NOD.ARKO mice. We hypothesize that if AR signaling is important for protection from T1D in in only the hematopoietic compartment, T1D incidence will be high in AR wild-type hosts that receive ARKO bone marrow. In contrast, if AR signaling is critical only in the non-hematopoietic compartment,

ARKO hosts that receive AR wild-type bone marrow will display high diabetes incidence rate. Lastly, if both the hematopoietic and non-hematopoietic compartments are targets of AR signaling that contribute to male protection from T1D, neither of said hosts will develop high rates of diabetes.

To understand the gene regulatory network driven by AR, we focused on identifying AR binding sites in DN and CD8SP thymocytes, which had the highest expression of *Ar* within the T cell compartment **(Figure 3.6.A)**. Multiple binding sites mostly in the regulatory regions of genes **(Figure 3.17.A)** were found using two independent anti-AR antibodies in the ChIP-seq assay. Computational analysis of this gene cohort put them in multiple categories including genes involved in β-catenin signaling and regulation of the TCR signaling. We focused on the second category for the reasons of it being well-studied and of a likely importance for selection of autoreactive T cells. Among the top hits in this category, *Ptpn22* phosphatase (a.k.a. EST domain–enriched tyrosine phosphatase, or Lymphocyte Phosphatase, LYP, in humans) stood as a known negative regulator of TCR activation (Bottini and Peterson, 2014; Stanford and Bottini, 2014) and associated with multiple autoimmune disorders [70]. Notably, GWAS studies identified mutant (R620W [rs2476601, C1858T]) PTPN22 as a risk factor for RA, T1D, and SLE [52–54]. Moreover, manipulation of *Ptpn22* resulted in modulation of autoimmunity in several mouse models [71–73]. To assess the role of *Ptpn22* in the sexual dimorphism of autoimmunity, we first utilized a model of SLE, B6.NZM mice. Some of the manifestations of SLE were found to be sexually dimorphic: splenomegaly, secretion of ANA, C3 deposition in the kidney glomeruli and expansion of activated T cells with effector/effector memory phenotype were stronger in females and were enhanced in B6.NZM.PTPN22KO males. The importance of *Ptpn22* was previously tested in BXSB/Yaa model of lupus [72], where it was found not to have an effect in male mice. However, in this model, males suffer a very severe disease driven by Toll-like receptor 7 gene duplication and an additional increase in severity is hardly possible to detect. Other

parameters, such as proportion of marginal zone and follicular B cells were not affected by *Ptpn22* deficiency. Although *Ptpn22* has been implicated in regulating BCR signaling and B cell tolerance [74, 75], these effects could be secondary to perturbations to T cell signaling caused by *Ptpn22* deficiency [57, 76]. B cells seem to have low AR expression **(Figure 3.5)**. Thus, even if *Ptpn22* signaling has a B cell-intrinsic role, it may not be sensitive to regulation by sex hormones.

The possibility of *Ptpn22* regulation by sex hormones became rather attractive and led to the search for AR binding site in *Ptpn22* regulatory elements **(Figure 3.21)**. Luciferase expression driven by bits of 1.5Kb region upstream of translation start was measured in the presence of AR and the AR agonist. We found a 56bp sequence within 5'UTR of *Ptpn22* gene to contain the stimulatory activity. Interestingly, this region was highly conserved within about 60 mammalian species and was subsequently narrowed down to an octamer sequence of GCTnnGCT. This sequence was different from the consensus *ARE* sequence identified by studies of prostate cancer in humans [77, 78]. However, *ARE* of multiple genes in multiple tissues have quite variable sequences [79, 80]. Localization of *ARE* to the 5'UTR of the gene is also quite common [81, 82], including AR itself [83]. Notably, the short 56nt sequence containing the GCTnnGCT octamer stimulated much higher luciferase expression by itself compared to being a part of a longer sequence **(Figure 3.21.B)** pointing at a presence of a currently undefined negative regulatory sequence upstream of it.

The functional significance of the novel *ARE* motif was subsequently validated *in vivo* **(Figures 3.23.B and 3.23.C)**. The primary concern was that *ARE* manipulation could affect the overall gene expression regardless of androgen presence. That was not the case because the lower expression of *Ptpn22* was only detected in mutant male but not female thymocytes **(Figure 3.23.A)**. Although the effect of *ARE* mutation potentially could be observed in multiple cell types where *Ptpn22* is normally expressed, T cell intrinsic effect was obvious: T cells from mutant male mice induced T1D efficiently in NOD.SCID recipient

males **(Figure 3.23.B)**, whereas transfer of T1D by T cells from mutant females was not different from transfer efficiency of the wild-type female T cells. Proliferation of $CD8^+$ T cells from G9C8 TCR transgenic NOD mouse strain *in vitro* in response to their cognate peptide was stronger for mutant male, but not female cells **(Figure 3.23.C)**. This observation is important because it argues that androgens make a lasting imprint on T cells during development and the presence of the hormone during activation is no longer required.

We then tested the input of $PTPN22^{AREmut}$ in development of the disease itself. Female NOD.$PTPN22^{AREmut}$ females showed a slight decrease in T1D incidence compared to wild-type females, but still had pretty high levels of it (about 75% at 30 weeks of age). That is what females in our facility usually demonstrate [7]. NOD.$PTPN22^{AREmut}$ males displayed a trend for increased T1D susceptibility compared to wild-type littermate male controls. However, the hazard ratios of overall female to male incidence were 8.83 in control vs. 2.32 in mutants. In NOD.$PTPN22^{-/-}$ mice [84], females were reported to have a significant increase in overall incidence, whereas males were not significantly affected. That brings us back to the point that the gender bias of T1D in NOD mice is highly dependent on the qualities of the microbiota [7]. The powerful anti-diabetic influence of the commensals could be comparable to or stronger than the input of *Ptpn22* loss.

On the other hand, reduction of *Ptpn22* expression in mutant males led to an increase of the proportion of $CD4^+FoxP3^+$ Treg cells **(Figure 3.22.B)**. It is important to consider that several research groups have reported conflicting data for the consequence of PTPN22 modulation in mouse models of autoimmunity in which both the removal and overexpression of PTPN22 led to a reduced susceptibility to autoimmunity [71, 73, 85, 86]. In the study by Brownlie Rebecca et al., the authors reported that $PTPN22^{-/-}$ effector ($CD4^+CD45RB^{hi}$) T cells, compared to PTPN22 wild-type effector T cells, induced more severe colitis in B6 mice [85]. However, co-transfer of $PTPN22^{-/-}$ Tregs, but not PTPN22 wild-type Tregs, was able to significantly ameliorate colitis. Their subsequent analyses on Treg function revealed that

while removal of PTPN22 affects both the effector and regulatory T cell compartments, the intrinsic enhancement of Treg suppression outweighs the elevated function of effector T cells that result from the loss of PTPN22 [85]. This finding indicates that different T cell subsets, which rely on a spectrum of TCR signaling threshold, have varying degree of dependency on regulation by PTPN22 signaling. In support of these findings, Maine et al. reported that PTPN22 deficiency confers protection from EAE in B6 mice [71]. This protection was in part due to an expanded Treg compartment because removal of $CD25^{+}$ T cell fraction rendered $PTPN22^{-/-}$ mice equally susceptible to EAE as PTPN22 wild-type mice [71]. Zheng and Kissler investigated the role of PTPN22 in NOD mice using doxycycline inducible RNAi approach [73]. PTPN22 silencing starting either at birth or 8 week of age (post-puberty) led to an expansion of only peripheral, but not thymic, Treg compartment. This effect seemed to be localized to the periphery as thymic Treg population was unaffected regardless of the timing of silencing. In contrast, the expansion of $CD4^{+}$ effector T cells ($CD44^{hi}CD62L^{lo}$) was sensitive to the timing of PTPN22 silencing, where PTPN22 silencing seemed to matter more during early developmental stages at birth compared to starting at 6 week of age [73]. This brings up an important point that PTPN22 in developing T cells may have lasting impact on T cell function in the periphery. Interestingly, this model revealed that between the 2 silencing shRNAs (P2 and P4) used in the studies, only the one with more potent silencing (P2) at the level of protein led to a decreased overall T1D incidence. Importantly, both groups of mice targeted either with P2 or P4 shRNAs shared the expansion of Treg and $CD4^{+}$ effector T cell compartments. This alludes to an important point that PTPN22 operates on a fine balance so that the precise dosage of PTPN22 matters and even a slight change in it can lead to drastically different outcomes in the course of disease progression. Yeh et al. took an opposite approach from these groups and overexpressed PTPN22 in T cell specific manner under the distal Lck promoter in NOD mice [86]. The authors chose to characterize 2 transgenic founder mice, dLPC and dLPE, who each had 2-5 and 10-20

copies of the transgene, respectively. The findings were surprising in that similar to the data obtained from PTPN22$^{-/-}$ mice, PTPN22 overexpression also resulted in protection from T1D. In these systems, the authors did not observe a significant difference in the overall size of the T cell compartments of the thymus and the periphery. However, they detected increased ratio of Tregs to pathogenic T cells ($CD4^{+}IFN\gamma^{+}$ and $CD8^{+}IFN\gamma^{+}$) in the pancreatic infiltrates [86]. These findings led the authors to question whether PTPN22 has a preferential effect on autoreactive T cells. To address this question, the authors adoptively transferred BDC2.5^{+} T cells that either do or do not express dLPC transgene into NOD.SCID recipients. They found that the proliferation of BDC2.5^{+} T cells was reduced in the PLNs only when dLPC was co-expressed [86]. This data is important in that it serves as another piece of evidence supporting the concept that the dosage of PTPN22 has different consequences for T cells with varying T cell signaling strength. In addition, the phenotypes characterized in this study were consistently more striking in mice with higher copy number of the transgene (dLPE over dLPC), indicative of the dosage of PTPN22 being an important factor for determining a T cell fate. Overall, considering that different T cell subsets have varying degrees of *Ar* expression **(Figure 3.5)**, it is likely that the intrinsic qualities of a given T cell including TCR signaling threshold and sensitivity to hormonal regulation contribute to the net physiological consequence of the tipping of the balance in PTPN22 regulation.

Considering that different mature T cell subsets have varying degrees of *Ar* expression **(Figure 3.5)**, it is likely that hormonal regulation contributes to T cell selection in the thymus and their functional properties in the periphery. Knowing that PTPN22 is sensitive to androgen regulation, it made sense to revisit clinical data on the input of known R620W mutation in PTPN22 gene associated with multiple autoimmune diseases including T1D. Interestingly, disease risk introduced by the mutation was in inverse correlation with the published degree of sexual dimorphism **(Figure 3.26.A)** and there was no difference in the

frequencies of that mutation between sexes regardless of the bias of the disease **(Figure 3.26.B)**. Moreover, that mutation introduced in NOD mice [84] did not affect T1D gender bias. Thus, we posit that it fixes PTPN22 in a certain functional state that supersedes the influence of sex hormones. That supports a possibility that PTPN22 most common 'normal' allele does contribute to disease development in a hormone dependent manner, making this protein, as well as potentially multiple other proteins that are controlled by androgens, a valid target for therapeutic interventions. It is important to emphasize that the immune response to modified-self in cancer demonstrates similarities with autoimmunity, despite the opposite goals of immunotherapy. Several studies have connected AR signaling with exhaustion of anti-tumor $CD8^+$ T cell responses limiting the efficiency of immunotherapy [50, 51, 87]. A negative role of *Ptpn22* in anti-tumor immunotherapy has been established in animal models [88, 89]. The knowledge of PTPN22 regulation by AR provides more options for cancer treatment as well.

Lastly, we have previously defined the 2 required signals—hormonal and microbial signals—for male protection from T1D in NOD males. It was important to test the relevancy of this finding in a systemic model of autoimmunity. The striking difference in the severity of SLE in B6.NZM mice at U of C vs. U of F prompted us to test the hypothesis that the variation in the composition of the microbiota influences the degree of systemic autoimmunity in B6.NZM mice. However, colonization of GF animals with cecal contents of SPF mice housed at U of C vs. U of F did not lead to recapitulation of severity seen in SPF mice housed at respective institutions. This finding demonstrated that the microbiota is not the main causative agent that modulates the severity of SLE in B6.NZM mice. Given that B6.NZM mice are poor breeders, we are entertaining the hypothesis that genetic drift within the colonies of B6.NZM mice housed at U of C vs. U of F resulted in genetic changes that contributed to variation in the severity of SLE in mice housed at different institutions. To this end, we are currently performing comparative analyses of whole genomic sequences of

B6.NZM mice raised either in GF setting or in SPF conditions at U of C or U of F to identify SNPs that could be linked to changes in the severity of SLE in B6.NZM mice.

Overall, our data define the cellular and molecular mechanisms by which androgens confer protection from T1D in NOD males. We discovered that T cell intrinsic androgen signaling through the AR is sufficient to attenuate T cell autoreactivity and yields reduction in T cell proliferation yet enhancement of IFNγ secretion by $CD8^+$ T cells following stimulation by cognate antigens. Furthermore, we revealed that androgens influence shaping of the TCR repertoire. Considering the widely distributed expression pattern of AR, it is likely that both T cell-intrinsic and -extrinsic AR signaling contribute to modulation of T cell autoreactivity. We show that T cell-extrinsic androgen signaling mediated regulation of AIRE represents at least one mechanism by which autoreactivity of mature T cells can be modulated. Our work also highlights androgen-AR mediated regulation of *Ptpn22* as a physiologically relevant route in altering T cell autoreactivity in mouse models of systemic or organ-specific autoimmunity. The inverse correlation between the degree of gender bias in human autoimmune conditions and the frequency of common nonsynonymous mutation in PTPN22 ($PTPN22^{R620W}$) supports our argument that wild-type allele of PTPN22 may contribute to autoimmunity through its sensitivity to regulation by sex hormones in humans. However, neither NOD.$AR^{f/y}$CD4Cre^+ males nor NOD.$PTPN22^{AREmut}$ males fully lost protection from T1D. Collectively, these data indicate that additional networks and/or cell types may be subjected to regulation by androgens to contribute to male-dependent protection from autoimmunity. Finally, our colonization studies performed with B6.NZM mice allude to the complexity of studying the interplay between host genetic factors and microbial agents in dictating the severity and gender bias in SLE of B6.NZM mice. The causative players for variations in the SLE severity of B6.NZM mice housed at different institutions remain to be determined.

REFERENCES

[1] Sheridan, L. A., Poulin, R., Ward, D. F. & Zuk, M. Sex differences in parasitic infections among arthropod hosts: is there a male bias? *Oikos* **88**, 327–334 (2000).

[2] Klein, S. L. & Flanagan, K. L. Sex differences in immune responses. *Nature Reviews Immunology* **16**, 626–638 (2016).

[3] Lopes-Ramos, C. M., Quackenbush, J. & DeMeo, D. L. Genome-wide sex and gender differences in cancer. *Frontiers in oncology* **10**, 597788 (2020).

[4] Gay, L. *et al.* Sexual dimorphism and gender in infectious diseases. *Frontiers in Immunology* **12** (2021).

[5] Pollard, K. M. Gender differences in autoimmunity associated with exposure to environmental factors. *Journal of autoimmunity* **38**, J177–J186 (2012).

[6] Hansen, M. P., Matheis, N. & Kahaly, G. J. Type 1 diabetes and polyglandular autoimmune syndrome: A review. *World journal of diabetes* **6**, 67 (2015).

[7] Yurkovetskiy, L. *et al.* Gender bias in autoimmunity is influenced by microbiota. *Immunity* **39**, 400–412 (2013).

[8] Peeva, E., Zandman-Goddard, G. & Shoenfeld, Y. Gender bias in murine lupus. *Handbook of Systemic Autoimmune Diseases* **9**, 21–27 (2008).

[9] Richard, M. L. & Gilkeson, G. Mouse models of lupus: what they tell us and what they don't. *Lupus science & medicine* **5**, e000199 (2018).

[10] Miller, S. D., Karpus, W. J. & Davidson, T. S. Experimental autoimmune encephalomyelitis in the mouse. *Current protocols in immunology* **88**, 15–1 (2010).

[11] Constantinescu, C. S., Farooqi, N., O'Brien, K. & Gran, B. Experimental autoimmune encephalomyelitis (eae) as a model for multiple sclerosis (ms). *British journal of pharmacology* **164**, 1079–1106 (2011).

[12] Ogino, Y., Miyagawa, S. & Iguchi, T. Testosterone/dihydrotestosterone. In *Handbook of Hormones*, 917–920 (Elsevier, 2021).

[13] Handelsman, D. J. Androgen physiology, pharmacology, use and misuse. *Endotext [Internet]* (2020).

[14] Ballou, S. P., Khan, M. A. & Kushner, I. Clinical features of systemic lupus erythematosus. *Arthritis & Rheumatism: Official Journal of the American College of Rheumatology* **25**, 55–60 (1982).

[15] Belman, A. L. *et al.* Characteristics of children and adolescents with multiple sclerosis. *Pediatrics* **138** (2016).

[16] MAKINO, S., KUNIMOTO, K., MURAOKA, Y. & KATAGIRI, K. Effect of castration on the appearance of diabetes in nod mouse. *Experimental Animals* **30**, 137–140 (1981).

[17] Roubinian, J., Talal, N., Greenspan, J., Goodman, J. & Siiteri, P. Effect of castration and sex hormone treatment on survival, anti-nucleic acid antibodies, and glomerulonephritis in nzb/nzw f1 mice. *The Journal of experimental medicine* **147**, 1568–1583 (1978).

[18] Palaszynski, K. M., Loo, K. K., Ashouri, J. F., Liu, H.-b. & Voskuhl, R. R. Androgens are protective in experimental autoimmune encephalomyelitis: implications for multiple sclerosis. *Journal of neuroimmunology* **146**, 144–152 (2004).

[19] Verheul, H., Verveld, M., Hoefakker, S. & Schuurs, A. Effects of ethinylestradiol on the course of spontaneous autoimmune disease in nzb/w and nod mice. *Immunopharmacology and immunotoxicology* **17**, 163–180 (1995).

[20] Wen, L. *et al.* Innate immunity and intestinal microbiota in the development of type 1 diabetes. *Nature* **455**, 1109–1113 (2008).

[21] Gilliver, S. C. Sex steroids as inflammatory regulators. *The Journal of steroid biochemistry and molecular biology* **120**, 105–115 (2010).

[22] Varanasi, V., Avanesyan, L., Schumann, D. M. & Chervonsky, A. V. Cytotoxic mechanisms employed by mouse t cells to destroy pancreatic β-cells. *Diabetes* **61**, 2862–2870 (2012).

[23] Dultz, G. *et al.* The protein tyrosine phosphatase non-receptor type 22 c1858t polymorphism is a joint susceptibility locus for immunthyroiditis and autoimmune diabetes. *Thyroid* **19**, 143–148 (2009).

[24] Zhou, Y. *et al.* Metascape provides a biologist-oriented resource for the analysis of systems-level datasets. *Nature communications* **10**, 1–10 (2019).

[25] Davey, R. A. & Grossmann, M. Androgen receptor structure, function and biology: from bench to bedside. *The clinical biochemist reviews* **37**, 3 (2016).

[26] Dart, D. A., Waxman, J., Aboagye, E. O. & Bevan, C. L. Visualising androgen receptor activity in male and female mice. *PloS one* **8**, e71694 (2013).

[27] Tan, M., Li, J., Xu, H. E., Melcher, K. & Yong, E.-l. Androgen receptor: structure, role in prostate cancer and drug discovery. *Acta Pharmacologica Sinica* **36**, 3–23 (2015).

[28] Shaffer, P. L., Jivan, A., Dollins, D. E., Claessens, F. & Gewirth, D. T. Structural basis of androgen receptor binding to selective androgen response elements. *Proceedings of the National Academy of Sciences* **101**, 4758–4763 (2004).

[29] Horie-Inoue, K., Bono, H., Okazaki, Y. & Inoue, S. Identification and functional analysis

of consensus androgen response elements in human prostate cancer cells. *Biochemical and biophysical research communications* **325**, 1312–1317 (2004).

[30] Dahiya, V. & Bagchi, G. Non-canonical androgen signaling pathways and implications in prostate cancer. *Biochimica et Biophysica Acta (BBA)-Molecular Cell Research* 119357 (2022).

[31] Heng, T. S. *et al.* The immunological genome project: networks of gene expression in immune cells. *Nature immunology* **9**, 1091–1094 (2008).

[32] Lee, P. P. *et al.* A critical role for dnmt1 and dna methylation in t cell development, function, and survival. *Immunity* **15**, 763–774 (2001).

[33] Wong, F. S., Visintin, I., Wen, L., Flavell, R. A. & Janeway Jr, C. A. Cd8 t cell clones from young nonobese diabetic (nod) islets can transfer rapid onset of diabetes in nod mice in the absence of cd4 cells. *The Journal of experimental medicine* **183**, 67–76 (1996).

[34] Stadinski, B. D. *et al.* Chromogranin a is an autoantigen in type 1 diabetes. *Nature immunology* **11**, 225–231 (2010).

[35] Verdaguer, J. *et al.* Acceleration of spontaneous diabetes in tcr-beta-transgenic nonobese diabetic mice by beta-cell cytotoxic cd8+ t cells expressing identical endogenous tcr-alpha chains. *The Journal of Immunology* **157**, 4726–4735 (1996).

[36] Bhat, P., Leggatt, G., Waterhouse, N. & Frazer, I. H. Interferon-γ derived from cytotoxic lymphocytes directly enhances their motility and cytotoxicity. *Cell death & disease* **8**, e2836–e2836 (2017).

[37] Padovan, E. *et al.* Expression of two t cell receptor α chains: dual receptor t cells. *Science* **262**, 422–424 (1993).

[38] Niederberger, N. *et al.* Allelic exclusion of the tcr α-chain is an active process requiring tcr-mediated signaling and c-cbl. *The Journal of Immunology* **170**, 4557–4563 (2003).

[39] Von Boehmer, H. & Melchers, F. Checkpoints in lymphocyte development and autoimmune disease. *Nature immunology* **11**, 14–20 (2010).

[40] Heath, W. R. *et al.* Expression of two t cell receptor α chains on the surface of normal murine t cells. *European journal of immunology* **25**, 1617–1623 (1995).

[41] Anderson, M. S. *et al.* Projection of an immunological self shadow within the thymus by the aire protein. *Science* **298**, 1395–1401 (2002).

[42] Malchow, S. *et al.* Aire enforces immune tolerance by directing autoreactive t cells into the regulatory t cell lineage. *Immunity* **44**, 1102–1113 (2016).

[43] Zhu, M.-L. *et al.* Sex bias in cns autoimmune disease mediated by androgen control of autoimmune regulator. *Nature communications* **7**, 1–14 (2016).

[44] Hale, J. S. & Fink, P. J. Back to the thymus: peripheral t cells come home. *Immunology and cell biology* **87**, 58–64 (2009).

[45] Webb, S. R. & Sprent, J. Induction of neonatal tolerance to mlsa antigens by cd8+ t cells. *Science* **248**, 1643–1646 (1990).

[46] Ben-Nun, A. & Cohen, I. R. Spontaneous remission and acquired resistance to autoimmune encephalomyelitis (eae) are associated with suppression of t cell reactivity: suppressed eae effector t cells recovered as t cell lines. *J. Immunol* **128**, 1450–1457 (1982).

[47] Chau, L. *et al.* Thymic re-entry of mature activated t cells and increased negative selection in vascularized allograft recipients. *Clinical & Experimental Immunology* **127**, 43–52 (2002).

[48] Gardner, J. M. *et al.* Deletional tolerance mediated by extrathymic aire-expressing cells. *Science* **321**, 843–847 (2008).

[49] Gardner, J. M. *et al.* Extrathymic aire-expressing cells are a distinct bone marrow-derived population that induce functional inactivation of cd4+ t cells. *Immunity* **39**, 560–572 (2013).

[50] Kwon, H. *et al.* Androgen conspires with the cd8+ t cell exhaustion program and contributes to sex bias in cancer. *Science Immunology* (2022).

[51] Yang, C. *et al.* Androgen receptor-mediated cd8+ t cell stemness programs drive sex differences in antitumor immunity. *Immunity* **55**, 1268–1283 (2022).

[52] Begovich, A. B. *et al.* A missense single-nucleotide polymorphism in a gene encoding a protein tyrosine phosphatase (ptpn22) is associated with rheumatoid arthritis. *The American Journal of Human Genetics* **75**, 330–337 (2004).

[53] Bottini, N. *et al.* A functional variant of lymphoid tyrosine phosphatase is associated with type i diabetes. *Nature genetics* **36**, 337–338 (2004).

[54] Kyogoku, C. *et al.* Genetic association of the r620w polymorphism of protein tyrosine phosphatase ptpn22 with human sle. *The American Journal of Human Genetics* **75**, 504–507 (2004).

[55] Velaga, M. *et al.* The codon 620 tryptophan allele of the lymphoid tyrosine phosphatase (lyp) gene is a major determinant of graves' disease. *The Journal of Clinical Endocrinology & Metabolism* **89**, 5862–5865 (2004).

[56] Morel, L. *et al.* Genetic reconstitution of systemic lupus erythematosus immunopathology with polycongenic murine strains. *Proceedings of the National Academy of Sciences* **97**, 6670–6675 (2000).

[57] Hasegawa, K. *et al.* Pest domain-enriched tyrosine phosphatase (pep) regulation of effector/memory t cells. *Science* **303**, 685–689 (2004).

[58] Hogquist, K. A. *et al.* T cell receptor antagonist peptides induce positive selection. *Cell* **76**, 17–27 (1994).

[59] Li, M. O. & Rudensky, A. Y. T cell receptor signalling in the control of regulatory t cell differentiation and function. *Nature Reviews Immunology* **16**, 220–233 (2016).

[60] Onengut-Gumuscu, S. *et al.* Fine mapping of type 1 diabetes susceptibility loci and evidence for colocalization of causal variants with lymphoid gene enhancers. *Nature genetics* **47**, 381–386 (2015).

[61] Padyukov, L. *et al.* A genome-wide association study suggests contrasting associations in acpa-positive versus acpa-negative rheumatoid arthritis. *Annals of the rheumatic diseases* **70**, 259–265 (2011).

[62] Frommer, L. & Kahaly, G. J. Autoimmune polyendocrinopathy. *The Journal of Clinical Endocrinology & Metabolism* **104**, 4769–4782 (2019).

[63] Frommer, L. & Kahaly, G. J. Type 1 diabetes and autoimmune thyroid disease—the genetic link. *Frontiers in endocrinology* **12**, 618213 (2021).

[64] Zeldovich, L. Genetic drift: the ghost in the genome. *Lab animal* **46**, 255–257 (2017).

[65] Chervonsky, A. V. Microbiota and autoimmunity. *Cold Spring Harbor perspectives in biology* **5**, a007294 (2013).

[66] Gascoigne, N. R., Rybakin, V., Acuto, O. & Brzostek, J. Tcr signal strength and t cell development. *Annual review of cell and developmental biology* **32**, 327–348 (2016).

[67] Constant, S. L. & Bottomly, K. Induction of th1 and th2 cd4plus t cell responses: The alternative approaches. *Annual review of immunology* **15**, 297 (1997).

[68] Leitenberg, D., Boutin, Y., Constant, S. & Bottomly, K. Cd4 regulation of tcr signaling and t cell differentiation following stimulation with peptides of different affinities for the tcr. *The Journal of Immunology* **161**, 1194–1203 (1998).

[69] Rogers, P. R. & Croft, M. Peptide dose, affinity, and time of differentiation can contribute to the th1/th2 cytokine balance. *The Journal of Immunology* **163**, 1205–1213 (1999).

[70] Siminovitch, K. A. Ptpn22 and autoimmune disease. *Nature genetics* **36**, 1248–1249 (2004).

[71] Maine, C. J. *et al.* Ptpn22 alters the development of regulatory t cells in the thymus. *The Journal of Immunology* **188**, 5267–5275 (2012).

[72] Maine, C. J. *et al.* The effect of the autoimmunity-associated gene, ptpn22, on a bxsb-derived model of lupus. *Clinical Immunology* **156**, 65–73 (2015).

[73] Zheng, P. & Kissler, S. Ptpn22 silencing in the nod model indicates the type 1 diabetes–associated allele is not a loss-of-function variant. *Diabetes* **62**, 896–904 (2013).

[74] Menard, L. *et al.* The ptpn22 allele encoding an r620w variant interferes with the removal of developing autoreactive b cells in humans. *The Journal of clinical investigation* **121** (2011).

[75] Schickel, J.-N. *et al.* Ptpn22 inhibition resets defective human central b cell tolerance. *Science immunology* **1**, aaf7153–aaf7153 (2016).

[76] Maine, C. J., Marquardt, K., Cheung, J. & Sherman, L. A. Ptpn22 controls the germinal center by influencing the numbers and activity of t follicular helper cells. *The Journal of Immunology* **192**, 1415–1424 (2014).

[77] Mitchell, S. H., Murtha, P. E., Zhang, S., Zhu, W. & Young, C. Y. An androgen response element mediates lncap cell dependent androgen induction of the hk2 gene. *Molecular and cellular endocrinology* **168**, 89–99 (2000).

[78] Riegman, P., Vlietstra, R., Van der Korput, J., Brinkmann, A. & Trapman, J. The promoter of the prostate-specific antigen gene contains a functional androgen responsive element. *Molecular endocrinology* **5**, 1921–1930 (1991).

[79] Nelson, C. C. *et al.* Determinants of dna sequence specificity of the androgen, progesterone, and glucocorticoid receptors: evidence for differential steroid receptor response elements. *Molecular endocrinology* **13**, 2090–2107 (1999).

[80] Wang, Q. *et al.* A hierarchical network of transcription factors governs androgen receptor-dependent prostate cancer growth. *Molecular cell* **27**, 380–392 (2007).

[81] Hay, C. W., Hunter, I., MacKenzie, A. & McEwan, I. J. An sp1 modulated regulatory region unique to higher primates regulates human androgen receptor promoter activity in prostate cancer cells. *PloS one* **10**, e0139990 (2015).

[82] Wilson, S., Qi, J. & Filipp, F. V. Refinement of the androgen response element based on chip-seq in androgen-insensitive and androgen-responsive prostate cancer cell lines. *Scientific reports* **6**, 1–15 (2016).

[83] Hay, C. W. *et al.* Negative regulation of the androgen receptor gene through a primate-specific androgen response element present in the 5 utr. *Hormones and Cancer* **5**, 299–311 (2014).

[84] Lin, X. *et al.* Crispr-cas9–mediated modification of the nod mouse genome with ptpn22r619w mutation increases autoimmune diabetes. *Diabetes* **65**, 2134–2138 (2016).

[85] Brownlie, R. J. *et al.* Lack of the phosphatase ptpn22 increases adhesion of murine

regulatory t cells to improve their immunosuppressive function. *Science signaling* **5**, ra87–ra87 (2012).

[86] Yeh, L.-T. *et al.* Different modulation of ptpn22 in effector and regulatory t cells leads to attenuation of autoimmune diabetes in transgenic nonobese diabetic mice. *The Journal of Immunology* **191**, 594–607 (2013).

[87] Guan, X. *et al.* Androgen receptor activity in t cells limits checkpoint blockade efficacy. *Nature* 1–6 (2022).

[88] Cubas, R. *et al.* Autoimmunity linked protein phosphatase ptpn22 as a target for cancer immunotherapy. *Journal for immunotherapy of cancer* **8** (2020).

[89] Ho, W. J. *et al.* Systemic inhibition of ptpn22 augments anticancer immunity. *The Journal of clinical investigation* **131** (2021).

[90] Belman, A. *et al.* Characteristics of children and adolescents with multiple sclerosis. *PEDIATRICS* **138**, e20160120–e20160120 (2016).